DURBAN UNIVERSITY OF TECHNOLOGY
INYUVESI YASETHEKWINI YEZOBUCHWEPHESHE

Increasing catalytic activity of a fructosyltransferase using site-directed mutagenesis

Submitted in complete fulfilment for the Degree of Master of Applied Science in Biotechnology in the Department of Biotechnology and Food Science, Durban University of Technology, Durban, South Africa

Fanzhi Wang

December 2023

SUPERVISOR : **Prof. Kugen Permaul**
CO-SUPERVISOR : **Prof. Suren Singh**

REFERENCE DECLARATION

I, Mr Fanzhi Wang – 21836081 and Prof Kugen Permaul do hereby declare that in respect of the following dissertation:

Title: Increasing catalytic activity of a fructosyltransferase using site-directed mutagenesis

1. As far as we ascertain:

a) no other similar dissertation exists;
b) the only similar dissertation(s) that exist(s) is/are referenced in my dissertation as follows:

_____

_____

_____

2. All references as detailed in the dissertation are complete in terms of all personal communication engaged in and published works consulted.

	2024/03/22
Signature of student	**Date**
	2024/03/22
Signature of supervisor	**Date**
	2024/03/22
Signature of co-supervisor	**Date**

AUTHOR'S DECLARATION

This study presents original work by the author. It has not been submitted in any form to another academic institution. Where use was made of the work of others, it has been duly acknowledged in the text. The research described in this dissertation was carried out in the Department of Biotechnology and Food Science, Faculty of Applied Sciences, Durban University of Technology, South Africa, under the supervision of **Prof Kugen Permaul**.

Student's signature

TABLE OF CONTENTS

ACKNOWLEDGEMENTS

The author would like to acknowledge the following people:

Prof Kugen Permaul, for academic supervision, guidance and mentorship which was always a motivation to carry on.

The staff of the Department of Biotechnology for academic and technical assistance.

ABSTRACT

Fructooligosaccharides (FOS) are naturally occurring metabolites that have a wide application in the food industry. They are one of the most well-studied prebiotics and have been used as an alternative sweetener to sucrose, as the modern diet demands healthier and calorie-reduced foods. FOS is commercially produced either by hydrolysis of inulin into inulin-type FOS or by sucrose transfructosylation into levan-type FOS. The levan-type FOS are short-chain FOS and are produced under the catalysis of fructosyltransferase (FTase) or fructofuranosidase (FFase). In this study, FOS production was studied using a fructosyltransferase, SucC, which was originally isolated from *Aspergillus niger* and was functionally expressed in *Pichia pastoris*. The tertiary structure of SucC was determined by bioinformatics analysis and catalytic sites were verified and validated by wet and dry experiments where the amino acid residues D64, D194 and E271 were proved to form the catalytic triad. Three mutants, C66S, G273V, L313H were constructed aiming to improve the enzyme performance. Only the C66S mutant showed improved enzymatic activity which was 61% increase in specific activity. The other mutants, G273V and L313H, led to a complete loss of enzyme activity. By simulating saturated mutagenesis, tertiary structure alignment, and molecular docking, it was predicted that the C66S mutation could increase the hydrophilic environment surrounding the active site without visible changes in its structure. Two more amino acid residues (E296, H310) in addition to D64, D122, R193, D194, E271 in mutant C66S were predicted to be interacting with sucrose, and the binding energy changed from -3.65 to -4.14 kcal/mol. Subsequently, mutant C66S was constructed by site-directed mutagenesis and expressed in *Pichia pastoris* GS115. The purified mutant C66S showed improved enzymatic activity with a 61.3% increase in its specific activity. Its K_m value was decreased by 13.5% while the k_{cat} value increased by 21.6%. Its transfructosylation efficiency significantly improved during the initial reaction stages of FOS production. These results clearly revealed that the increase of hydrophilicity surrounding the active site enhanced the transfructosylating activities. Therefore, modification of the hydrophilic micro-environment surrounding the active site could be an alternative way to artificially evolve an enzyme's catalytic efficiency.

Keywords: Fructooligosaccharides, Prebiotics, Transfructosylation, Enzyme engineering, Fructosyltransferase.

LIST OF FIGURES

LIST OF TABLES

CHAPTER 1: INTRODUCTION

Sucrose, also well known as "table sugar", is the most used carbohydrate consumed by human beings (Mathlouthi and Reiser, 1995). It is a naturally occurring sugar and is largely manufactured from sugarcanes and sugar beets (Carter, 1987). Sucrose is not only found in many naturally occurring fruits and vegetables but is also used as a sweetener that is added to processed foods and beverages (White, 2014). It has been used for thousands of years as a food additive that provides a sweet taste and a source of energy. It is abundant and relatively easy to obtain (Sen et al., 2019). In the modern sugar industry, about 80% of the production of sugar is mostly based on the extraction of sucrose from sugarcanes in the tropical regions while the rest of the commercial sugar being produced are extracted from sugar beets in temperate climatic regions (Zhu and Pan, 2022). It was reported in 2022 that the global sugar production reached 183.2 million tons, where Brazil, Russia, India, China, USA and Pakistan are the main sucrose-producing countries (https://www.fas.usda.gov/data/sugar-world-markets-and-trade). Although sugar has been one of the most important food additives, the excessive consumption of sugar in foods, mainly sucrose, may lead to health issues such as obesity, diabetes, tooth decay, etc (Prada et al., 2022). As the modern diet encompasses a healthier life style which mainly involves low-calorie intake, dietary modulation, dental health and prebiotic effects in intestines, fructooligosaccharides may act as an alternative option for substitution of sucrose. Fructooligosaccharides (FOSs) are functional oligosaccharides formed by β-2,1-glycosidic bonding of fructose with a typical polymerization degree of 2 to 9 (Sangeetha et al., 2005). It exhibits a general sweetness level between 30 to 50% comparing to sucrose and has very similar biochemical properties such as taste, reductivity, viscosity, humidity, thermostability. Therefore, FOS can be an outstanding alternative sweetener that partially substitutes the use of sucrose in the daily diet (Kherade et al., 2021). The commercial application of FOS emerged around the 1980s and are widely applied in the diary industry, food industry and medical products. This is due to its following attractive features: i) stimulating the growth of probiotics in the intestines such as bifidobacteria that strengthens the immune system; ii) facilitating the intake of minerals and trace elements; and iii) reducing the intake of calories in food due to its non-digestibility (Sánchez-Martínez et al., 2020). Although FOS is a natural sugar found in many plants and fruits, its bulk production relies on modern biotechnological processes. Inulin-type FOS is manufactured from hydrolysis of inulin into long-chain FOS while levan-type FOS is manufactured from transglycosylation of sucrose into short-chain FOS (Nobre et al., 2015). The inulin-type FOS has been well studied and its bulk production has been applied in industry since the last two decades (Singh and Singh, 2010) and is relatively

easy to obtain compared to levan-type FOS. However, it has been proved that levan-type FOS is more stable and will induce better growth of bifidobacteria and more effectively suppress potential pathogens comparing to inulin-type FOS because the FOS with a smaller degree of polymerization is largely non-digestible and serves as feed for bifidobacteria (Sabater-Molina et al., 2009). In addition, the modern production of both types of FOS replies on enzymatic methods for bulk production because the use of enzymes for FOS production guarantees higher specificity, higher efficiency and a more environment-friendly manufacturing process compared to the traditional chemical processes (Pang et al., 2021). Nowadays, the enzymatic production of FOS relies on two enzymes: fructosyltransferase (FTase) and fructofuranosidase (FFase), which have been well studied over 20 years in Japan, South Korea, etc. Many examples of these enzymes have been identified, and the mechanism of enzymatic reaction as well as the structure-function relationships have been investigated and revealed (Antošová and Polakovič, 2001). The improvement in yield of FOS and lower capital investment during FOS production mainly relies on the optimization of fermentation techniques, screening for new strains that produce novel enzymes and enhancement of down-stream processing techniques (Zhang et al., 2017). Moreover, a major limitation of the enzymatic production technique is that the conversion rate of substrates into FOS is not by satisfactory. The amount of products obtained is limited by the inhibition by glucose, which is a main by-product that not only inhibits the conversion of sucrose into FOS but also increases the capital cost of removing such by-products (Vega and Zuniga-Hansen, 2014). Site-directed mutagenesis of enzymes is a powerful protein engineering technique for improvement of enzyme performance. This technique not only improves the enzyme's characteristics, but also sheds light on structure-function relationships (Bachman, 2013). Many successful cases have showed improved fructosyltransferase performance such as higher kestose yield catalyzed by a mutated fructosyltransferase which was originally cloned from *Aspergillus niger* N74 (Alvarado-Obando et al., 2022) and better thermostability of a mutated fructosyltransferase which was originally cloned from another *Aspergillus niger* strain (Xia et al., 2022). In this project, a fructosyltransferase, SucC, was used as the enzyme for structural characterization and evolution in order to obtain better catalytic activity for production of FOS.

CHAPTER 2: LITERATURE REVIEW

2.1. Enzymes

Enzymes are direct products of certain specific genes through transcription and translation that catalyze chemical reactions in living organisms (Adrio and Demain, 2014). Enzymes act as biological catalysts that facilitates reactions which are necessary for various physiological processes, such as metabolism, DNA replication, and cellular respiration (Robinson, 2015). These catalysts increase the rate of chemical reactions by lowering the activation energy required in such processes without being consumed or permanently altered where this acceleration is responsible for the timely execution of cellular activities, such as metabolism and DNA replication (Roduner, 2014). Enzymes are characterised by their: i) high specificity for particular substrates to produce precise products which ensures the accuracy and efficiency of biochemical pathways; ii) high efficiency that significantly enhances the rate of chemical reactions in which allows cells to carry out essential processes at physiological temperatures and pressures; iii) reusability that are capable of catalyzing multiple rounds of reactions where enzymes return to their original state and are available to additional cycles of catalysis after catalyzing a reaction; and iv) regulations in metabolic pathways including feedback inhibition, allosteric modulation, and post-translational modifications that enables organisms to control the intensity of biochemical reactions which are vital for energy production, nutrient utilization, and the synthesis of biomolecules (Robinson, 2015). Therefore, they are not only the life fundamentals but also has have various applications in: i) biotechnology manufacturing such as in production of biofuels, pharmaceuticals, and chemicals (Fogarty and Kelly, 2012); ii) food industry for various purposes, including the production of prebiotics, alcohols, bread, cheese and beverages (Raveendran et al., 2018); iii) medical diagnostics typically in diagnostic tests and assays, such as enzyme-linked immunosorbent assays (ELISAs) to detect and quantify biomolecules (Singh et al., 2019); iv) environmental technology particularly in bioremediation that break down pollutants and contaminants in soil and water and clean-up of environmental hazards (Bhandari et al., 2021); and 5) textile industry for processes of desizing and biofinishing that helps improve the quality of textiles (Madhu and Chakraborty, 2017).

2.2. Prebiotics

Prebiotics are mainly a group of fructans that are non-digestible in animal intestines. They must meet three criteria in order to be classified as prebiotics, i.e., being non-digestible by human enzymes, fermentable by host microbes in intestines and

stimulating growth and activity of beneficial bacteria (Slavin, 2013). The market for prebiotic ingredients globally is valued at 7.15 billion dollars in 2022 and it is predicted to be worth around 22.71 billion dollars by 2032, with a growth rate of 12.30% annually from 2023 to 2032 (Precedence Research, 2022) The production of prebiotics such as inulin, FOS, GOS using enzymes in modern industries offers significant advantages which guarantees high specificity, high efficiency in producing sole products with high quality and are environmentally-friendly that does not lead to pollutions (Vera et al., 2021). The mechanisms of how prebiotics function in human intestines is revealed where prebiotics are primarily served as substrates for specific intestine bacteria, such as *Bifidobacterium*, *Lactobacillus*, *Enterococcus* which promotes their proliferation (Macfarlane, 2009). This selective stimulation results in a favourable change in the composition and activity of the gastrointestinal microbiota that exerts numerous downstream effects on human health. Some typical types of prebiotics which have been studied and applied in industry over decades are fructooligosaccharides (FOS), galactooligosaccharides (GOS), inulin, pectin, lactulose, xylooligosaccharides (XOS), mannan-oligosaccharides (MOS) (Davani-Davari et al., 2019). Prebiotics as supplementary nutrients have been attracted lots of interest in their pivotal role in modulating the gastrointestinal microbiota and health promoting properties. By stimulating the growth of probiotics in human's intestines, prebiotics are involved in maintaining gastrointestinal health in which reduce inflammation and alleviate symptoms such as irritable bowel syndrome and constipation (Zhang et al., 2023); prebiotics also takes part in metabolic pathways in which produces short-chain fatty acids through prebiotic fermentation that carries profound metabolic implications where short-chain fatty acids affect glucose metabolism, lipid homeostasis, and may contribute in controlling glycemic level and lipid profiles (Roberfroid et al., 2010).

2.2.1. Fructooligosaccharides (FOS)

Fructooligosacchride (FOS) are a typical prebiotic that have gained lots of interest in research and application. They are oligosaccharide fructans, which are polymers of D-fructose residues linked by β (2→1) bonds with a terminal α (1→2) linked D-glucose. General structures of FOS can be expressed in Glu-Fru_n, in which n ranges from 2 – 7 that represents the number of fructose units linked to the glucose unit. As a sugar, it is of 30 – 60% sweetness level to commercial (Mudannayake et al., 2022) sucrose (Ibrahim O, 2018). The main components of commercial FOS are kestose (GF_2), nystose (GF_3), fructosylnystose (GF_4), in which two, three, and four fructosyl units are bound at the β-2,1 position of glucose, respectively (Figure 1). These FOS are naturally found in a large number of plants, especially in Jerusalem artichoke, chicory and the

blue agave plant (Mudannayake et al., 2022). They are also found in fruits and vegetables such as bananas, onions, chicory root, garlic, asparagus, and leeks. Some grains and cereals, such as wheat and barley, also contain FOS (Campbell et al., 1997). FOS exhibits outstanding characteristics in its high solubility in water (~80%, m/v) and high stability between a range of pH 4.0 – 7.0 (Sabater-Molina et al., 2009). FOS is widely used in dairy industry, food industry and medical products due to its attractive features in promoting growth of probiotics in human body's intestines which benefits health in reducing blood lipids, promoting intake of minerals and trace elements and reducing calories intake due to its feature of non-digestibility. As also reported that a demand of 2-2.5 g/day FOS will maintain the healthy gastrointestinal microbiota (Flamm et al., 2001). So, it is widely supplemented in milk products, condiments, infant food and feed, health care products and other fields. However, naturally occurring FOS are limited in the amount and relies on biotechnological way for bulk production of FOS by using enzymes, in which fructosyltransferase is well studied among these years and successfully applied to catalyse the production of FOS (Sabater-Molina et al., 2009).

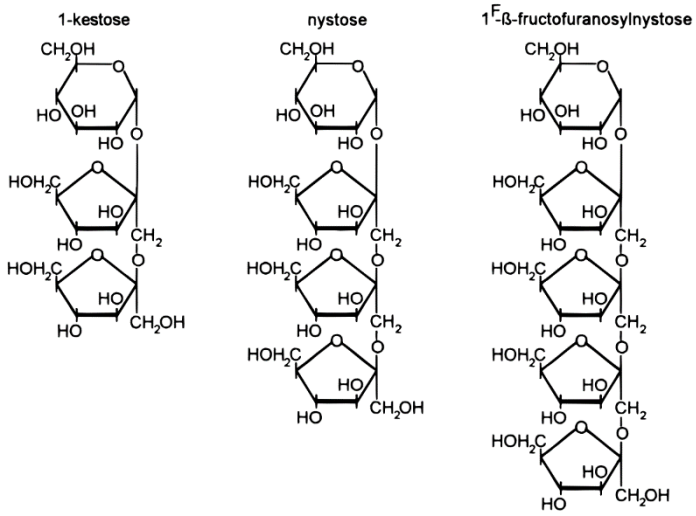

Figure 1: Structure of 1-kestose (GF_2), nystose (GF_3) and 1^F-β-fructofuranosylnystose (GF_4), from left to right, respectively (Campbell et al., 1997). The FOS (GF_2, GF_3 and GF_4) showed the typical structure linkage where one or several D-fructose residues were linked by β (2→1) bonds with a terminal α (1→2) linked D-glucose that forms a FOS.

2.2.2. Galactooligosaccharides (GOS)

Galactooligosaccharides (GOS) are another class of prebiotics that have gained significant interests in recent years due to their health benefits in bifidogenic effect (Souza et al., 2022). Galactooligosaccharides are food-grade oligosaccharides which are composed of galactose units. They are found to form linkages by β-glycosidic bonds

(Figure 2) which are β-(1→2), β-(1→3), β-(1→4), or β-(1→6) to galactose moieties and generally have a degree of polymerization (DP) of 3 – 8 (Gänzle, 2011). GOS are naturally occurred in mammals' milk with a relatively low quantity but are commercially produced by β-galactosidase (EC 3.2.1.23) with the substrate lactose in industrial scales (Sako and Tanaka, 2011). GOS as prebiotic ingredients are featured in their functional property being non-digestible, which are not hydrolyzed by human intestine enzymes but are fermented by the probiotic microbes residing in human gastrointestines (Macfarlane et al., 2008). Natural accumulation of GOS is relatively low, mainly in certain mammal milk, legumes, and root vegetables (Pico et al., 2021; Raman et al., 2019). Chemical and enzymatic ways of manufacturing GOS have been investigated due to the due to the increasing GOS demands in various applications particularly in the food and pharmaceutical industries (Torres et al., 2010). Therefore, the use β-galactosidases with high transglycosylation activities in GOS production has emerged as an outstanding method (Guerrero et al., 2015). Several studies have been conducted in identifying microorganisms with high transglycosyaltion activities such as *Lactobacillus plantarum* (Iqbal et al., 2010), *Lactobacillus pentosus* (Maischberger et al., 2010), *Aspergillus oryzae* (Urrutia et al., 2013), *Kluyveromyces lactis* (González-Delgado et al., 2016), *Sulfolobus solfataricus* (Park et al., 2008). Numerous studies have been carried out to investigate the prebiotic effects of GOS, especially in their health benefits on the gastrointestinal microbiota. Briefly, GOS selectively stimulate the growth and activity of certain beneficial bacteria, typically *Bifidobacterium* spp and *Lactobacillus* spp. Such bacteria play a crucial role in gastrointestinal microbiota modulation, immune system modulation, digestion and absorption of nutrients, reducing inflammation in the gastrointestinal tracts, synthesizing vitamins, producing short-chain fatty acids, inhibiting pathogenic bacteria growth that contribute to the overall health (Holzapfel and Schillinger, 2002; Williams, 2010). Thus, the prebiotic effects of GOS along with probiotics exhibit many benefits for nutrient intake, metabolic health and immune function. GOS are applied in various industries due to their prebiotic and physiological effects. For example, GOS are utilized as functional ingredients in the food industry in dairy products, beverages, and infant foods to enhance the nutritional values and reduce calories intake (Dekker and Daamen, 2011). GOS are also explored in pharmaceuticals where therapeutic interventions are developed for gastrointestinal disorders and gastrointestinal microbiota modulation (Vulevic et al., 2018). Although GOS has many promising applications, challenges remain in fully understanding the interactions between GOS and the gastrointestinal microbiota. It was found that the overconsumption of GOS may lead to discomfort of human beings, which was comparable to the lactose-intolerant individuals in overconsumption of lactose (Gänzle, 2011). Further research of GOS is required in

study on its optimal dosage, structural characteristics, and long-term effects of GOS consumption. By exploring novel sources of GOS, refining its production processes and identifying additional health-promoting properties, more comprehensive understandings and applications of GOS may gain increased interest.

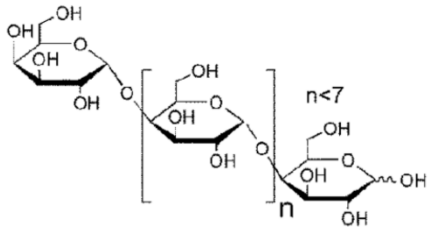

Figure 2: Generic structure of galactooligosaccharides (GOS) where n represents the number of galactosyl units linked to the glucosyl unit (Berezovskaya et al., 2020).

2.2.3. Xylooligosaccharides (XOS)

Xylooligosaccharides (XOS) are another type of oligosaccharides which are derived from hydrolysis of xylan by xylanase. They are components of hemicellulose and are naturally accumulated in plant cell walls (Pinto et al., 2023). Different from the FOS and GOS discussed above, XOS are polymers of five carbon sugar (C5) instead of six carbon sugar (C6). XOS are composed of xylose units that are linked to each other through β (1→4) glycosidic bonds (Figure 3) with a general degree of polymerization between 2 to 10 (Ibrahim O, 2018). The degree of polymerization of XOS plays a crucial role in their biological activities in which influence their solubility and fermentability (Kabel et al., 2002). XOS are also featured in their non-digestibility and health-promoting properties in selectively stimulating the growth of beneficial bacteria in the human gastrointestinal tracts (Aachary and Prapulla, 2011). Similar to the other types of prebiotics, XOS not only stimulate the growth of *Bifidobacterium* and *Lactobacilli*, facilitate nutrients intake, but also supress the growth or activity of pathogenic microbes. Moreover, it was reported that XOS served as the dietary supplements are more effective than the other prebiotics such as FOS, GOS (Mhetras et al., 2019). Besides its prebiotic effects, XOS also find applications in which are served as additives in food industry such as beverages, dairy products, alcohols and functional foods. In the pharmaceutical industry, the consumption of XOS guarantees the therapeutic applications in reducing blood sugar and lipid, laxation and immune modulation. In agriculture, XOS supplied as animal feed additives promotes the growth and health of livestock by positively modulating their gastrointestinal microbiota (Chen et al., 2021). XOS is primarily derived from xylan, which is a hemicellulose component

of the plant cell walls. In modern industry, XOS are usually extracted from certain woods, cereal grains and agricultural residues using alkaline chemicals such as NaOH (Rowley et al., 2013). The production of XOS through enzymatic hydrolysis of xylan by xylanases is also a common way of manufacturing XOS (de Menezes et al., 2009). The difference between chemical production and enzymatic production is in their requirements where chemical ways of manufacturing XOS will result in the accumulation of the XOS with a wider DP range while manufactured by enzymatic ways will reduce the formation of degradation products, which satisfies the demand for food and pharmaceutical industries (Mhetras et al., 2019). Additionally, the development of enzyme technology in modifying xylanases have led to more efficient production of XOS, suggesting a potential more efficient production process and higher yield for industry use. Several studies have been conducted in improving the catalytic efficiency of xylanase (Cheng et al., 2015; Li et al., 2017; Song et al., 2012) and thermostability (Dumon et al., 2008; Wang et al., 2017) by directed evolution strategies.

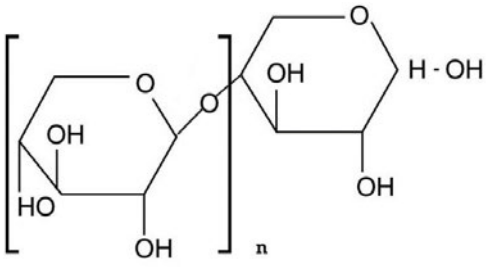

Figure 3: Structure of xylooligosacchairdes (XOS) where n represents the number of xylose units linked to another xylose by β (1→4) glycosidic bonds (Ibrahim O, 2018).

2.2.4. Mannan-oligosaccharides (MOS)

Mannan-oligosaccharides (MOS) are another type of prebiotics which are primarily derived from yeast cell walls, particularly in *Saccharomyces cerevisiae.* They are composed of mannose units linked by either α-(1,3) or α-(1,6) bonds with a polymerization degree up to 10 (Tungland, 2018). Like the other prebiotics such as FOS and GOS, MOS also stimulate the growth of beneficial bacterium in intestines and positively influence the gastrointestinal health with modulations. However, different from the other prebiotics, MOS gained its interests and applications mainly in animal feeds. Several studies have been conducted investigating the effects of administration of MOS for animals in which all reported positive effects on animals performance (Baurhoo et al., 2007; Halas and Nochta, 2012; Torrecillas et al., 2014; White et al., 2002). The use of MOS as a food supplement for animals have improved their overall well-being and longevity. Besides its prebiotic effects, MOS has also been applied in aquaculture that reduced the microbial load in which significantly reduced the *Vibrio*

spp levels in the live and aquatic feed cultures (Dimitroglou et al., 2010). When combined with certain probiotics for administration, such as *Enterococcus faecalis*, it was reported that such administration has greatly reduced the number of pathogens, *Vibrio*, coliforms and *Salmonella*, resulting in a greater feed efficiency and performance in rainbow trout aquaculture (Denji et al., 2015; Dimitroglou et al., 2010).

2.3. Probiotics

Probiotics are live microorganisms with positive effects on body health when administrated in adequate amount. They particularly take part in the modulation of microbial balance in the gastrointestinal tracts, resulting in a promoted gastrointestinal health (Sarao and Arora, 2017). Probiotics have been associated with human health over a lone time, with the first insight into human beings where Eli Metchnikoff (1907) illustrated the benefits of lactic acid bacteria present in the fermented milk and their positive impact on modifying the microflora in gastrointestinal tracts (Holzapfel and Schillinger, 2002). After that, scientists have gained attentions and insights in identifying the lactic acid bacteria species, in which the *Bifidobacterium* and *Lactobacillus* were found to be the predominant components of the microflora in intestines (Fooks and Gibson, 2002; O'Sullivan et al., 1992). As research goes on, more strains of lactic acid bacteria have been identified that are responsible for probiotic effects, such as *L. acidophilus, L. lactis, L. plantarum, B. bifidum, B. infantis, E. faecalis, S. salivarius, S. cremoris* (Parvez et al., 2006). However, concerns have been raised in using *Enterococcus* spp as probiotics due to their possible pathogenicity (Williams, 2010). Therefore, certain criteria have been established for a microorganism to be regarded as probiotics (Harish and Varghese, 2006): i) isolated from same species as its intended hosts; ii) non-pathogenic; iii) have specified beneficial effects on hosts; iv) be alive and viable in sufficient numbers; and v) stable and able to survive prolonged periods during manufacturing and storage. Probiotics beneficially effect on gastrointestinal health by various mechanisms, in which lower the intestinal pH, competitively exclude pathogenic microbes, produce antimicrobial substances and are involved in the modulation of host's immune response (Plaza-Diaz et al., 2019). The most effective clinical use in probiotics was that it has been used in treatment of acute diarrhoea which was mostly caused by rotavirus and pouchitis (Williams, 2010). Probiotics are also able to alleviate symptoms of irritable bowel syndrome and inflammatory bowel diseases, which provides insights in modulation of immune system (Lescheid, 2014). Besides its clinical uses, probiotics are also widely applied in functional food industry, especially served as food additives in fermented dairy products, functional beverages, cereals, snack bars, capsules and tablets (Kechagia et

al., 2013; Latif et al., 2023). Although probiotics have provided huge beneficial effects on gastrointestinal tracts, challenges still exist mainly in demonstrating strain-specific effects and improving viability during storage (Foligné et al., 2013). Addressing these challenges will offer better probiotic performance various applications.

2.4. Sucrose

Sucrose is a naturally occurring sugar that is abundant in many plants on Earth. It is the most consumed sugars among all the other sugars such as maltose, glucose, fructose for human beings over centuries. In history, the first chemically refined sugar occurred about 2500 years ago and this technology eventually spread to most of the world after 13th century. The ancient art of refining sugar techniques seemed to be firstly mastered by Persians. After that the Venetians attempted to produce the refined sugar and made a success in sugar trade. Around 16th century, the technique of refining sugar spread to Germany but the Dutch mastered the refinery technique and soon dominated the European market (Ballinger, 1971). Although the sugar extraction technology from sugarcane or beets was developed since thousands of years ago, refined and pure sugar used to be a luxurious commodity that are only available to rich people rather than an ordinary condiment in daily diet because the refining technology was not mature enough during those ages (Eggleston, 2019). Nowadays, most of the countries in the world are able to manufacture sugars on their own but the top ten countries (Australia, Brazil, China, USA, India, EU-27, Pakistan, Thailand, Russia, Mexico) accounted for approximately 70% sugar production globally (Mnisi and Dlamini, 2012). It was reported in 2022 that the global sugar production reached 183.2 million tons where Brazil, Russia, India, China, The US, Pakistan are the main sucrose-producing countries (https://www.fas.usda.gov/data/sugar-world-markets-and-trade). Although sucrose is very easy to obtain, its sources for commercial production mainly relies on sugarcane and beets where 80% of the production of sugar is mostly based on the extraction of sucrose from sugarcane in the tropical regions while the rest of the commercial sugar being produced are extracted from sugar beets in temperate climatic regions (Zhu and Pan, 2022). Meanwhile, the cultivation of sugarcane not only provides sugar but also generates lots of by-products such as fibre, livestock feed, bioethanol and the cane bagasse can be used for generation of electricity (Sahu, 2018). The development of sugar industry over centuries which involves raw sugar production and down-stream processing have offered great opportunities and contributed to the economic growth in which sugar crops cultivators, processors and related food companies benefited a lot from it (Higgins et al., 2007).

In modern sugar industry, more concerns are raised not only on sugar production, but also on its sustainability and other utilizations that make sucrose into more valuable substances (Prada et al., 2022). The conversion of sucrose into more valuable substances is a meaningful way for the comprehensive utilization of sucrose. One relevant topic is the overconsumption of sucrose may lead to many health issues, such as obesity, diabetes, dental caries, hyperlipidemia, etc. (Prada et al., 2022). A successful solution to reduce the sucrose intake is to convert sucrose into oligofructans such as fructooligosaccharides, which is a type of prebiotic that is featured in its prebiotic effects such as promoting the growth of bifidobacteria in human intestines, stimulating the production of short chain fatty acids by prebiotic fermentation that maintain gastrointestinal health, managing and regulating the gastrointestinal disorders, reducing inflammation, enhancing the absorption of nutrients such as calcium and magnesium by increasing their solubility in the gastrointestinal tracts (de Paulo Farias et al., 2019). Also, prebiotics, typically FOS is featured in its non-digestibility which means it is calories-free that does not contribute the energy intake by human bodies so that FOS served as a great alternative to sucrose to be applied as food additives in food industry (Ibrahim, 2021). The sucrose application through traditional chemical methods has been studied since a half-century ago that are applied in food, chemistry and pharmaceutical industries (Queneau et al., 2007), but biotechnological investigations in converting sucrose into valuable compounds has gained lots of interest in the last 30 years due to its environmental-friendly and sustainable properties (Ni et al., 2022). Specifically in production of FOS, several enzymes were studied and applied in industry such as fructosyltransferase, β-fructofuranosidase, levansucrase, inulosucrase, sucrose isomerase and amylosucrase that specifically convert sucrose to functional sucrose isomers, oligosaccharides, or polysaccharides (Flores-Maltos et al., 2016). In summary, the enzymatic conversion of sucrose into those compounds with higher value represents a significant approach for comprehensive utilization of sucrose.

2.5. FOS Producing Enzymes

Fructosyltransferase (EC.2.4.1.9) belongs to GH32 family and is a glycosyltransferase which specifically catalyses the chemical reaction where a fructosyl group is transferred to a molecule of sucrose or a FOS when a FOS with a chain longer by one fructosyl unit is formed with sucrose as the substrate (Henry and Darbyshire, 1980). This enzyme also participates in polymerization reactions where FOS with various numbers of fructosyl units are formed (Antošová and Polakovič, 2001). Fructosyltransferase is widely found in plants and microorganisms intracellularly and extracellularly, but differs in molecular weight and other properties due to the difference of culture and

relative culture medium composition. However, only few strains are reported to produce the fructosyltransferase that have potential use in industry while most of the wild-type ones can not meet the industrial requirements (Kawakami and Yoshida, 2002). Several fungal strains are reported as fructosyltransferase producers with high transfructosylating activities such as *Aspergillus niger* ATCC 20611, *A. niger* AN 166, *Aspergillus foetidus*, *Aspergillus oryzae* CFR 202, *Aureobasidium pullulans* CFR 77, *A. oryzae* KB, *Aspergillus awamori* GHRTS, *Aspergillus aculeatus* (Antošová and Polakovič, 2001; Ghazi et al., 2007). Fructosyltransferases are produced by solid and liquid fermentation, and the factors such as temperature, pH, substrate concentration affecting the optimal growth conditions vary in different sources of enzymes while generally this enzyme works best between 50 to 60℃ and 4.5 to 6.5 in pH (Manoochehri et al., 2020).

2.5.1. Enzymatic Production of FOS

Industrial production of FOS is based on either enzymatic hydrolysis of inulin using inulinase or transfructosylation of sucrose using fructosyltransferase. Kestose (GF_2), nystose (GF_3), 1F (1-β-fructofuranosyl) nystose (GF_4), 1F(1-β-fructofuranosyl) 4 sucrose (GF_5) are the main oligosaccharide products (Yoshikawa et al., 2006). Several microorganisms were reported to secrete fructosyltransferase that are suitable for industrial production of FOS, which were mainly isolated from *Aspergillus niger*, *A. japonicus*, *A. pullulans* (Picazo et al., 2019). However, current isolated fructosyltransferases are fragile, sensitive and are not of high catalytic activity. In order to increase the enzyme activity and yield of products, immobilization techniques of cells or enzymes using alginate, chitosan etc, are usually applied that decreases the cost of enzyme preparations (Sirisansaneeyakul et al., 2000). Besides screening on wild-type fructosyltransferase producers for better enzyme activity, modification of existing FOS-producing enzymes is also an effective way to improve the enzyme's performance where bioinformatic techniques are used to predict the homologous fructosyltransferase's 3-D structure followed by molecular-docking to study the interaction between protein and substrate, thus guiding the selection of the target for amino acid sequences modification to modify the enzyme protein structure for possible improvements of enzyme activity (Choukade and Kango, 2021).

2.5.2. Mechanism of Transfructosylation

Fructosyltransferase is a typical glucoside hydrolase with transfructosylating activities in GH32 families. The enzymes classified in this family shares the most prominent feature in consisting of a distinctive β-propeller catalytic domain with three acidic amnio acid residues which are two Asp and one Glu that forms a catalytic triad. In this catalytic triad, one Asp in the highly conserved sequence of "WMNDPNG" acts as a nucleophilic; one Glu in the highly conserved sequence of "EC" acts as a general acid/base catalyst and the other Asp in the highly conserved sequence of "RDP" acts as a transition state stabilizer (Lafraya et al., 2011). This catalytic triad is very common in all GH32 enzymes. What's more, a number of hydrophobic residues surrounding the catalytic domain are vital for substrate binding. Another unique structure found in GH32 family is the possess of a C-terminal β-sandwich domain which helps stabilize the enzyme structure (Álvaro-Benito et al., 2010). The transfructosylation reaction undergoes a double displacement mechanism, where the nucleophile (Asp) attacks the anomeric carbon of the fructosyl moiety of the donor substrate, such as sucrose, which forms the enzyme-fructose intermediate while the general acid/base catalyst (Glu) will protonate the leaving group in the first step. After that, the general acid/base catalyst will deprotonate the acceptor molecule and then the intermediate will react with the acceptor molecule over the anomeric carbon of the fructosyl moiety. If water serves as the acceptor molecule in the case of a hydrophilic environment, then free fructose will be released. If the sucrose serves as the acceptor molecule in the case of hydrophobic environment, then the final product will be FOS (Figure 2).

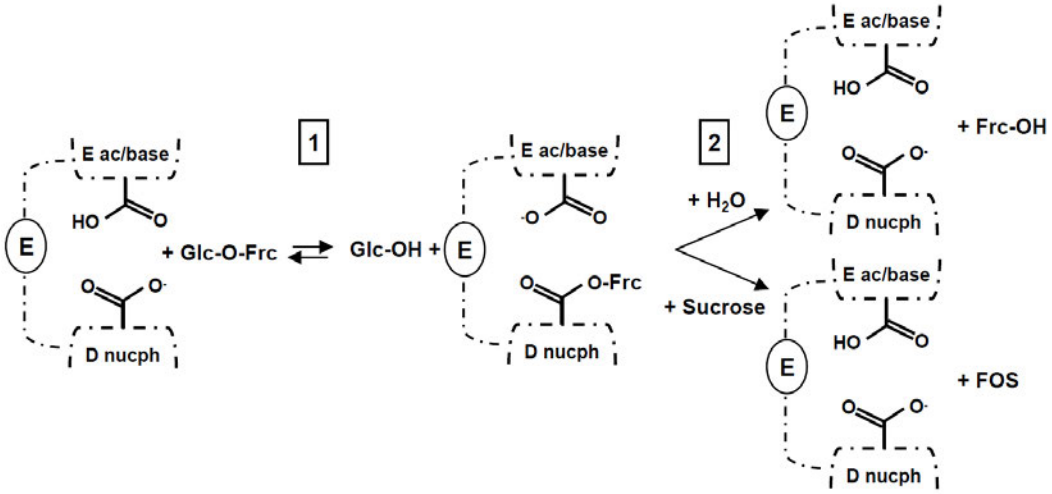

Figure 4: The overall double displacement reaction mechanism in GH32 enzymes. A Asp acts as a nucleophile and a Glu acts as a general acid/base catalyst. The sucrose will firstly be broken down into a fructosyl unit and a free glucose. If water acts as the acceptor molecule, free fructose will be generated

eventually. If another sucrose acts as the acceptor, FOS will be generated instead. A hydrophilic reaction leads to the hydrolysis of sucrose into glucose and fructose while a hydrophobic reaction leads to the transfructosylation of a fructosyl unit to another sucrose that forms a FOS (Lafraya et al., 2011).

2.6. Substrate Access Tunnel

In order to carry out a successful catalyzed reaction, substrates must get access to the enzyme's active sites. The active site, is a specific region structurally for and complementary region in the enzyme which is structurally complementary to the substrate that allows a specific binding of substrates with active sites, thus promoting the conversion chemical reaction of the substrate into product(s). For understanding the enzymatic catalysis mechanisms, several models have been created (Figure 5). Among the whole last century, the traditional theory of lock-and-key model for enzyme catalysis was firstly raised by Emil Fischer in 1894 (Fischer, 1894) and was widely accepted until, the induced-fit model for illustrating the catalysis occurring on the surface was introduced by Koshland in 1958 (Koshland Jr, 1958) and the keyhole-lock-key model for elucidating the enzyme's catalysis where tunnels take part in the transportation of substrates and products to and from the buried active sites within the enzyme, respectively (Prokop et al., 2012) in which described that the enzyme allows slight conformational changes so that guarantees the flexibility of both the enzyme and substrate (ligand), which encounters the limitation of Fischer's theory when enzymes being fully rigid that do not fit to all models (Chakraborty and Di Cera, 2017). Clearly, a specific region in an enzyme molecule surrounding the active site and the factors effected on are being much more concerned in either fundamental research or application requirement (Buller et al., 2023). Although the induced-fit model has well illustrated the catalysis occurring on the surface of enzyme, it is well studied that over 60% of enzymes carry out their catalysis with their active site buried inside the enzyme's structure, which are located in the internal cavities, and substrates must get access to the buried active site through tunnels from the surface of enzyme (Marques et al., 2016). Tunnels are pathways that are crucial during the catalysis where substrates, cofactors and solvents are transported to the active site while products are transported out of the active site to be released (Kokkonen et al., 2019). Therefore, a new concept of enzyme-substrate catalysis model, keyhole-lock-key model, has been proposed to elucidate the enzyme's catalysis where tunnels take part in the transportation of substrates and products to and from the buried active sites within the enzyme, respectively (Prokop et al., 2012). The proposed keyhole-lock-key model is a relatively new field of research and describes the interactions and impact of access tunnels on enzyme activity, specificity, and stereoselectivity (Prokop et al., 2012). Studies have

been conducted in investigating the binding of ligands (substrates) to the enzyme's active site which illustrated that the substrate must travel through the tunnel to get access to the active site and subsequently bind to the active site. Therefore, in the keyhole-lock-key model, ligands are not only complementary to the active site, but also to the binding tunnel in which the tunnel also affects the substrate specificity for an enzyme reaction (Kingsley and Lill, 2015). There have been abundant of researches in engineering access tunnels in enzymes that addressed the impact of tunnels on catalysis, ligand binding and products release (Kaushik et al., 2018; Kingsley and Lill, 2015; Kokkonen et al., 2019; Koudelakova et al., 2013; Lu et al., 2019; Seo et al., 2022) where emphasized the effect of tunnel engineering significantly improved the enzyme's performance.

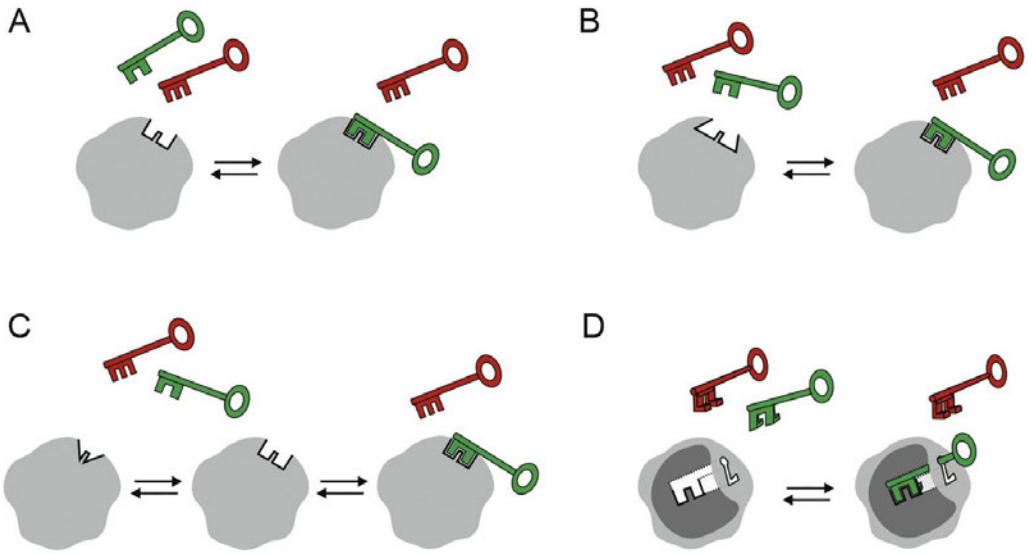

Figure 5: Schematic depictions of models describing enzymatic catalysis. (A) lock-key model, (B) induced-fit model, (C) selected-fit Model, and (D) keyhole-lock-key model. The green key represents the binding substrate while the red key represents the unbinding substrate (Kokkonen et al., 2019).

It is well-known that many factors influence the physio-chemical microenvironment of the active site, and hence effect on or even control the enzyme activity, such as volume (Ma et al., 2024), hydrophilicity/hydrophobicity (Yang et al., 2022), acidity/alkalinity (Lu et al., 2002) and positively/negatively charged (Meiering et al., 1992). One notable factor is that the hydrophilicity/hydrophobicity of the catalytic environment surrounding the active sites plays crucial importance in catalysis (Yang et al., 2022). Typically, the hydrophilic residues resident in the tunnel will interact with the hydrophilic groups of the substrates that promote substrate transport and binding to the active site (Singh and Anand, 2021). The hydrophilicity/hydrophobicity for different

amnio acid residues has significant impacts on the structure-function relationships (Kaushik et al., 2018). Since most of enzymatic reactions are naturally occurred in aqueous environments, the hydrophilic/hydrophobic micro-environment surrounding the active site of an enzyme may highly determine its catalytic activity (Wang et al., 2021; Yang et al., 2022)

2.7. Fructosyltransferase Engineering

In order to improve the enzyme performance that meets the higher demand of FOS-producing enzymes in industry besides screening for new enzymes with more favourable characteristics, abundant studies have been carried out in order to tackle the demand pressure and increases the yield of FOS. One of the most effective ways to artificially evolve fructosyltransferase is site-directed mutagenesis (Xia et al., 2022). As reported of the first fructosyltransferase being revealed in crystallization which was cloned from *Aspergillus japonicus*, its crystal structure was determined where D60, D191 and E292 forms the catalytic triad that plays its functions. It was also determined that residues Lys-78, Phe-118, Asp-119, Ile-143, His-144, Arg-190, Glu-318, His-332, Tyr-369, Ala-370, Trp-398 and Tyr-404 form a negatively charged active-site pocket (Chuankhayan et al., 2010). Several mutagenesis studies have been carried out and many successful cases were listed: The mutant N52S and P232V of β-fructofuranosidase from *Schwanniomyces occidentalis* (GenBank: ADN34605.1) built by Alvaro-Benito et al. (2010) improved the transferase activity of the wild-type enzyme about 1.6-fold; The mutant F254H of a fructosyltransferase from *Aspergillus niger* N74 (GenBank: GU145136.1) built by Alvarado-Obando et al. (2022) increased 1-kestose production; The combinatory mutant W39Y-N41S-N44S of a β-fructofuranosidase (GenBank: NP_012104.1) built by Engel et al. (2022) increased the synthesis of 6-kestose up to 10-fold (Lafraya et al., 2011). These mutants constructed through site-directed mutagenesis showed improved characteristics comparing to their wild type enzymes and contribute a lot to the research in modifying FOS producing enzymes.

CHAPTER 3: TERTIARY STRUCTURE OF SucC AND VERIFICATION OF ITS ACTIVE SITE

3.1. Introduction

The fructosyltransferase, SucC, expressed as a recombinant protein in *P. pastoris* was obtained from the Biocatalysis and Biotransformation laboratory at the Tianjin University of Science and Technology, Tianjin, China. It was identified from a wild-type strain of *Aspergillus niger* which was isolated from a food processing sample. Its encoding gene was cloned and functionally expressed in *Pichia pastoris* GS115. SucC has been prepared at a commercial scale and has been applied for manufacturing fructooligosaccharides in China and many other countries for over ten years. However, there is a lack in the fundamental research on SucC to reveal its structure-function relationships. Although SucC has been applied in industrial scale for FOS production, it is necessary to study its tertiary structure for a better understanding of the mechanism of its enzymatic reactions and the amino acid residues involved in the interactions between the enzyme and substrates. In addition, prediction of its 3D structure will provide more information for future modification and improvement of the enzyme's properties.

Once the active sites in SucC were identified through *in silico* homologous alignment, it was vital to prove the validity of the active site prediction through *in vitro* experiments. Thus, the amino acids constituting the catalytic triad were each replaced by the other possible 19 amino acids and the tertiary structures of these mutants were predicted. The constructed mutated enzymes as well as the wild-type SucC were docked with the substrate in order to assess the impact of mutations on their interactions with substrate. Theoretically, some mutants may show different sucrose binding sites from the wild-type enzyme docked with sucrose, indicating the collapse of enzyme tertiary structure that leads to nonspecific binding of sucrose. Some other mutants may exhibit the same sucrose binding sites but poor affinity, indicating the reduced enzyme activity. For those mutants with better affinity to sucrose and share the same sucrose binding sites compared with the wild-type SucC, it is vital to carry out *in vitro* experiments to prove their loss of enzyme activity. In this chapter, a total of 57 mutations for D64, D194 and E271 in SucC were simulated and docked with sucrose to examine the impact of saturated mutagenesis on the three catalytic residues. The mutants with their binding sites and affinity energies to sucrose were presented. Among the saturated mutagenesis, the mutants with best interactions to sucrose in each catalytic residue were constructed

through site-directed mutagenesis. The mutated genes were generated by overlapping PCR technique, then transformed into *E. coli* JM109 and subsequently transformed into *P. pastoris* GS115 for expression. The mutated enzymes were then characterized in their activity. If no activity was detected for the generated mutants, it was then convinced that the loss of enzyme activity was caused by the mutations, which validated the predicted catalytic residues that were non-substitutable.

3.2. Materials and Methods

3.2.1. Construction of an evolutionary tree

The evolutionary analysis was conducted by the Maximum Likelihood method using the MEGA11 software (Tamura et al., 2021). The tree with the highest log likelihood (-37853.29) was chosen. Initial trees for the heuristic search were obtained automatically by applying the Neighbour-Join and BioNJ algorithms to a matrix of pairwise distances estimated using the JTT model, and then selecting the topology with superior log likelihood value. The tree was drawn to scale, with branch lengths measuring the number of substitutions per site. This analysis involved 32 amino acid sequences from different microbial sources, selected from the NCBI database.

3.2.2. Enzyme structure prediction

SucC (AHC54391.1) was modelled using the SWISS-MODEL server (https://swissmodel.expasy.org/). Fructofuranosidase, 5XH8 (Nagaya et al., 2017) was used as the existing template for modelling of SucC. The output results showed sequence similarities and GMQE scores of each generated structure where GMQE stands for "Global Model Quality Estimation" and is a score used to estimate the quality of the 3-D model generated by Swiss-Model. The GMQE score was expressed as a value between 0 and 1 where a higher score indicates a better model with better quality (Waterhouse et al., 2018). The value of QMEANDisCo (Qualitative Model Energy Analysis Discrimination Score) Global was also generated and provided a measure of the overall reliability of the protein structure model (Studer et al., 2020). The structure produced from SWISS-MODEL was then rendered or visualized using PyMOL (Schrodinger, 2015)

The amino acid sequence and primary structure alignments to determine the conserved sequences with active sites was carried out using ClustalW (Thompson et al., 1994). The amino acid sequences of three fructosyltransferases, two invertases and one fructofuranosidase from different microbial sources which are responsible for synthesizing FOSs with identified catalytic residues (Olarte-Avellaneda et al., 2018) were selected as the reference sequences.

3.2.3. *In silico* saturation mutagenesis of SucC

The *in silico* saturation mutagenesis of SucC was done through systematically replacing wild-type amino acid coding sequences into the other 19 non wild-type amino acids,

and subjecting them to tertiary structure constructions by SWISS-MODEL (https://swissmodel.expasy.org/) as described in section 3.2.2. The residues D64, D194 and E271 were substituted by the other 19 possible amino acids and all 57 variants were constructed through SWISS-MODELING processes. The tertiary structures of generated variants were then visualized by PyMOL (Schrodinger, 2015).

3.2.4. Molecular docking and screening for mutants

Autodock 1.5.7 (Morris et al., 2009) was used where a Lamarckian genetic algorithm GA was specifically applied to predict how sucrose interacts with SucC by predicting the most energetically favourable binding mode of sucrose within the active site of SucC. Dockings were run 60 times and sucrose binding was restricted to the catalytic region. The amino acid residues interacting with sucrose in the active site were firstly determined, and then the mutations were designed in order to modify the catalytic regions. The tertiary structures of SucC and its mutant candidates were predicted using SWISS-MODEL (Waterhouse et al., 2018) using aid of a best identical model, the fructofuranosidase from *Aspergillus kawachii* (PDB ID: 5XH8) (Nagaya et al., 2017). The interactions between proposed mutants and sucrose were predicted by Autodock (Morris et al., 2009) and visualized by PyMOL (Schrodinger, 2015).

3.2.5. Site-directed mutagenesis, molecular cloning and expression

3.2.5.1. Isolation of genomic DNA from *P. pastoris*

The source of *sucC* gene was obtained and acknowledged from the lab of Biocatalyst and Biotransformation in Tianjin University of Science and Technology, Tianjin, China. It was originally cloned from *A. niger* and functionally expressed in *P. pastoris* GS115. The recombinant *P. pastoris* containing the *sucC* gene was then used as the source of template DNA. The *sucC* gene is 1941 bp in size. The Dr. GenTLE^{TM} (from Yeast) High Recovery Kit (Takara) was used to isolate the genomic DNA. The isolated genomic DNA was used for DNA application.

3.2.5.2. Amplification of up-stream and down-stream fragments of mutations

The SucC mutants were created by site-directed mutagenesis using the over-lapping PCR technique (Hussain and Chong, 2016). Primers were designed to obtain overlapping regions with the template SucC to create the desired mutants and were

designed in such a way where the three bases coding for the target amino acid were deliberately replaced by the desired amino acid codons. The different set of primers still shared a common sequence to each other and the generated up-stream and down-stream fragments for over-lapping PCR. Primers designed for amplifying up-stream and down-stream fragments of D64S, D194Q and E271R are listed below in Table 1. The expected products to be obtained are listed in Table 2. The hot-start PCR technique was performed for amplifications and the programs being used in a thermocycler were optimized as follows: pre-heating at 95℃ for 300 seconds; denaturation at 94℃ for 10 seconds; annealing at 58℃ for 30 seconds; extension at 72℃ for 120 seconds; and a final extension at 72℃ for 300 seconds. 30 cycles of PCR were performed. The *Taq* DNA polymerase was not added until the end of pre-heating stage. The ingredients in the PCR reaction mixture are listed in Table 3.

Table 1: Primers used for mutagenesis on SucC active site residues

Primers	**Sequence (5′ to 3′)**
SucC-F	GTAAAGCTTCAAACGGCTTCCG
SucC-R	TGCTCTAGAATTAAGACTGACGATCCGGCC
D64S-F	CAATGGCCAGATCGGT***TCT***CCCTGCCTGCATTACA
D64S-R	GGG***AGA***ACCGATCTGGCCATTG
D194Q-F	TCACCGCATTCCGG***CAA***CCCTACGTCTTCCAAAAC
D194Q-R	GGG***TTG***CCGGAATGCGGTGA
E271R-F	GCTGGGCCTTCAACTTC***AGA***ACGGGCAACGTCTTCA
E271R-R	CGT***TCT***GAAGTTGAAGGCCCAGC

* The underlined sequence represents the *Xba*I recognized restriction site. The bold and italicized sequences symbolize the mutated region.

Table 2: Amplification products for SucC active site mutants

Primers	**Product**	**Expected size (bp)**
SucC-F, D64S-R	D64S-up	200
SucC-R, D64S-F	D64S-down	1700
SucC-F, D194Q-R	D194Q-up	600
SucC-R, D194Q-F	D194Q-down	1300
SucC-F, E271R-R	E271R-up	800
SucC-R, E271R-F	E271R-down	1100

Table 3: Ingredients in PCR reaction mixture

50 μL reaction mix	Amount
ddH_2O	up to 50 μL
10 × *Pyrobest*™ buffer II	5 μL
dNTPs (2.5 mM each)	4 μL
Forward primer	0.5 μM
Reverse primer	0.5 μM
chromosomal DNA	＜500 ng
**Pyrobest*™ DNA polymerase (5 units/μL)	0.5 μL

* The Pyrobest DNA polymerase was added after pre-denaturation in a hot-start PCR process.

3.2.5.3. Cross-over PCR of D64S, D194Q, E271R

Overlapping PCR products generated from the previous step were diluted with ddH_2O into 50 ng/μL before use. 1 μL of each mixture was then used as the template for PCR. The SucC-F and SucC-R primers were not added in the first 5 cycles while the later 25 cycles were performed by adding SucC-F and SucC-R primers. PCR procedure programs were the same as described above for hot-start PCR.

3.2.5.4. Preparation of pPIC9K

The pPIC9K plasmid was isolated from its host, *E. coli* JM109, which was obtained from the laboratory of Biocatalysis and Biotransformation at Tianjin University of Science and Technology using the alkaline lysis with SDS method (Birnboim and Doly, 1979). pPIC9K/JM109 was recovered from stock cultures on LB plates containing ampicillin (100 μg/mL) at 37℃ for 12 hours. Pellets of *E. coli* JM109 (50-100 mg) were collected and resuspended in 100 μL of solution I that contains EDTA (10 mM, pH 8), Tris-HCl (25 mM, pH 8) and glucose (50 mM). 200 μL of Solution II containing NaOH (0.2 M) and SDS (1%, w/v) was then added to the cell suspension to lyse the cells where all the cell components are released, and the double stranded DNA became denatured due to the breakdown of hydrogen bonds by NaOH. The next step was adding 150 μL of solution III containing 3 M sodium acetate, pH 4.8 in order to neutralize the mixture and re-anneal the DNA molecules. The plasmid DNA is much easier to renature while it is almost impossible to renature the large genomic DNA, thus making it possible to isolate the plasmid without the contamination from the precipitated genomic DNA. About 450 μL of the supernatant that contains plasmid DNA was then treated with 900 μL of cold 100% ethanol to precipitate the plasmid DNA. After centrifugation,

70% ethanol was used to wash the pellet to remove impurities. Eventually, the plasmid DNA was dried, then dissolved into 50 µL TE buffer (10 mM Tris-HCl, 1 mM EDTA, pH 8) and stored at -20°C. The isolated pPIC9K is 9294 bp in size and was verified by restriction enzyme digestion by *Bam*HI at 30°C for 1 hour and agarose gel electrophoresis to check if obtained band is of the correct size. *Bam*HI digestion conditions are listed in Table 4. The plasmid map of pPIC9K is shown in Figure 6.

Table 4: Linearization of pPIC9K using *Bam*HI

10 µL reaction	Amount
ddH_2O	up to 10 µL
10×K Buffer	1 µL
pPIC9K (50 ng/µL)	≤1 µg
*Bam*HI (15 units/µL)	1 µL

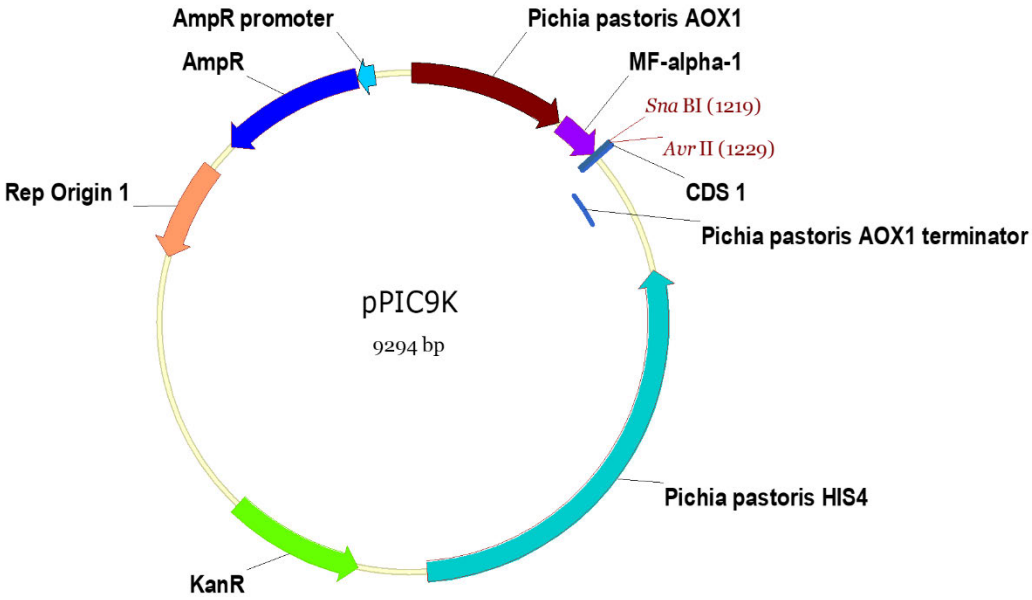

Figure 6: Map of pPIC9K. The vector is 9294 bp in size. Rep Origin 1 is used for its self-replication, AmpR is responsible for ampicillin resistance, KanR is responsible for kanamycin and G418 (geneticin) resistance, AOX1 for control the expression of inserted gene in the presence of methanol, CDS 1 refers to a 6x-His tag for expression and purification, α-factor (MF alpha 1) used as the secretion signal, HIS4 as the auxotrophic marker for selections of *his*$^+$ auxotrophs in transformation. The *Sna*BI and *Avr*II cloning sites for insertion of the foreign gene are also shown.

3.2.5.5. Ligation

Extracted and purified pPIC9K was digested by *Avr*II and *Sna*BI (Takara) at 37℃ for 1 hour to generate one sticky end and one blunt end, respectively. The generated crossover PCR products were digested by *Xba*I (Takara) at 37℃ for 1 hour to generate sticky ends that had the same tail digested by *Avr*II. The conditions of restriction reactions are listed in Table 5 and Table 6. Linearized and purified pPIC9K digested by *Avr*II and *Sna*BI was ligated with purified PCR product (*sucC* mutants) digested by *Xba*I. Ligation was performed using T4 DNA ligase (ThermoFisher). The ligation mixture was incubated at 16℃ for 4 hours in a water bath, followed by incubating at 4℃ overnight in the fridge. The ingredients in the ligation mixture are listed in Table 7.

Table 5: Digestion of pPIC9K by *Avr*II and *Sna*BI

10 μL reaction	Amount
ddH_2O	up to 10 μL
10×Tango Universal Buffer	1 μL
pPIC9K (50 ng/μL)	≤1 μg
*Sna*BI (15 units/μL)	1 μL
*Avr*II (15 units/μL)	1 μL

Table 6: Digestion of PCR products of *sucC* mutants using *Xba*I

10 μL reaction mix	Amount
ddH_2O	up to 10 μL
10×M Buffer	1 μL
BSA	1 μL
sucC (30 ng/μL)	2 μL
*Xba*I (15 units/μL)	1 μL

Table 7: Ligation reaction for linearized pPIC9K and *sucC* (mutated)

10 μL reaction mix	Amount
pPIC9K (50 ng/μL)	2 μL
*suc*C (30 ng/μL)	5 μL
10×T4 DNA ligase buffer	1 μL
50% (w/v) PEG 4000	1 μL
T4 ligase	1 Weiss U

3.2.5.6. Heat-shock transformation

E. coli competent cells were prepared freshly before use. The 10 µL ligation mixtures were mixed with 80 µL *E. coli* competent cells gently and incubated on ice for 10 min. The reaction mixture was heat-shocked by incubating at 42°C for 90 seconds in a water bath. After heat-shock, cells were transferred to ice immediately and incubated for 2 minutes. The cells were then incubated at 37°C for 1 hour with addition of 900 µL warm LB medium. After incubation, 100 µL cell suspension was used for spread plates on LB medium containing ampicillin. The remaining cell mixtures were centrifuged and resuspended into a final volume of 100 µL and spread on another LB plate containing ampicillin. Plates were incubated at 37°C overnight and the obtained colonies were selected for further screening processes.

3.2.5.7. Screening for correct *E. coli* JM109 transformants

The correct *E. coli* JM109 transformants were screened through plasmid extraction and restriction enzyme digestion. 20 *E. coli* JM109 transformants were subcultured onto LB plates with ampicillin and plasmid extraction of each culture was performed. The extracted 20 plasmids were digested by *Hin*dIII and four fragments were expected which are 350 bp, 2300 bp, 3600 bp and 5000 bp. The different strands generated from the digestion were separated by agarose gel (1.0%) electrophoresis. The transformants with correct insertions have a specific 2300 bp band containing the 1900 bp *sucC* gene while absence of this specific 2300 bp indicated the lack the *sucC* gene. The culture containing the correct insert was subcultured to obtain single colonies on LB plates with ampicillin and were preserved in 15% glycerol solution at -70°C.

3.2.5.8. Electrotransformation of recombinant pPIC9K into *P. pastoris* GS115

The *E. coli* JM109 transformants containing the inserted *sucC* gene were recovered on LB plates with ampicillin after incubation at 37°C for 12 hours. Plasmid extraction was performed as described in 3.2.5.4. to obtain recombinant plasmids of pPIC9K-D64S, pPIC9K-D194Q and pPIC9K-E271R. These recombinant plasmids were linearized by *Sal*I and were electro-transformed into *Pichia pastoris* GS115 for homologous recombination into the chromosome. *P. pastoris* transformants were selected on histidine-deficient medium and screened for their level of resistance to geneticin (G418). The ability to grow in high concentrations of geneticin indicates that multiple copies of the kanamycin resistance gene and the gene of interest were integrated into the genome.

The competent *P. pastoris* GS115 cells were prepared freshly prior to transformation, then 80 µL competent *P. pastoris* GS115 cells were mixed with 10 µL linearized recombinant plasmids in a 0.2 cm electroporation cuvette (Invitrogen) and incubated on ice for 5 minutes. After incubation, the ligation mixture was then transformed into *P. pastoris* GS115 using standard fungal electroporation conditions of 1.5 kV, 6 ms, 25 µF capacitance and 200 Ω resistance. After electroporation, 900 µL cold sorbitol (1 M) solution was immediately added to the mixture and then 100 µL of the cell mixture was spread onto MD agar which lacks histidine. The rest of the mixture was centrifuged at 6000 × g for 5 minutes, the supernatant was discarded and the pellet was resuspended by 100 µL sorbitol (1 M) solution and then spread onto MD agar plates. All MD plates were incubated at 30℃ for 72 hours. After incubation, white colonies appeared on MD plates indicated positive clones and were subcultured on YPD agar plates containing 0.5 mg/mL geneticin (G418) and incubated at 30℃ for 72 hours. The growing colonies were then subcultured on another YPD agar plate containing 2 mg/mL geneticin (G418) and incubated at 30℃ for 72 hours. The largest colonies for each transformation was picked and subcultured and preserved at -70℃ in 15% (V/V) glycerol solution.

3.2.5.9. Verification of correct GS115 transformants

The culture obtained in the previous section was verified by the colony PCR technique. The transformants were recovered on YPD agar plates at 30℃ for 72 hours. One colony was picked up and mixed with the PCR reaction mixture. 30 cycles of PCR were performed using the following program: pre-heating at 95℃ for 300 seconds; denaturation at 94℃ for 10 seconds; annealing at 58℃ for 30 seconds; extension at 72℃ for 120 seconds; and final extension at 72℃ for 300 seconds. The ingredients used in the PCR reaction are listed in Table 8. The obtained PCR products were visualized by agarose gel (1.0%) electrophoresis where the presence of a 1900 bp band indicated the correct insertion of foreign DNA into *P. pastoris* GS115 chromosome.

Table 8: Ingredients in the colony PCR reaction mixture

Ingredients	Amount
ddH_2O	up to 20 µL
2×Es *Taq* Master Mix	10 µL
SucC-F	0.5 µM
SucC-R	0.5 µM
Colony	*

*Colony was directly picked up from the agar plate and mixed in the reaction.

3.2.6. Expression of mutated enzymes

The *sucC* mutants were cloned downstream of the α-factor in pPIC9K to ensure functional expression in *Pichia pastoris* GS115 (Invitrogen) as described by the manufacturer's guidelines. The recombinant *P. pastoris* GS115 strains containing *sucC*, *sucC*-D64S, *sucC*-D194Q and *sucC*-E271R were recovered on YPD [1% yeast extract (w/v); 2% peptone (w/v); 2% glucose (w/v)] agar plates containing 2 mg/mL geneticin (G418) at 30ºC and 220 rpm for 72 h. Shake flask fermentations in 50 mL scale were performed to express the enzymes, where one colony was sub-culured into 20 mL liquid YPD medium and incubated at 30ºC and 200 rpm for 16 h. The 250 µL culture suspension was inoculated into 25 mL BMGY [1% yeast extract (w/ v); 2% peptone (w/v); 2% glucose (w/v); 1 M potassium phosphate buffer (pH 6.0 ± 0.2; 1% glycerol (w/v); 4 × 10-5 % biotin (w/v); 1.34% yeast nitrogen base (Oxoid) (w/v)] medium to represent a 1% inoculum and then incubated at 30℃ and 200 rpm to get the cell suspension reached an OD600 of around 4 to 5. Cells were then collected through centrifugation at 6000 × g and 4℃ for 5 min and resuspended by 2 mL BMMY [1% yeast extract (w/ v); 2% peptone (w/v); 2% glucose (w/v); 1 M potassium phosphate buffer (pH 6.0 ± 0.2; 1% glycerol (w/v); 4 × 10-5% biotin (w/v); 1.34% yeast nitrogen base (w/v)] medium. The fermentation medium was inoculated with the cell suspension to reach an OD600 of 1.0 at the start of the fermentation. The fermentation was supplemented with 250 µL methanol (0.5%, v/v) as the inducer, every 24 h and the whole fermentation period lasted up to 120 h at 30℃ and 200 rpm. The supernatants were collected as the crude enzymes for characterization.

3.2.7. Characterization of mutated enzymes

3.2.7.1. SDS-PAGE to examine the expression of enzymes

The SDS-PAGE technique (Laemmli, 1970) was used to examine if enzymes were expressed through visualization of separated protein bands on acrylamide gels by electrophoresis. The separation of different protein bands was based on their molecular weights. In this project, a 5% stacking gel and a 12% separation gel was used and their preparation recipes are listed in Table 9 and Table 10. The obtained crude enzymes were desalted using PD-10 desalting columns (Merck), and then 5 µL protein solution was mixed with 20 µL 5 × Sample Buffer, followed by boiling at 100℃ for 5 minutes in a water bath. The boiled samples were then centrifuged at 12000 × g for 5 minutes to pellet any debris and 20 µL of each sample and a molecular weight standard was loaded into the gel lanes. The chamber was then closed and a constant voltage of 80 V

was then supplied to the chamber to let the samples run out of the stacking gel for about 30 minutes. After that, a constant voltage of 110 V was then supplied to the chamber to separate the protein samples in the separation gel for about 90 minutes. After electrophoresis, only the separation gel was collected and stained by Coomassie blue dye (G-250) solution for 1 hour. The gel was soaked in the dye and the excess stain was then removed with destaining solvent for 12 hours. This treatment enables the visualization of blue bands that represents the denatured proteins.

Table 9: Ingredients to make a 6 mL 5% stacking gel

Stacking gel (5%)	Amount
ddH_2O	4.2 mL
30% acrylamide	1.0 mL
0.5 M Tris-HCl (pH 6.5)	0.75 mL
10% APS	60 µL
TEMED	0.1%

Table 10: Ingredients to make a 15 mL 12% separation gel

Stacking gel (5%)	Amount
ddH_2O	5.1 mL
30% acrylamide	6.0 mL
1.5 M Tris-HCl (pH 8.8)	3.8 mL
10% APS	150 µL
TEMED	0.1%

3.2.7.2. Enzyme activity assay

The activities of SucC and its mutants were determined by detecting the amount of glucose generated in the enzymatic reaction using a glucose detector (Yoo and Lee, 2010). The enzymatic reaction occurred in a 10% (M/V) sucrose solution in 100 mM sodium phosphate buffer at 50ºC and pH 5.5 for 1 h. The reaction was terminated by boiling the reactions at 100ºC for 10 min. The enzyme activity (U) was defined as the amount of enzyme required to generate 1 µmol of glucose per minute at 50ºC and pH 5.5. The protein concentrations of purified SucC and its mutants were quantified using the Bradford method (Bradford, 1976). The enzyme activity was calculated according to the formula:

$$U = \frac{A \times 10^{-2} \times 1 \times 10^{-3}}{180 \times 60} \times 10^{6} \times \mathrm{D} \times 10$$

Where A represents the reading produced from the glucose detector; D represents the dilution factor of enzyme solution.

3.3. Results and Discussion

3.3.1. Phylogenetic tree

A phylogenetic tree was generated where the amino acid sequence of the fructosyltransferase SucC from *Aspergillus niger* (GenBank: AHC54391) was aligned and compared to the other 30 reference enzymes with transfructosylating activities (Figure 7). This phylogenetic tree included 8 bacterial, 13 fungal, 2 protozoan and 8 plant strains. The genetic distances between these organisms were indicated where longer branches suggested greater genetic divergences. SucC was distinguished from plant, bacterial and protozoan species, and was homologous to a group of fungal species while the other fungal species were distinctly more homologous to plant species. Moreover, it was found that the encoding amino acid sequence of SucC (AHC54391) was closely homologous to four *Aspergillus* spp (CAB89083, CBS 115571 PYI19045, ADK46938, AOD74986), suggesting a common ancestor.

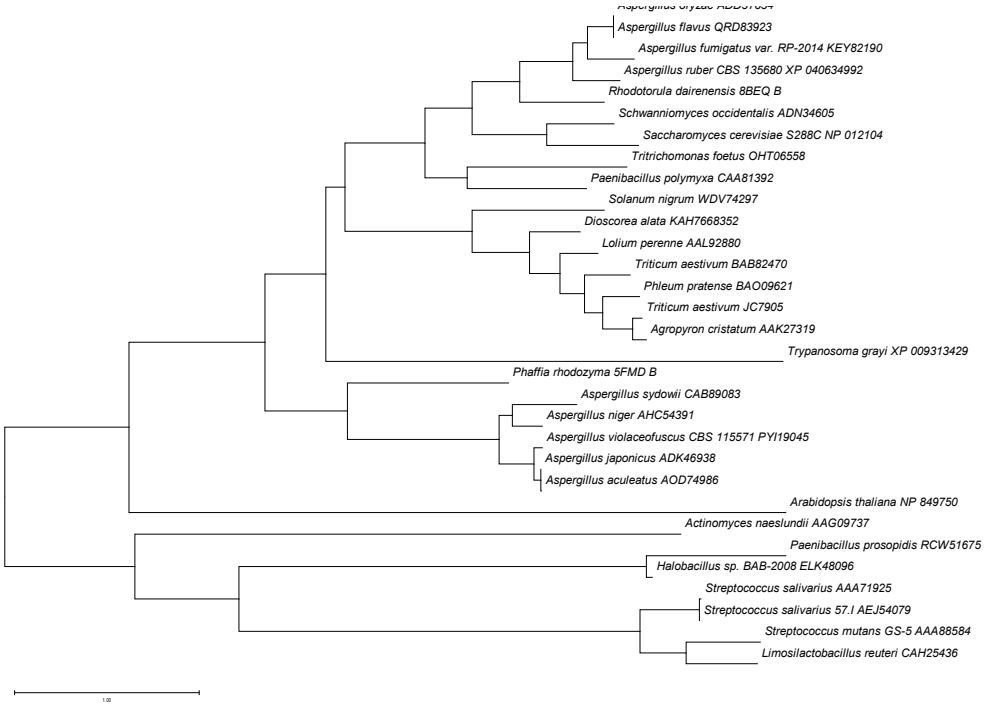

Figure 7: Bayesian phylogenetic tree showing the evolutionary relationship between 31 glycoside hydrolases of the GH32 family. All reference enzymes were named by their original microbial sources and GenBank accession numbers. SucC was most homologous to *Aspergillus sydowi* CAB89083.

3.3.2. Structural characteristics of *A. niger* fructosyltransferase SucC

The amino acid sequence alignment amongst fructosyltransferase SucC from *A. niger* and the other six FOS generating enzymes with identified catalytic residues was made and the catalytic residues in SucC were predicted and characterized (Figure 8A). Although the amino acid sequences from different sources of microbes were quite distinct to each other, the typical two Asp and one Glu in the highly conserved domains were 100% identical at the sites of D64, D194 and E271 in SucC where one Asp (D64) in Domain A was the catalytic nucleophile, the other Asp (D194) in Domain D was a transition stabilizer, and Glu (E271) in Domain E was the general acid/base catalyst. They together formed a catalytic triad that was responsible for catalysis (Figure 8A & 9B) in which the catalytic triad formed with two Asp and one Glu residue is a typical and unique characteristic among the GH32 and GH68 family of glycoside hydrolase (Manoochehri et al., 2020; Olarte-Avellaneda et al., 2018; Sainz-Polo et al., 2013).

SucC was further modeled by SWISS-MODELING with a crystal structure of fructofuranosidase (PDB ID: 5XH8) from *Aspergillus kawachii* (Nagaya et al., 2017) as template which was the most closely-related model to SucC (Figure 8B). The GMQE value of the generated SucC tertiary structure was 0.91 and the QMEANDisCo Global score was 0.88 ± 0.05, which indicated a reliable model being generated with high quality. According to the crystal structure created by Nagaya et al. (2017) and through homologous sequence alignment, the 3-D structure of SucC was composed of: an N-terminal small component (residues 25–59, component NS); a β-propeller domain (residues 60–440); an α-helical linker (residues 441–452); and a C-terminal β-sandwich domain (residues 453–628). Specifically, the 5-fold β-propeller catalytic domain was present with Asp-64, Asp-194, Glu-271 being the active sites forming a catalytic triad (Figure 8B). In summary, SucC from *A. niger* belonged to the GH32 family as it shared a common characteristic among GH32 enzymes (invertases, inulinases and fructosyltransferases) that contained an additional β-sandwich structure which was attached to the 5-fold β-propeller domain (Lammens et al., 2009). The identification of the acidic catalytic triad (D64, D194 and E271) in the three highly conserved motifs (Domain A, Domain D and Domain E) within the 5-fold β-propeller domain was a typical and unique characteristic among the Glycoside Hydrolase Family 32 (Alméciga-Díaz et al., 2011; Lammens et al., 2009; Pons et al., 2004; Yuan et al., 2006). The bioinformatic data showed that a reliable SucC 3-D structure was produced which served as the basis for further analysis.

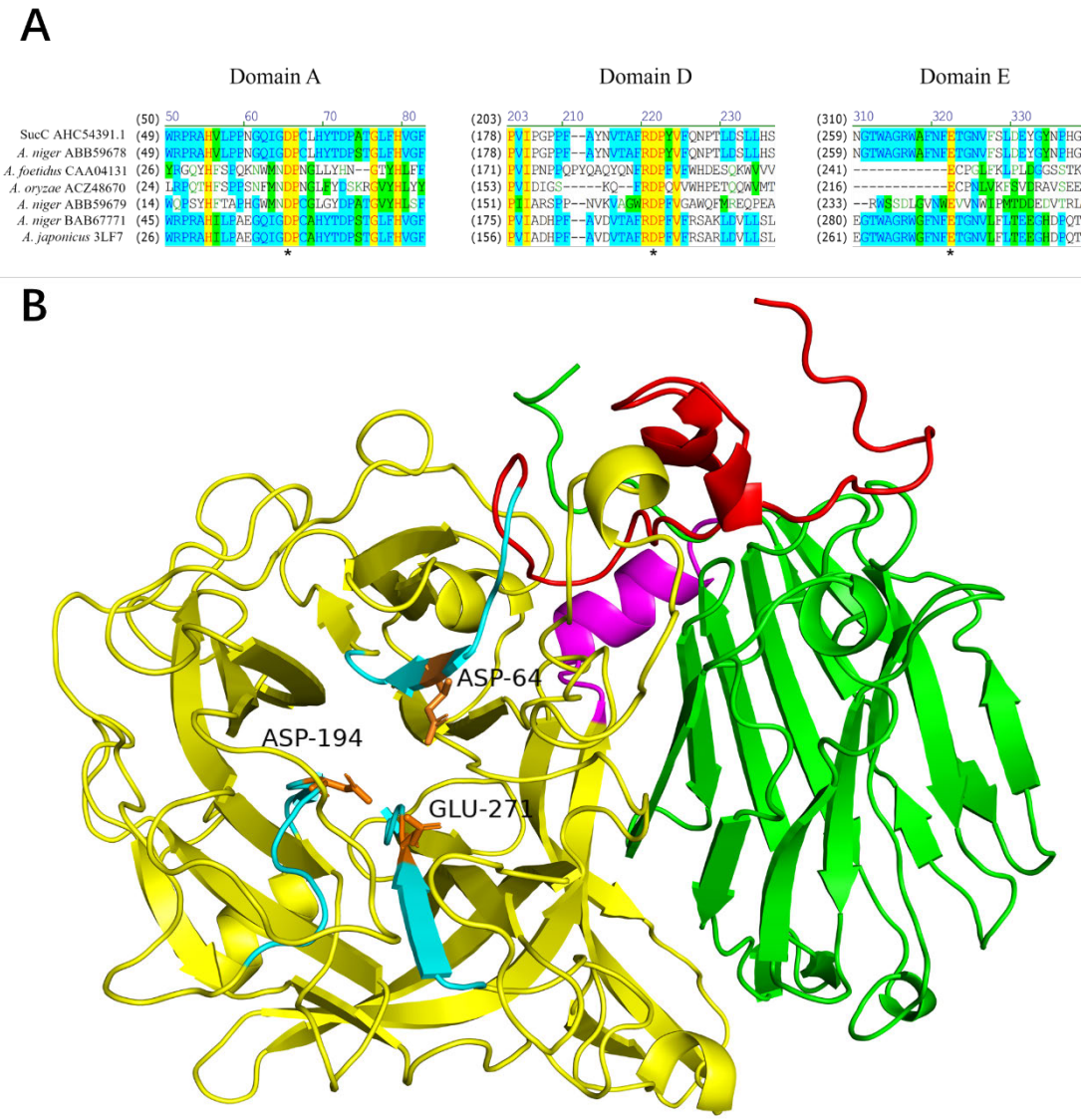

Figure 8: The structure analysis of SucC. A: Primary sequence alignment of SucC with the other FOS generating enzymes (Olarte-Avellaneda et al., 2018). The active site was predicted where D64 in domain A, D194 in domain D and E271 in domain E were identified as the catalytic triad (marked with asterisk). Yellow identifies the identical residues, green represents block of similar residues, cyan represents conserved residues and non-coloured residues are non-similar. The selected reference sequences included: a fructosyltransferase from *A. foetidus* (GenBank accession number: CAA04131); a fructosyltransferase from *A. oryzae* N74 (ACZ48670); an intracellular invertase from *A. niger* (ABB59679); an extracellular invertase from *A. niger* (ABB59678); a fructosyltransferase from *A. japonicus* (PDB ID: 3LF7); and a β-fructofuranidase from *A. japonicus* ATCC (BAB67771). B: Predicted tertiary structure of SucC. The SucC tertiary structure was predicted through PyMOL where the enzyme was modelled by SWISS-MODEL, with the fructofuranosidase, 5XH8 used as template. The components of all regions were determined and presented in different colours. Red represents a N-terminal small component (25–59), yellow represents the β-propeller domain (60–440), magenta represents the α-helical linker (residues

441–452), and green represents the C-terminal β-sandwich domain (453–628). Three highly conserved domains are coloured cyan with Asp-64, Asp-194, Glu-271 (orange) being the active sites, forming a catalytic triad.

3.3.3. *In silico* saturated mutagenesis of SucC

The wild-type SucC model docked with sucrose displayed a binding energy of -0.59 kcal/mol where V179 and W242 were interacting with the sucrose through hydrogen bonds. The binding of sucrose to SucC was restricted on the surface of the enzyme, close to the active sites. Among the 57 mutants (Table 11), 29 mutants had a different binding site between sucrose and enzyme comparing to the wild-type model and sucrose binding did not fit to a pocket structure, indicating the collapse of enzyme structure that led to the nonspecific interacting conditions, thus resulting in the loss of enzyme activity. For the remaining mutants, where binding of sucrose remained in the same pocket structure as observed in the surface models compared to the wild-type binding situation, three mutants had the most negative affinity energies to sucrose in each mutated active site, i.e., D64S (-1.68 kcal/mol), D194Q (-1.21 kcal/mol) and E271R (-1.19 kcal/mol). This represented better interacting conditions to sucrose than the wild-type interacting model (-0.59 kcal/mol), as the more negative the affinity energy is, the better the enzymatic reaction will theoretically take place. If D64S, D194Q and E271R were proven to have lost enzyme activity, it suggests that these three residues, D64, D194 and E271 were the active sites of SucC and are non-substitutable. The D64S, D194Q and E271R mutants were then constructed through molecular cloning processes to assess their enzyme activity.

Table 11: Summary of dockings and affinity energies of WT-SucC and its 57 mutants between sucrose

Protein model	Binding energy (kcal/mol)	Binding residues	Binding sites	Surface model
SucC (WT)	-0.59	Val^{179} Trp^{242}	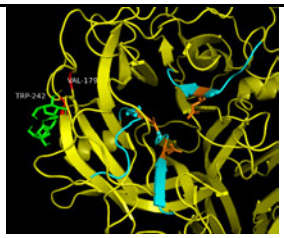	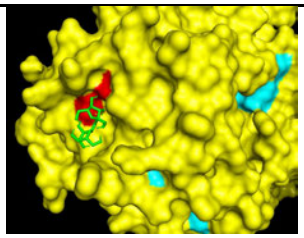
D64A	-0.31	Trp^{242}	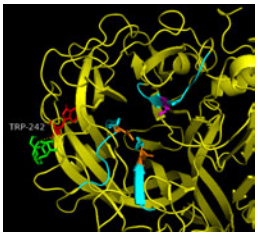	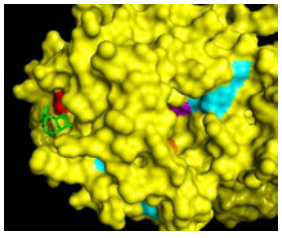

D64C	-0.22	Gly^{260} Gly^{264} Ala^{544}		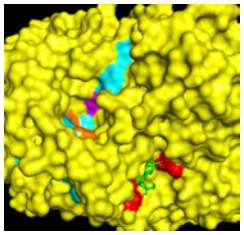
D64E	-0.24	Glu^{129} Asn^{131} Ser^{237} Asp^{238}		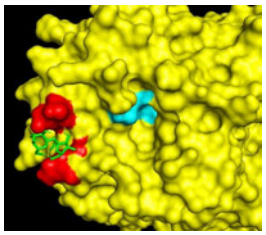
D64F	-0.46	Asn^{406} Ser^{424} Ser^{425}	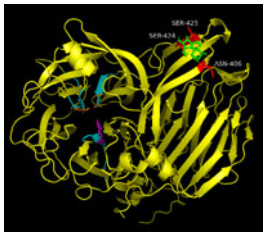	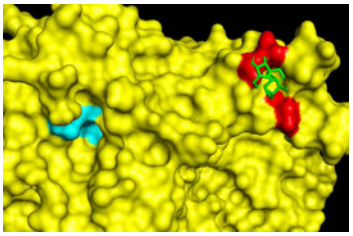
D64G	-0.75	Asp^{311} Trp^{337} Ala^{544}	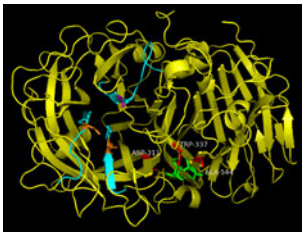	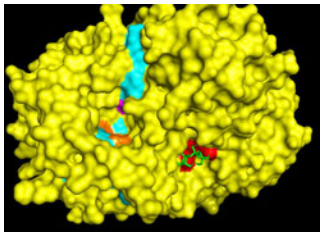
D64H	-1.33	Gly^{182} Tyr^{232} Trp^{242} Tyr^{244}	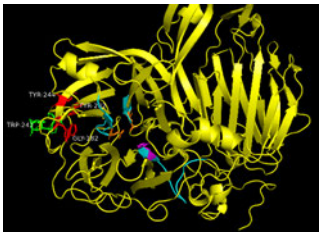	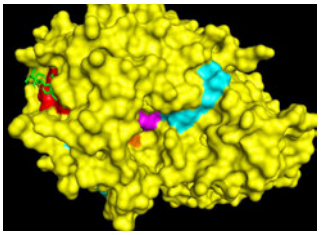
D64I	-1.09	Glu^{415} Val^{422}	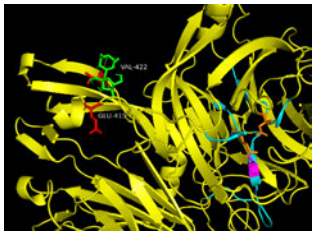	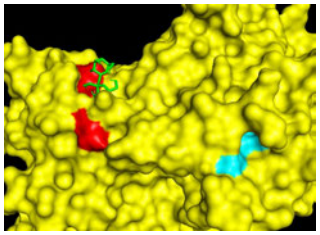
D64K	0.7	Asn^{579} Arg^{581}	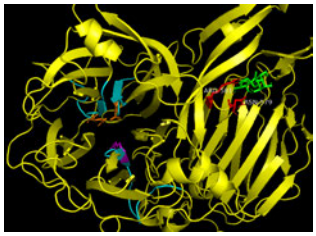	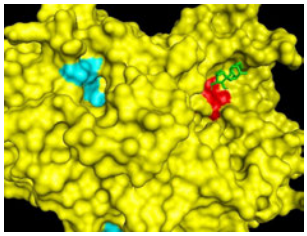

D64L	0.15	Asn^{170} Phe^{171} Lys^{173}	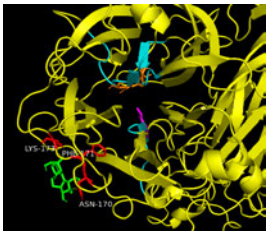	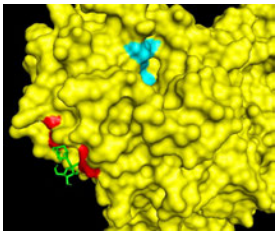
D64M	-0.68	Gly^{182} Trp^{242}		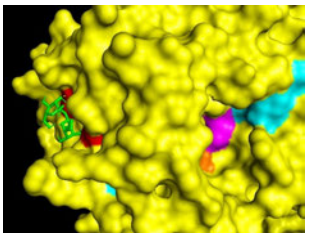
D64N	-0.89	Thr^{261} Trp^{337} Ala^{544}	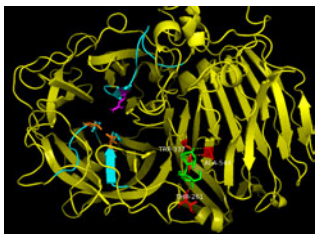	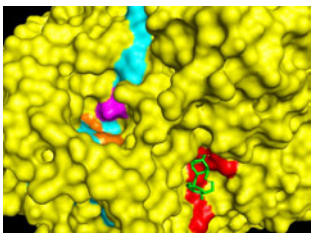
D64P	0.00	Gly^{417} Ala^{418} Trp^{420} Val^{422}	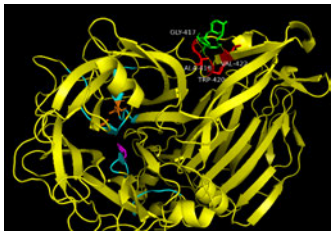	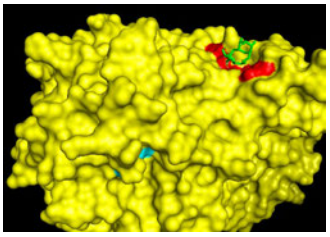
D64Q	-0.25	His^{250} Glu^{251} Thr^{256} Trp^{266}	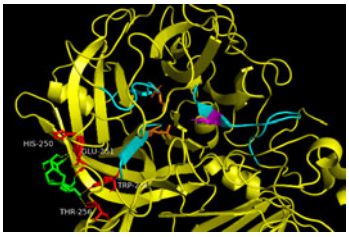	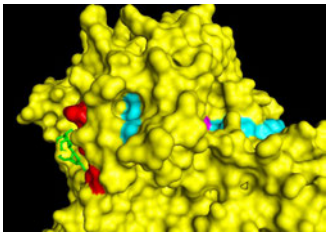
D64R	-0.33	Val^{110} Phe^{171} Lys^{173}	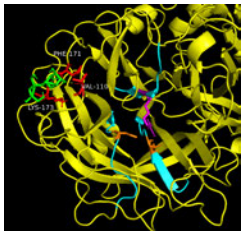	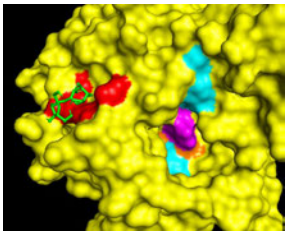
D64S	-1.68	Gly^{182} Tyr^{232} Trp^{242} Tyr^{244}	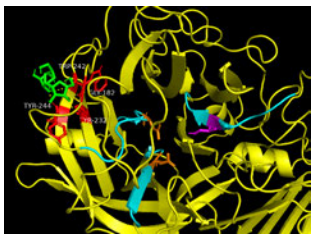	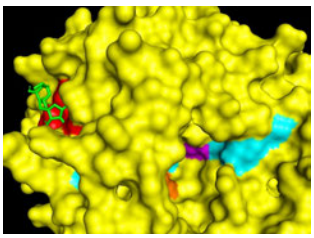

D64T	-0.39	Val[179] Trp[242]	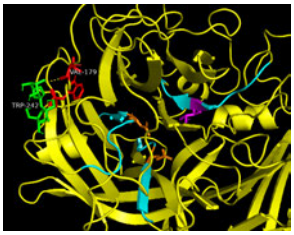	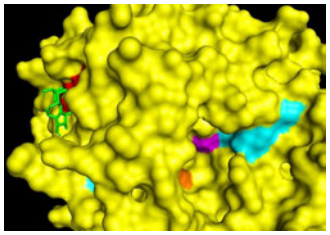
D64V	0.01	Glu[224] Thr[253]		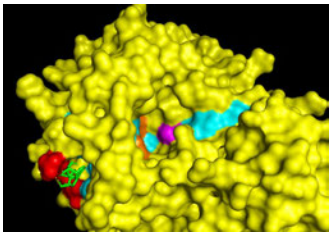
D64W	-0.78	Val[179] Gly[182] Trp[242]	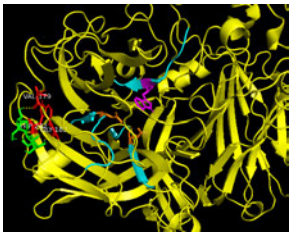	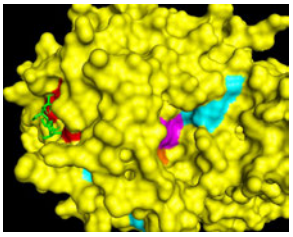
D64Y	-0.39	Gly[182] Trp[242]	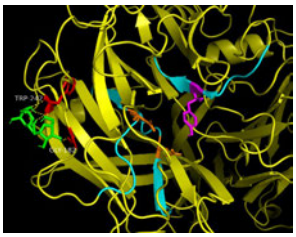	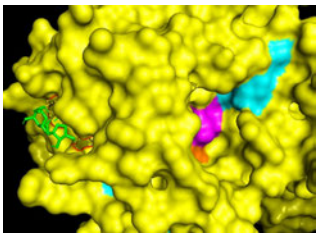
D194A	0.02	His[223] Glu[224] Val[302]	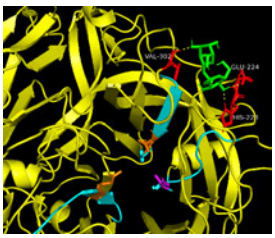	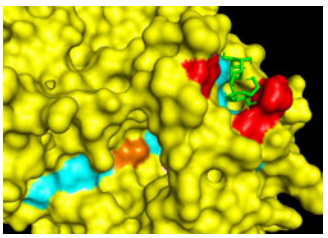
D194C	-0.24	Tyr[232] Trp[242] Tyr[244]	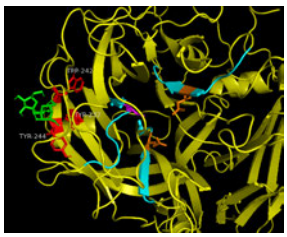	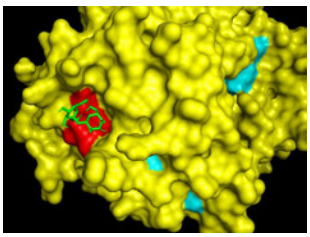
D194E	-0.3	Gly[182] Trp[242]	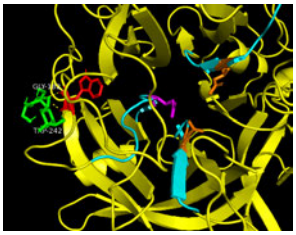	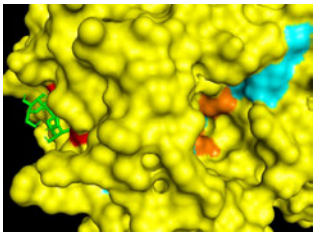

D194F	-0.77	Val^{179} Trp^{242}	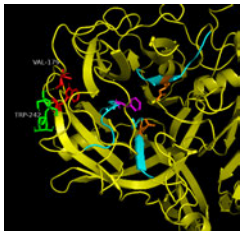	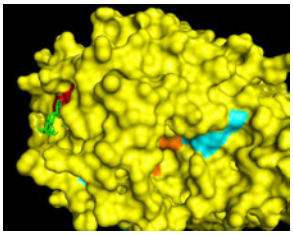
D194G	-0.31	Gly^{182} Phe^{185} Trp^{242}	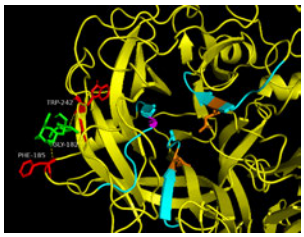	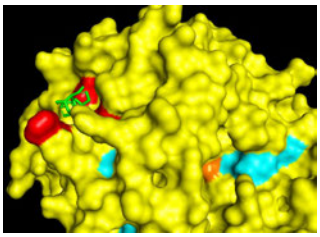
D194H	-0.31	Arg^{414} Gly^{417} Ala^{418} Trp^{420} Val^{422}	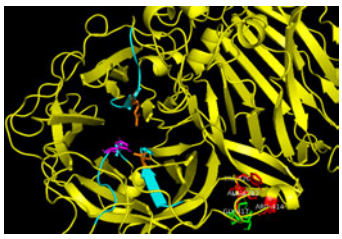	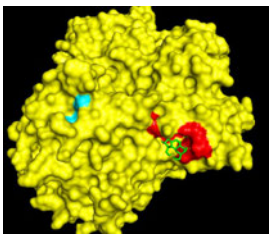
D194I	-0.85	Trp^{337} Ala^{542} Ala^{544}	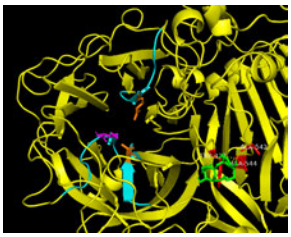	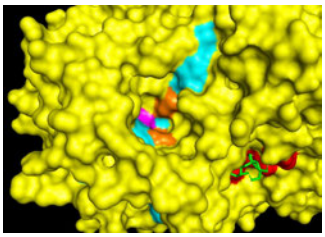
D194K	-0.35	Ser^{149} His^{223} Glu^{224}	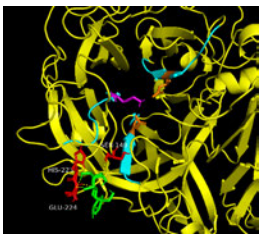	
D194L	-0.72	Gly^{182} Trp^{242}	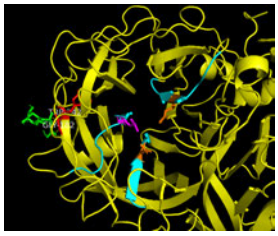	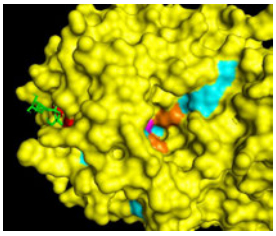
D194M	-0.22	Trp^{242}	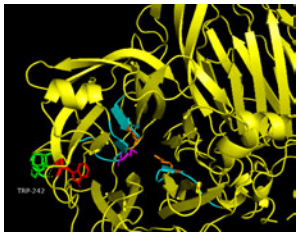	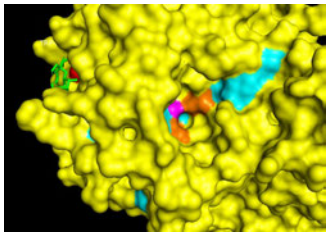

D194N	-0.43	Gly[182] Pro[183] Trp[242]	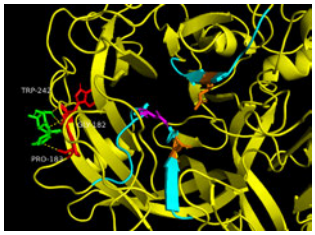	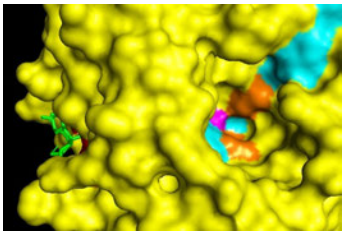
D194P	0.03	Gly[182] Phe[185]	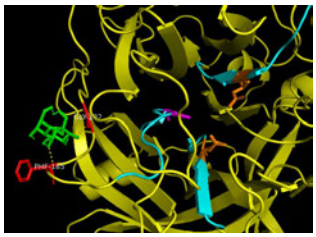	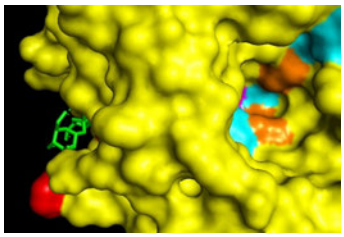
D194Q	-1.21	Gly[182] Trp[242] Tyr[244]	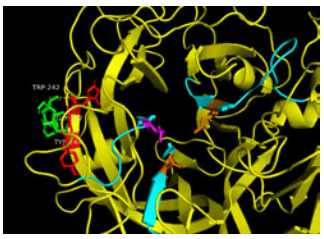	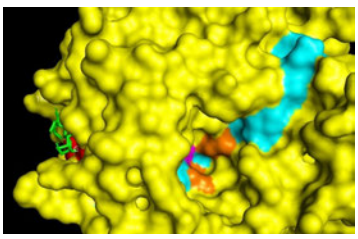
D194R	-0.44	Asn[406] Asp[426] Asp[555]		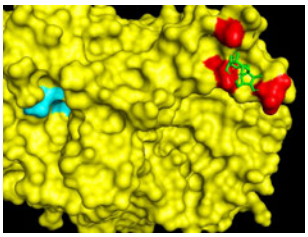
D194S	-0.75	Val[179] Gly[182] Trp[242]	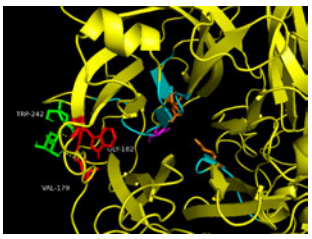	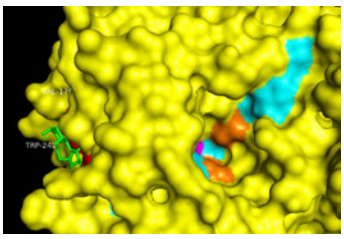
D194T	0.04	Asn[330] Val[422]	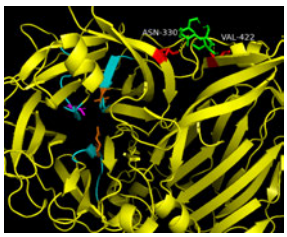	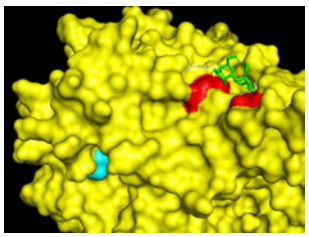
D194V	-0.75	Gly[182] Trp[242]	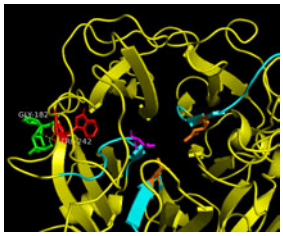	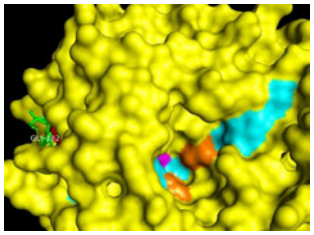

D194W	0.18	Phe[185] Trp[242]	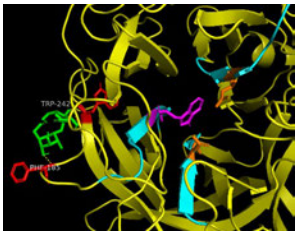	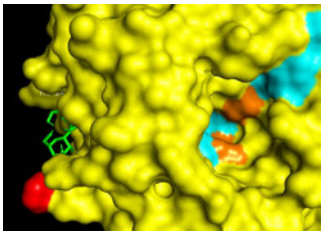
D194Y	-0.73	Val[27] Asp[29]	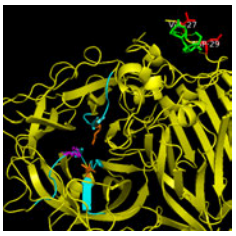	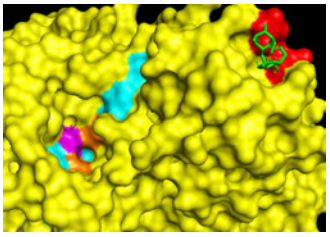
E271A	-0.36	Thr[261] Gly[264] Asp[311]	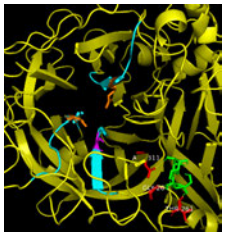	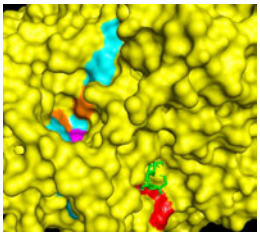
E271C	0.02	Ala[411] Arg[492] Asp[551] Gln[558]	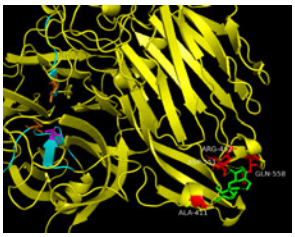	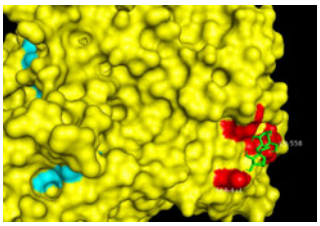
E271D	-0.22	Gly[182] Pro[183] Trp[242]	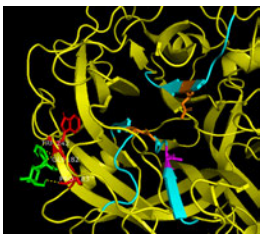	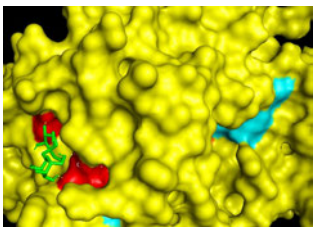
E271F	-0.39	Gly[287] Ile[289] Val[319]	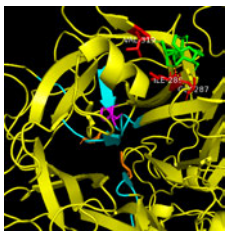	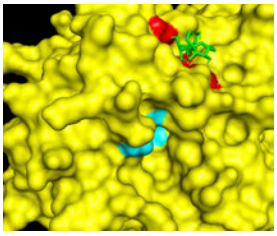
E271G	-0.69	Gly[182] Trp[242]	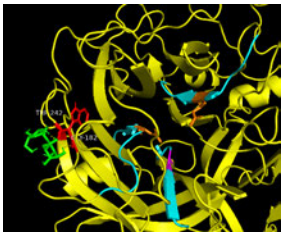	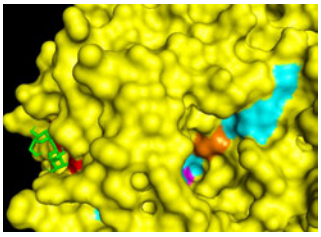

E271H	-1.1	Val[179] Gly[182] Trp[242]	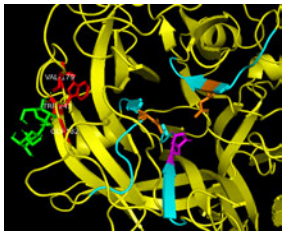	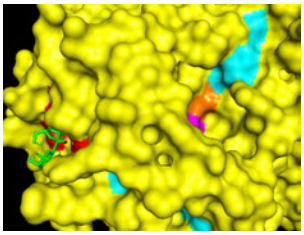
E271I	0.05	Asn[128] Asn[211] Asn[212] Trp[214] Gln[234]	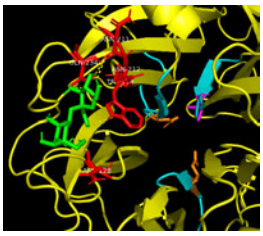	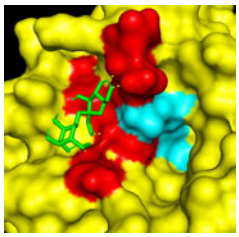
E271K	-0.62	Tyr[152] Tyr[187] Asn[188]		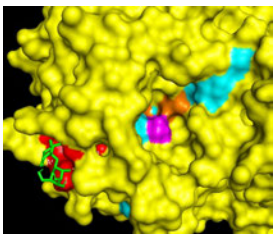
E271L	-0.71	Trp[242] Tyr[244]	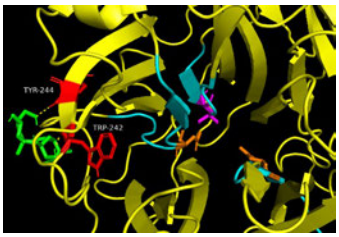	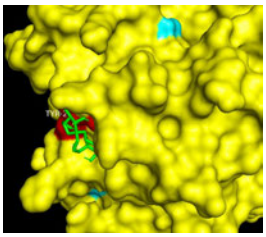
E271M	-1.01	Trp[242] Tyr[244]	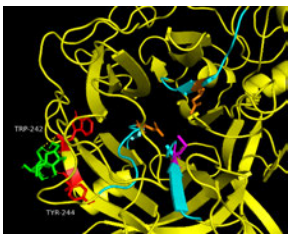	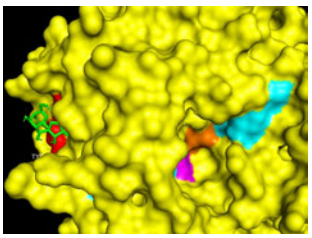
E271N	-0.74	Trp[242] Tyr[244]	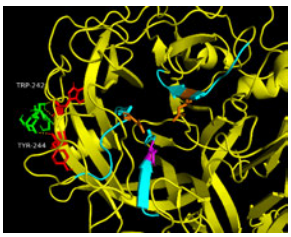	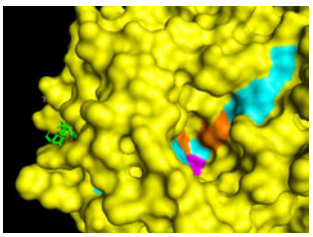
E271P	0.07	Asn[131]	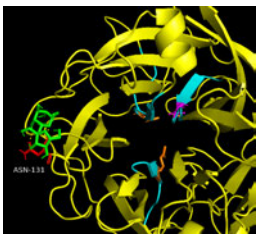	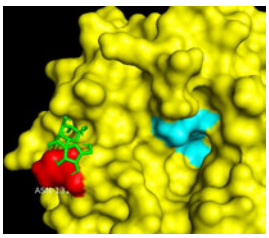

E271Q	-1.05	Ile^{146} Gln^{305} Thr^{307} Phe^{376}	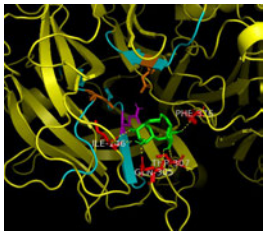	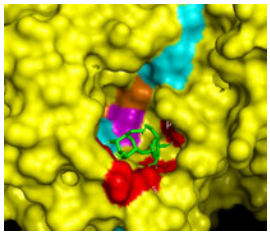
E271R	-1.19	Gly^{182} Trp^{242}	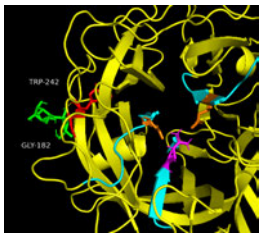	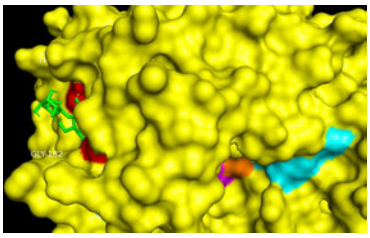
E271S	-0.45	Val^{179} Trp^{242}	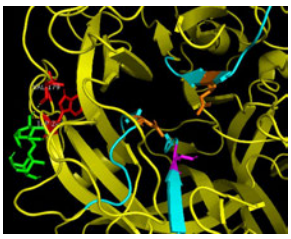	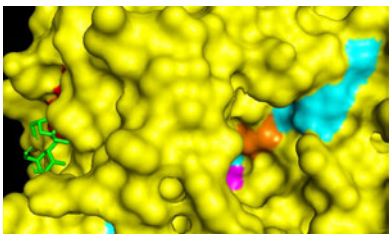
E271T	-0.07	Gly^{182} Trp^{242} Tyr^{244}	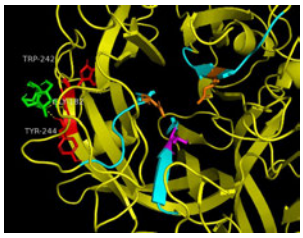	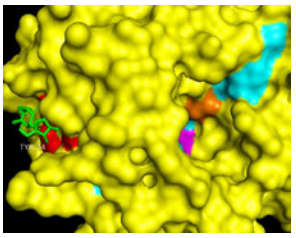
E271V	-0.71	Val^{27} Asp^{29}	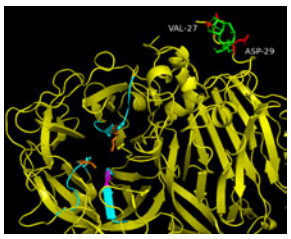	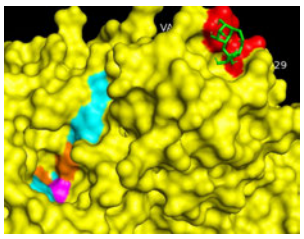
E271W	-0.38	Trp^{242}	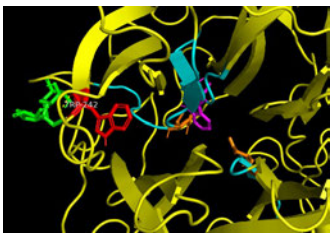	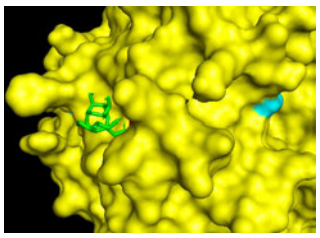
E271Y	0.09	Val^{27} Asp^{29}	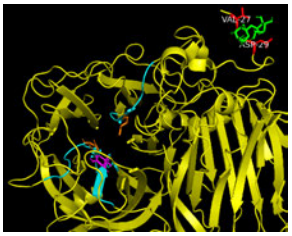	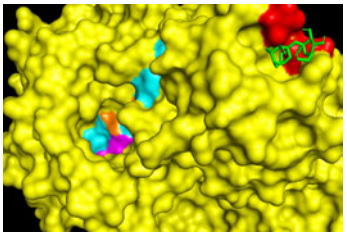

* The conserved motifs were labelled cyan, the catalytic triad was labelled orange, the mutated residues were labelled magenta and the interacting amino acids with sucrose were labelled red.

3.3.4. Isolation of genomic DNA from *P. pastoris*

The genomic DNA of *Pichia pastoris* GS115 is around 9.5 Mb and was isolated using Dr. GenTLE (from Yeast) High Recovery Kit. The majority of the isolated genomic DNA appeared as a diffuse band of high molecular weight above the 10 kb marker (Figure 9). A smear, typical of all genomic DNA isolation was seen below this diffuse band, representing numerous smaller DNA fragments. The presence of high molecular weight fragments was therefore verified and the genomic DNA was used for PCR amplification of the *sucC* gene.

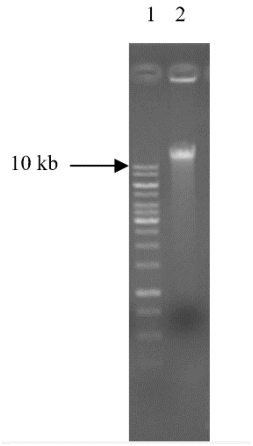

Figure 9: Genomic DNA isolated from *P. pastoris* through agarose gel (0.8%) electrophoresis at a constant 110 V for 30 minutes. In lane 2, the gDNA was spliced into fragments during isolation procedures but most fragments were larger than 10 kb. Lane 1 contains the molecular weight marker (GeneRuler 1 kb Plus DNA Ladder).

3.3.5. Amplification of up-stream and down-stream fragments of mutations

The up-stream and down-stream fragments of D64S, D194Q and E271R were amplified through the overlapping PCR technique (Hussain and Chong, 2016) with different sets of primers according to Table 1 and Table 2. The obtained PCR products (Figure 10) were of expected sizes summarized in Table 2, where D64S-up, D64S-down, D194Q-up, D194Q-down, E271R-up and E271R-down were of 200 bp, 1700 bp, 600 bp, 1300 bp, 800 bp, 1100 bp, respectively. The single bands obtained were bright and distinct, indicating a successful overlapping PCR was performed.

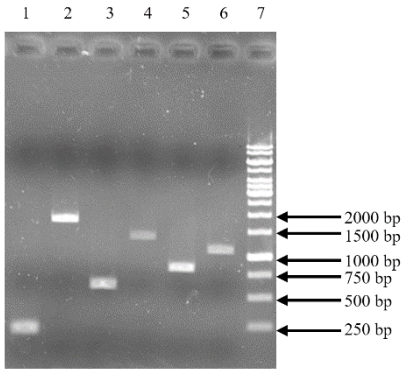

Figure 10: Up-stream and down-stream fragments after the overlapping PCR reaction. The agarose gel (1.0%) electrophoresis was done at a constant 110 V for 30 minutes. From left to right, the bands were D64S-up (lane 1), D64S-down (lane 2), D194Q-up (lane 3), D194Q-down (lane 4), E271R-up (lane 5) and E271R-down (lane 6) which are of 200 bp, 1700 bp, 600 bp, 1300 bp, 800 bp, 1100 bp, respectively. Lane 7 was the molecular weight marker (GeneRuler 1 kb Plus DNA Ladder).

3.3.6. Cross-over PCR of D64S, D194Q, E271R

The cross-over PCR products of D64S, D194Q and E271R were obtained after a second PCR reaction to combine the overlap PCR products. The obtained products were visualized by gel electrophoresis and were expected to be 1.9 kb. The gel map showed a clear visualization of the correctly-sized DNA bands, indicating a successful cross-over PCR products with high quality (Figure 11). Although there was little smearing in the gel image, the concentration of products was high enough to negate this impact in the following applications. No non-specific amplifications were observed, indicating a high purity of obtained DNA products. The successful amplification of full-length *sucC* genes after overlap and cross-over PCR suggested that the gene was correctly mutated and recombined. While this could have been confirmed by DNA sequencing, it was decided to proceed with expression of these mutated genes to determine their effects on the enzyme.

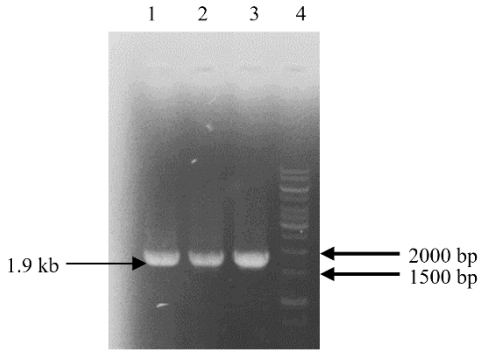

Figure 11: Combined mutated DNA fragments of D64S, D194Q and E271R after overlap and cross-over PCR and agarose gel (1.0%) electrophoresis at a constant 110 V for 30 minutes. From left to right, the bands are D64S (lane 1), D194Q (lane 2) and E271R (lane 3), respectively and all of these DNA fragments were 1.9 kb. The molecular weight marker (GeneRuler 1 kb Plus DNA Ladder) is present in lane 4.

3.3.7. pPIC9K isolation

The pPIC9K was isolated from *E. coli* JM109 through standard plasmid isolation technique (Birnboim and Doly, 1979). The map of pPIC9K was shown in Figure 6 and its size was verified to be 9.2 kb through linearization by *Bam*HI, followed by gel electrophoresis (Figure 12). A bright single band of linearized pPICK9K indicated its good quality for further applications.

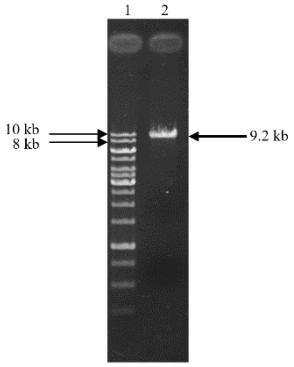

Figure 12: Linearized pPIC9K (9.2 kb) after agarose gel (1.0%) electrophoresis at a constant 110 V for 30 minutes. The plasmid was verified to be 9.2 kb in lane 2 while lane 1 was the molecular weight marker (GeneRuler 1 kb Plus DNA Ladder).

3.3.8. Ligation and heat-shock transformation into *E. coli* JM109

The mutated *sucC* genes (D64S, D194Q and E271R) were inserted into the cloning sites of *Sna*BI and *Avr*II in pPIC9K (Figure 13). The recombinant vector was 11225 bp

in size. The highlighted *Hin*dIII cloning sites (873, 1212, 1223, 3532, 3544, 7143) were used to screen for correct transformants with correct recombinant pPIC9K, in which will produce 350 bp, 2300 bp, 3600 bp and 5000 bp bands.

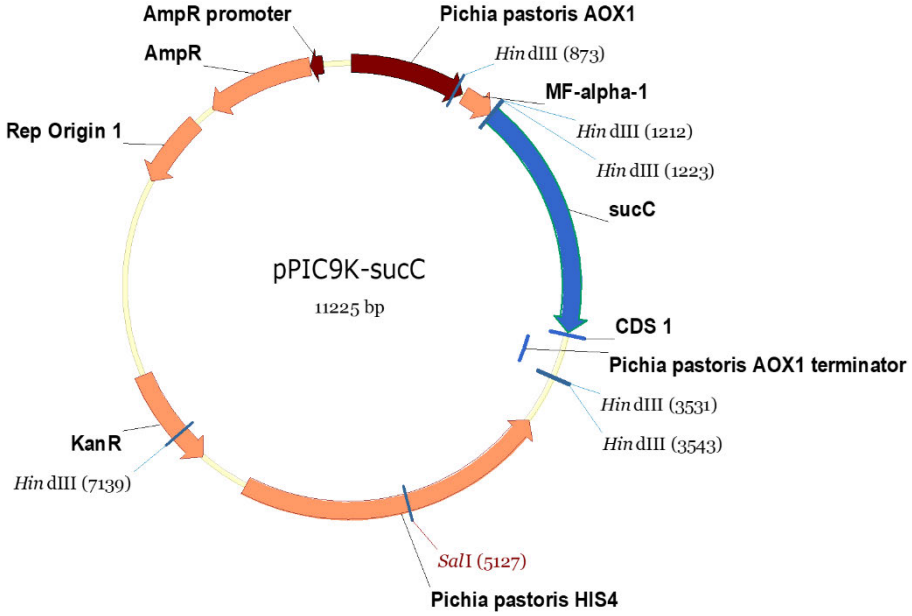

Figure 13: Map of pPIC9K with inserted *sucC* gene (purple) as an example for all 3 mutations (D64S, D194Q, E271R). The foreign DNA was inserted into the *Sna*BI and *Avr*II cloning sites upstream of the MF-alpha-1 promotor. Restriction sites for *Hin*dIII are indicated for the verification of recombinant vectors with desired sizes (350 bp, 2300 bp, 3600 bp and 5000 bp). The restriction sites of *Avr*II in pPIC9K were destroyed after ligation.

Spread plates (Figure 14) of JM109 transformants (D64S, D194Q and E271R) after heat-shock transformation were performed to detect if cloning was successful. The obtained transformants after 11 h incubation on LB-Amp plates at 37°C were round, creamy white and were of small sizes, which were the typical morphology of *E. coli* JM109 strains. They were closely packed, indicating a big density of cells. Colonies formed were sparse but were of good uniformity. Empirically, the good uniformity of obtained transformants usually implies that transformation occurred with high efficiency. 20 colonies from each plate were randomly selected and screened for transformants with correct inserts.

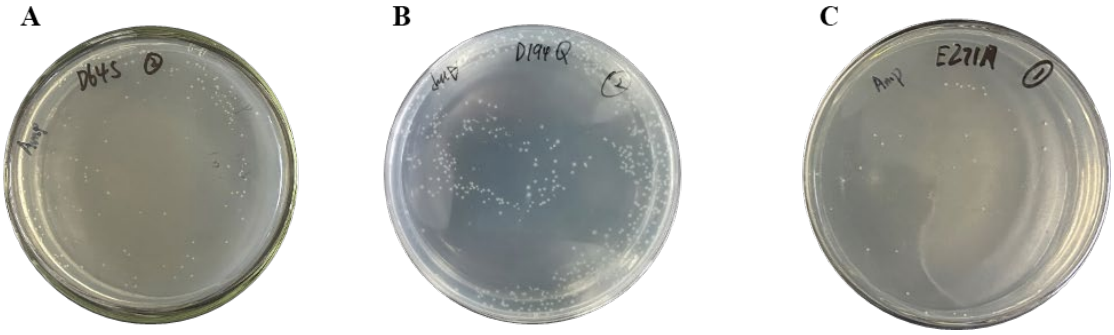

Figure 14: Spread plates of heat-shocked *E. coli* JM109 cells for each mutation, D64S (A), D194Q (B), E271R (C), on LB plates with ampicillin (100 µg/mL) for 11 hours. 20 obtained transformants for each mutation (D64S, D194Q, E271R) were subcultured and plasmid extraction technique was performed followed by *Hin*dIII digestion and agarose gel electrophoresis to screen for the correct recombinant pPIC9K.

3.3.9. Screening for correct JM109 transformants

20 obtained *E. coli* JM109 transformants were subcultured and the plasmid extraction technique was performed. Restriction enzyme digestion was then applied using *Hin*dIII to screen for correct transformants that contain the correct inserts. The original restriction sites used for cloning (*Sna*BI and *Avr*II) could not be used for this purpose, as they were destroyed during ligations. The digestion of recombinant pPIC9K by *Hin*dIII gave a specific 2300 bp band indicating the correct insert of mutated *sucC* gene as the 1900 bp insert sits in between two *Hin*dIII sites with a gap of 400 bp. As shown in Figure 15 below, the correct JM109 mutants that contained the desired inserts were obtained for D64S (A2), D194Q (B2) and E271R (C2), as they produced a specific 2300 bp band. The correct *E. coli* JM109 transformants containing the desired recombinant vectors (pPIC9K-D64S, pPIC9K-D194Q, pIC9K-E271R) were then subcultured and preserved for later use. The recombinant plasmids of pPIC9K-D64S, pPIC9K-D194Q and pIC9K-E271R were then isolated from their hosts and were transformed into *Pichia pastoris* GS115 for enzyme characterization.

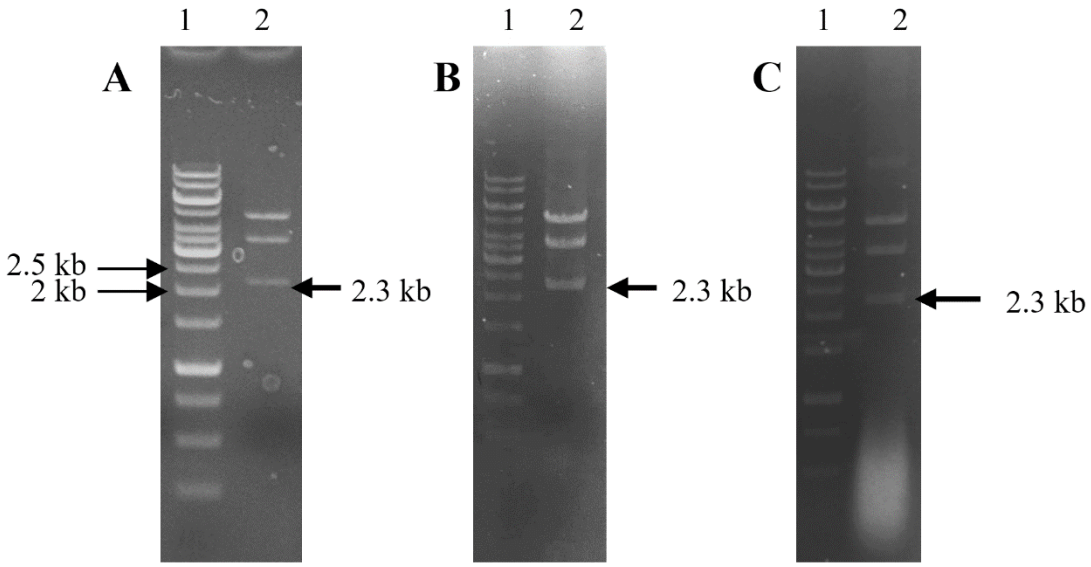

Figure 15: Recombinant pPIC9K digested by *Hin*dIII (pPIC9K-D64S (A), pPIC9K-D194Q (B) and pPIC9K-E271R (C)), in which obtained bands were of correct sizes (5000 bp, 3600 bp, 2300 bp, the 350 bp was too faint to be visualized). According to the map of recombinant pPIC9K (Figure 12), the obtained 2300 bp band indicated the successful insertion of foreign DNA fragment into pPIC9K.

3.3.10. Electrotransformation of recombinant pPIC9K into *P. pastoris* GS115

The pPIC9K-D64S, pPIC9K-D194Q and pIC9K-E271R recombinant plasmids were linearized by *Sal*I prior to transformed into *Pichia pastoris* GS115. The recombinant plasmids were electrotransformed into GS115 and survivors were cultivated on MD agar plates (Figure 16) to screen for histidine auxotrophs. Large, round, smooth, creamy white colonies with similar sizes to each other were formed on MD plates after 72 h incubation at 30°C. Although they were evenly spread and well separated, the number of colonies obtained were very small, indicating a low efficiency in electrotransformation. As a result, only 7 colonies for D64S, 4 colonies for D194Q and 2 colonies for E271R colonies were obtained. It was, however, expected that transformation of vectors that integrated into the chromosome occur at a low frequency than for autonomous vectors. Furthermore, the transformations were not emphasized as only one successful transformant was sufficient for further experiments.

The *Pichia* host strains GS115 have a mutation in the histidinol dehydrogenase gene (*his4*) which prevents them from synthesizing histidine (Balamurugan et al., 2007). The expression plasmid pPIC9K carries the *HIS4* gene that complements *his4* in the host, so transformants are selected for their ability to grow on histidine-deficient medium such as MD agar medium. GS115 will not grow on MD medium alone as it is His^-. The

transformants on MD plates were then subcultured onto YPD plates with 0.5 mg/mL geneticin (G418) at 30°C for 72 h to screen for high expression strains (Figure 17) where 7 colonies for D64S, 4 colonies for D194Q and 2 colonies for E271R colonies were obtained. The obtained colonies on YPD-geneticin plates were large, round and creamy white. However, one colony of D194Q and the colonies of E271R did not grow well compared to the other colonies on the plate. This may be caused by different expression levels of the transformed genes in different transformants where colonies expressing fewer copies of the geneticin resistance gene could have led to smaller sizes of the colonies.

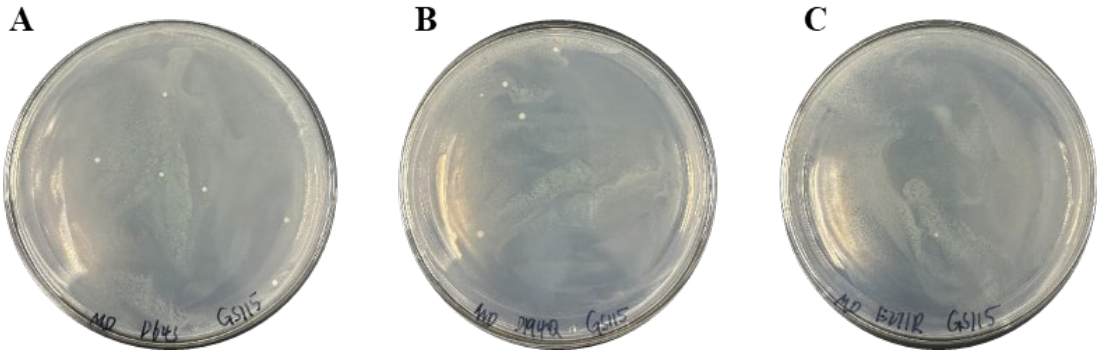

Figure 16: Transformants of *Pichia pastoris* GS115 after electroporation on MD plates to screen for *his*$^{+}$ auxotrophs. Plates were incubated at 30°C for 48 hours. 7 colonies for D64S, 5 colonies for D194Q and 2 colonies for E271R were obtained.

Figure 17: Screening for geneticin-resistant strains where the *his*$^{+}$ auxotrophs from MD plates were subcultured onto YPD agar plates with 0.5 mg/mL geneticin (G418) and incubated at 30°C for 72 hours.

3.3.11. Verification of correct GS115 transformants

The best growing colony of each mutant (D64S, D194Q, E271R) from GS115 transformants were subcultured and colony PCR was performed to verify if recombinant pPIC9K contained the correct insert or not. As a result, the insert of D64S, D194Q and E271R were of 1.9 kb (Figure 18), indicating the correct insert of recombinant pPIC9K into GS115 hosts. The GS115 mutants were then subcultured and preserved. In Summary, the correct GS115 recombinants containing desired inserts (D64S, D194Q, E271R) have been constructed through the whole processes of molecular cloning and will be used for expression.

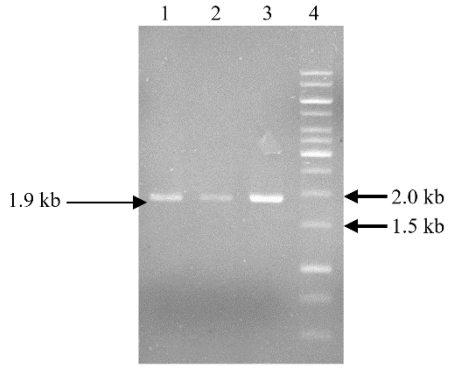

Figure 18: Confirmation of D64S (lane 1), D194Q (lane 2) and E271R (lane 3) mutants inserted in *P. pastoris* after colony PCR through agarose gel (1.0%) electrophoresis at a constant 110 V for 30 minutes. All of these three mutants were of 1.9 kb in size. Lane 4 is the molecular weight marker (GeneRuler 1 kb Plus DNA Ladder).

3.3.12. Determination of enzyme activity of SucC, D64S, D194Q, E271H

The SucC D64S, D194Q and E271R mutant enzymes were expressed through the method described in section 3.2.6. and the enzyme activities of D64S, D194Q and E271R were determined using the method described in section 3.2.7.2. The enzyme activity of SucC was measured at 232±18.5 U/mL while no enzyme activity was detected for all the three mutants (Table 12). Besides enzyme activity determination, it was also necessary to prove the mutated enzymes were expressed in order to prove the complete loss of enzyme activity was caused by mutation of the active sites rather than inappropriate molecular cloning processes that led to unsuccessful expression of inserts.

Table 12: Results of enzyme activity for SucC, D64S, D194Q and E271R

Enzyme	Enzyme activity (U/mL)
SucC	232±18.5
D64S	N.D
D194Q	N.D
E271R	N.D

3.3.13. Protein gel electrophoresis

The SDS-PAGE technique was used to verify if the enzymes were expressed or not. As shown in Figure 19, SucC, D64S, D194Q and E271R (lane 2-5, respectively) were visualized by protein gel electrophoresis as described in section 3.2.7.1. The four enzymes were of 70 kDa and D64S, D194Q and E271R were expressed comparing to the wild-type SucC. The complete loss of enzyme activity was therefore caused by the mutation of the catalytic triad, which confirmed that the catalytic triad can not be substituted, which validated the bioinformatically identified active sites. Numerous other bands were also detected as proteins from the culture supernatant were not purified. The band intensities were also different as the protein loaded on the gel was not uniform.

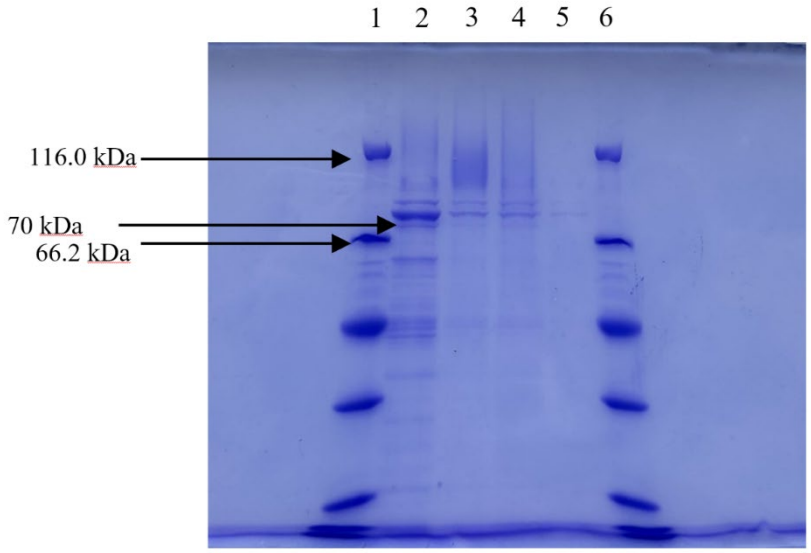

Figure 19: SDS-PAGE of SucC, D64S, D194Q and E271R (lane 2-5, respectively). SucC and its mutations were of 70 kDa. Lane 1 is the protein marker (Pierce Unstained Protein MW Marker)

CHAPTER 4: IMPROVEMENT OF SucC CATALYTIC PERFORMANCE BY A COMBINATION OF BIOINFORMATICS AND SITE-DIRECTED MUTAGENESIS

4.1. Introduction

Protein engineering is the process of synthesizing or modifying proteins with desired functions through the design and alteration of certain amino acid sequences in a protein (Dhanjal et al., 2019). Among these, rational design and directed evolution have been used as prominent strategies to mutate enzymes for specific characteristics (Kang et al., 2015). For rational design, it involves the deliberate substitution of those amnio acid sequences with comprehensive understanding in their structure-function relationships. While for directed evolution, it involves random mutagenesis and iterative cycles of mutation to select variants with desired traits for industrial applications. Both techniques have been studied with much understanding of protein folding and principles for mutation design (Woodley, 2022). Nowadays, site directed mutagenesis has been applied as the most-used method for improving an enzyme's characteristics. It introduces specific and precise mutations in the target amino acid sequence to attain desired characteristics with better understanding of the structure-function relationships in proteins (Hemsley et al., 1989). What's more, novel strategies for protein engineering have embraced bioinformatics tools, particularly in computational 3-D modelling and docking studies, have significantly facilitated the protein engineering processes in which not only have made the protein engineering easier, but also have offered valuable insights into the structure and function of engineered proteins (Rosenfeld et al., 2016).

Few successful proteins engineering have been carried out on fructosyltransferases where enzyme performance has been significantly. Two mutants, N52S and P232V, from a *Schwanniomyces occidentalis* β-fructofuranosidase constructed by Álvaro-Benito et al. (2010) had a 1.6-fold increase in the transferase activity. The mutant F254H from an *Aspergillus oryzae* fructosyltransferase constructed by Alvarado-Obando et al. (2022) had an approximately 1.3-fold increase in the transferase activity. Their efforts in engineering FOS-producing enzymes have shed light on the microenvironment of the enzyme active sites, revealing possible important amino acid residues interacting with substrates during catalysis. Understanding the role each amino acid residue plays during transfructosylation of sucrose is important in analysing the interactions between the catalytic residues of the enzyme and the substrate. Through homologous tertiary structure alignment, the mutants to be created for SucC in this

research were determined as C66S, G273V and L313H. Their impact on enzyme performance were comprehensively studied through *in silico* and *in vitro* approaches. These three mutants were subsequently constructed by site-directed mutagenesis and cloning into *P. pastoris* hosts for expressions and characterizations. The best mutant C66S was then studied by biochemical characterization, kinetic studies and assessment of its potential application for FOS production. The substitution of Cys-66 to Ser-66 in SucC was theoretically explained as the increase in hydrophilicity without significant changes in active site conformations, which favoured the transfructosylating efficiency by improved affinity to hydrophilic substrates. Therefore, in this chapter, a combination of docking studies and biochemical characterization of the C66S mutation revealed a possible strategy where the increase of hydrophilicity surrounding the active site may significantly enhance the transfructosylating activity and the artificial modification of hydrophilic micro-environment surrounding the active sites could be an alternative way to quickly evolve an enzyme's catalytic efficiency.

4.2. Materials and Methods

4.2.1. Selections of mutants

Previous research by Álvaro-Benito, et al (2010), identified two mutants N52S and P232V from a *Schwanniomyces occidentalis* β-fructofuranosidase (PDB ID: ADN34605.1) that had a 1.6-fold increase in the transferase activity. Another mutant F254H from an *Aspergillus oryzae* fructosyltransferase (PDB ID: GU145136.1) constructed by Alvarado-Obando et al. (2022) had an approximately 1.3-fold increase in the transferase activity. The tertiary structures of the above-mentioned enzymes were obtained from National Library of Medicine (https://www.ncbi.nlm.nih.gov/) via their unique PDB IDs. Tertiary structure alignment of SucC between these enzymes were carried out by PyMOL (Schrodinger, 2015) in which the homologous residues to N52, P232 and F254 in SucC were identified. The sequence alignment in PyMOL was followed by a structural superposition. Then several refinement cycles were performed to reject structural outliers.

4.2.2. Biosimulations on candidate mutants

The tertiary structures of candidate mutants were predicted by SWISS-MODELLING (Waterhouse et al., 2018) and the interactions between the mutants and sucrose were simulated by Autodock (Morris et al., 2009) and analysed by PyMOL (Schrodinger, 2015). All methods applied in this section were the same as described in section 3.2.4.

In Autodock, the substrate sucrose was restricted in the catalytic sites to specifically investigate its interactions with the catalytic triad, revealing the impact of mutation on the active sites.

4.2.3. Substrate access tunnel analysis

In order to further analyze the impact of mutations on the active site conformation, the access tunnels in SucC and mutants were simulated by the Caver 3.0.3 Plugin in PyMOL (Chovancova et al., 2012). The tertiary structures of SucC and its mutants were predicted and compared for protein structure analysis. The starting point was set in the centre of the catalytic triad in SucC. The minimum probe radius was set to 0.7 Å, and the shell depth and shell radius were set to 4 Å and 5 Å, respectively. The clustering threshold was set to 3.5 Å, the maximum distance was set to 3 Å and the desired radius was set to 5 Å.

4.2.4. Construction of mutants

4.2.4.1. Isolation of genomic DNA from *P. pastoris*

As described in section 3.2.5.1, genomic DNA from a recombinant *P. pastoris* containing the *sucC* gene was used as the source of template DNA. The *sucC* gene is 1941 bp in size. The Dr. GenTLE (from Yeast) High Recovery Kit was used to isolate the genomic DNA. The isolated genomic DNA was then used for the PCR amplification of *sucC* mutant genes.

4.2.4.2. Amplification of up-stream and down-stream mutated gene fragments

The SucC mutants were created by site-directed mutagenesis using the over-lapping PCR technique (Hussain and Chong, 2016) which was same as described in section 3.2.5.2. Primers designed for amplifying up-stream and down-stream fragments of C66S, G273V and L313H are listed below in Table 13. The expected PCR products are listed in Table 14. The constituents of PCR reaction mixtures are listed in Table 3.

Table 13: Primers used for the amplification of DNA fragments for site-directed mutagenesis of *sucC*

Primers	Sequence (5′ to 3′)*
SucC-F	GTAAAGCTTCAAACGGCTTCCG
SucC-R	TGCTCTAGATTAAGACTGACGATCCGGCC
C66S-F	CAGATCGGTGACCCC***TCT***CTGCATTACACCGATCCT
D66S-R	CAG***AGA***GGGGTCACCGATCTG
G273V-F	GCCTTCAACTTCGAGACG***GTT***AACGTCTTCAGTCTCGACG
G273V-R	GTT***AAC***CGTCTCGAAGTTGAAGGC
L313H-F	CAGCATCCACGACATG***CAT***TGGGTGTCCGGTACA
L313H-R	CCA***ATG***CATGTCGTGGATGCT

* The underlined sequence represents the *Xba*I recognized restriction site. The bold and italicized sequences symbolize the mutated regions.

Table 14: Amplification products for SucC mutants

Primers	Product	Expected size (bp)
SucC-F, C66S-R	D64S-up	200
SucC-R, C66S-F	D64S-down	1700
SucC-F, G273V-R	D194Q-up	800
SucC-R, G273V-F	D194Q-down	1100
SucC-F, L313H-R	E271R-up	940
SucC-R, L313H-F	E271R-down	960

4.2.4.3. Cross-over PCR for construction of C66S, G273V and L313H mutants

The overlapping PCR products generated from the previous step were subjected to the same processes as described in section 3.2.5.3. PCR procedure programs were same as described above for hot-start PCR.

4.2.4.4. Preparation of pPIC9K, ligation and transformation

The pPIC9K plasmid was isolated from its host, *E. coli* JM109, which was obtained from the Laboratory of Bio-catalysis and Biotransformation at the Tianjin University of Science and Technology using the modified alkaline lysis with SDS method (Bimboim and Doly, 1979). The plasmid isolation procedure was described in section 3.2.5.4. The techniques applied for digestion of pPIC9K and obtained PCR fragments prior to ligation, and the ligation conditions were described in section 3.2.5.5. *E. coli*

competent cells were prepared freshly before use. The heat-shock transformation procedures were described in section 3.2.5.6. After heat-shock transformation, spread plates were then incubated at 37℃ for overnight and the growth of colonies indicated the obtained colonies were applied for further screening processes.

4.2.4.5. Screening for correct JM109 transformants

The correct *E. coli* JM109 transformants were screened through plasmid extraction and restriction enzyme digestion techniques as described in section 3.2.5.7. The extracted plasmids were digested by *Hin*dIII in which four fragments were generated which are 350 bp, 2300 bp, 3600 bp and 5000 bp in size to verify if the transformants contained the insertion or not (Figure 13). Transformants with correct insertions have a specific 2300 bp band containing the 1900 bp *sucC* gene while the missing of this specific 2300 bp indicated the lack of insertion of *sucC* gene. The culture containing the correct insert was subcultured until obtaining homogenous single colonies on LB plates with ampicillin and were preserved in a 15% (v/v) glycerol solution at -70℃.

4.2.4.6. Electrotransformation of recombinant pPIC9K into *P. pastoris* GS115

The *E. coli* JM109 transformants containing the mutated *sucC* genes were recovered on LB plates containing ampicillin following the methods described in section 3.2.5.8. The plasmid extraction technique was then performed as described in 3.2.5.4. to obtain recombinant plasmids of pPIC9K-*sucC*, pPIC9K-C66S, pPIC9K-G273V and pPIC9K-L313H. These recombinant plasmids were linearized with *Sal*I and electro-transformed into *Pichia pastoris* GS115 chromosome via homologous recombination. Following the electrotransformation methods described in section 3.2.5.8., the GS115 recombinants were selected on YPD plates containing 0.5 mg/mL geneticin (G418). To get strains with potentially higher expression of the inserted *sucC* gene, an additional antibiotic selection on 2.0 mg/mL geneticin (G418) was performed. The best-growing colony for each transformation was picked and subcultured and finally preserved at -70℃ in 15% (v/v) glycerol solution.

4.2.4.7. Verification of correct GS115 transformants

The obtained recombinants were verified by colony PCR technique, following the colony PCR technique decribed in section 3.2.5.9. The obtained PCR products were

visualized by 1% agarose gel electrophoresis where the presence of a 1900 bp band confirmed the correct insert of *sucC* into the GS115 chromosome.

4.2.5. Expression of mutated enzymes

The *P. pastoris* GS115 strains containing *sucC*, *sucC*-C66S, *sucC*-G273V and *sucC*-L313H were grown on YPD agar plates containing 2 mg/mL geneticin (G418) at 30℃ for 72 hours. These enzymes were expressed through fermentation as described in section 3.2.6. The collected supernatant contained the expressed SucC and was used as the crude enzyme for further applications.

4.2.6. Enzyme purification by AKTA

The recovered enzyme-containing supernatant was desalted using a PD-10 Desalting Column (GE Inc.) and purified in an AKTA 100 purification system (Cytiva). A Superdex 200 Increase 10/300 GL (Cytiva) gel filtration column was used for size exclusion chromatography purification of proteins according to the manufacturer's guideline. The column as well as the purification system was equilibrated by the equilibration buffer (10 mM phosphate, 150 mM NaCl, pH 7.4). After equilibration, 500 μL sample was loaded. The elute rate was set to 1 mL/min. All protein fractions were collected in 300 μL volumes. The collected fractions were analysed by detecting their enzyme activity enzyme assays. The SDS-PAGE technique (Laemmli, 1970) was used to verify the purity of purified SucC.

4.2.7. Specific activity determination

The activity of purified enzymes was determined by the enzyme activity assay described in section 3.2.7.2. Their concentrations were then determined by the Bradford assay (Bradford, 1976). A standard curve was generated prior to the measurement of protein samples as the protein concentration is proportional to the absorbance of the reaction at 595 nm. The standard BSA solution from Solarbio (5 mg/mL) was diluted to 0.1 mg/mL, the working solution was prepared to dissolve 100 mg Coomassie Brilliant Blue G-250 dye powder in 50 mL 90% ethanol, then 25 mL of 85% (m/v) phosphoric acid was added into the solution. The G-250 solution was finally diluted into a final volume of 1 L with deionized water. A series of reactions were carried out with different concentrations of BSA (from 0.0017 mg/mL to 0.0133 mg/mL) where they were incubated with the working solution for 5 minutes to let the colour develop

and their absorbances at 595 nm were measured and plotted. The sample proteins which were collected from AKTA purification were then reacted with the Coomassie working solution for 5 min to determine their concentrations. Their absorbance at 595 nm were measured and the concentrations were determined according to the generated standard curve. The specific activity was subsequently determined as the ratio of enzyme activity to the protein concentration.

4.2.8. SDS-PAGE for analysis of mutated enzymes

The SDS-PAGE technique was used to examine the expression of enzymes as described in section 3.2.7.1. A 5% stacking gel and a 12% separation gel was used and their preparation recipes were listed in Table 9 and Table 10. The crude enzyme obtained from 4.2.5 was purified and then subjected for SDS-PAGE.

4.2.9. Impact of temperature and pH on enzyme activity and stability

The temperature and pH optima were determined using the standard enzyme activity assay at different temperatures (30-80ºC) and constant pH (5.5), and at different pH (4-9) at constant temperature (50ºC). The buffers (100 mM) used were: citric acid buffer (pH 4.0-6.0), phosphate buffer (pH 6.0-8.0) and Tris-HCl (pH 8.0-9.0). The thermostability and pH stability were assayed by incubating SucC and its mutants at different temperatures (4-80ºC) and pH (4-9) for 1 h, respectively. The remaining activities of these incubated enzymes were then determined by the standard enzyme activity assay.

4.2.10. Determination of kinetic parameters

The pure enzymes obtained from 4.2.6 were used to determine their K_m, V_{max} and k_{cat} values. A series of sucrose solutions were prepared with different concentrations (50, 80, 110, 150, 200, 250 mM). The reaction mixtures were composed of 900 µL substrates and 100 µL enzyme solution where the amount of enzyme added into the reaction mixtures was adjusted to a final activity of 5 U/mL in the 1 mL reaction mixture by dilutions prior to the reactions for determination of enzyme kinetics. The reactions were carried out for 5 min at 50℃ and pH 5.5 and the reactions were terminated by incubation at 80℃ for 10 mins. The generated glucose was then detected by a biosensor. Origin 9 (OriginLab) software was used to analyze the collected data and enzyme kinetics were then determined through its Nonlinear Fitting mode that fits the

Michaelis-Menten function. The values of K_m, V_{max} and k_{cat} for enzymes being analyzed were then determined.

4.2.11. FOS generation and sugar profile analysis by HPLC

Enzyme reactions were performed for SucC and its mutants in a 100 mL reaction mixture with 400 g/L sucrose as the substrate. The quantity of enzymes added into the different reactions were standardized to 9 U per 1 g sucrose and the reactions were optimized at 50℃ and pH 5.5 in a water bath. Six hours reactions were performed where 1 mL of the reaction mixture collected every hour and the reaction was terminated by incubating at 80℃ for 10 min. The collected reaction samples were diluted 5 times in distilled water, followed by precipitation with an equal volume of 100% ethanol at 4℃ for 2 h to remove the proteins. The samples were then centrifuged at 12000 × g for 5 min and then diluted 5 times with distilled H_2O. The FOS samples were eventually diluted 50 times and filtered with 0.22 μm sterile membrane filters. The FOS samples were then prepared for HPLC analysis.

An Agilent 1200 High Performance Liquid Chromatography (Agilent) was used for HPLC analysis. The Alltech ELSD 2000 (Grace Davison Discovery Sciences) was used as the detector. A Prevail Carbohydrate ES HPLC column (5.0 μm, 250×4.6 mm) was installed into the HPLC instrument and equilibrated with 65% (v/v) acetonitrile, which was used as the mobile phase. The speed flow rate was set to 1 mL/min. The wavelength to detect the sugars was set to 210 nm. The column temperature was set to 35℃ and the HPLC system was equilibrated until the baseline became stabilized. 20 μL of FOS samples as well as 4.5 g/L glucose standard and 10 g/L FOS standard were injected into the system and the samples were run for 20 min. The chromatogram was analyzed and the concentrations of different FOS components were calculated based on peak areas from a calibration curve generated from the glucose and FOS standard solution. After analysis, the column was washed with 20% (v/v) methanol with a flow rate of 2 mL/min to remove any remaining sample residues.

4.3. Results and Discussion

4.3.1. Determination of homologous residues in SucC

The homologous residues of N52 and P232 from a *Schwanniomyces occidentalis* β-fructofuranosidase (PDB ID: ADN34605.1) and F254 from an *Aspergillus oryzae* fructosyltransferase (PDB ID: GU145136.1) to SucC were determined as C66, G273 and L313 (Figure 20). Although these three residues (C66, G273 and L313) were not same to the aligned residues (N52, P232 and F254), the alignment of tertiary structure guarantees the accurate determination of the corresponding positions of these residues in the conformational structure. The homologous residues in SucC were then determined as C66, G273 and L313. The potential mutants C66S, G273V and L313H were subsequently analyzed through molecular docking to assess their impact on interactions with sucrose.

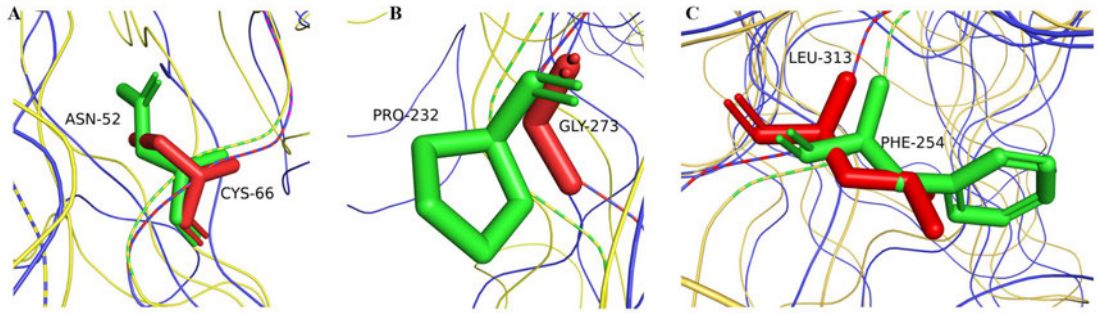

Figure 20: Partial tertiary structure alignment of a β-fructofuranosidase (PDB ID: ADN34605.1) (A and B) and a fructosyltransferase (PDB ID: GU145136.1) (C) to SucC. The residues in SucC were coloured red while the aligned residues were coloured green. It was determined that C66, G273 and L313 in SucC were homologous to the aligned N52, P232 and F254.

4.3.2. Docking analysis on candidate mutants

Three candidate mutants (C66S, G273V and L 313H) were studied for their interactions to sucrose restricted in their active sites (Figure 21). Compared with the wild type SucC interacting with sucrose having an affinity energy of -3.65 kcal/mol (Figure 21A), C66S (Figure 21B) exhibited the best affinity to sucrose (-4.14 kcal/mol) while the affinity energies were -2.79 kcal/mol for G273V (Figure 21C) and -3.37 kcal/mol for L313H (Figure 21D). These results suggested potential changes in enzyme activity caused by these mutations, where C66S may improve its enzyme activity due to its stronger affinity to sucrose than the wild type SucC. But the activities for G273V and L313H may decrease due to the weaker affinity to sucrose than that of wild type SucC. Moreover, besides the five residues (Asp-64, Asp-122, Arg-193, Asp-194, Glu-271)

that directly interact with sucrose, two additional residues (Glu-296, His-310) were predicted to directly interact with sucrose in the C66S mutant. This suggests that the mutation from Cys to Ser positively modified the chemical microenvironment surrounding the active site which resulted in a stronger affinity to sucrose. The mutation from Cys to Ser may cause a more hydrophilic environment and does not greatly change the conformation due to their similar side chains where the thiol group (-SH) in the side chain of Cys was replaced by the hydroxyl group (-OH). The more hydrophilic environment may favour the interactions between sucrose and the active site residues due to the presence of multiple hydroxyl groups in sucrose that favours hydrophilic environments (Chen et al., 2022; Yang et al., 2022). Therefore, C66S was predicted to be a promising candidate mutant that may have great improvements in the enzyme performance.

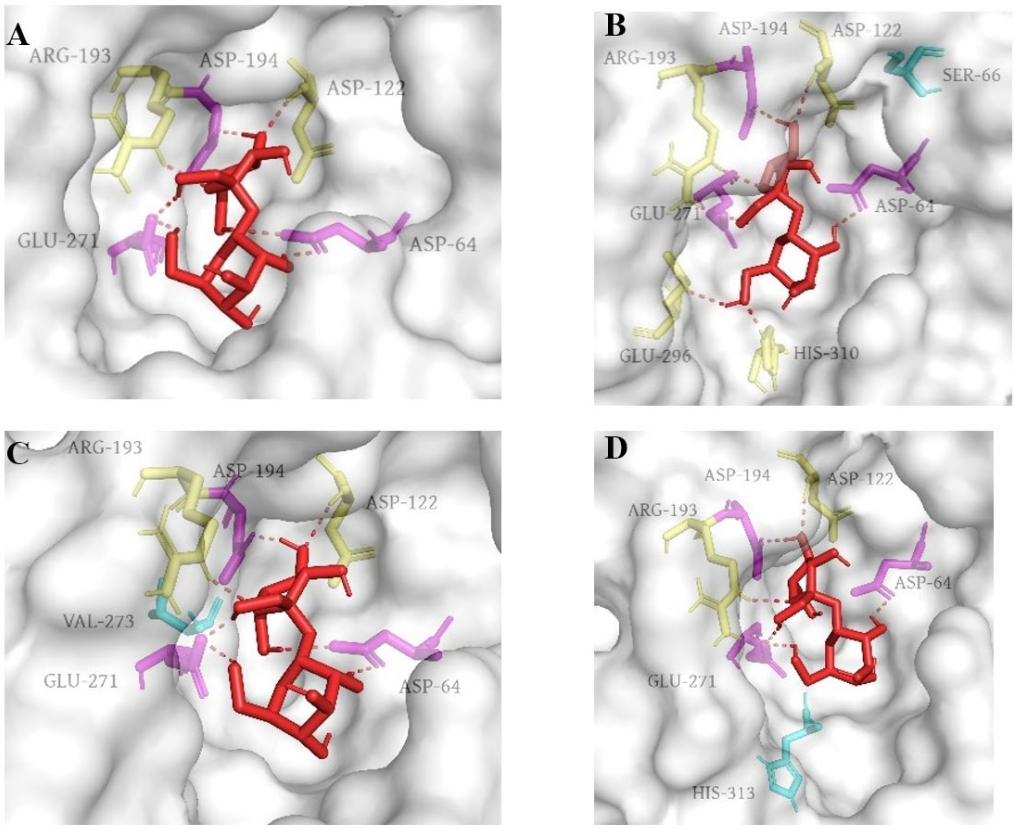

Figure 21: Binding models of sucrose with wild type SucC (A), SucC-C66S (B), SucC-G273V (C) and SucC-L313H (D) with affinity energies of -3.65, -4.14, -2.79 and -3.37 kcal/mol, respectively. Sucrose is coloured red, the catalytic triad (Asp-64. Asp-194 and Glu-271) were coloured magenta and were involved in interactions with sucrose for all models. The other amino acid residues interacting with sucrose (Asp-122, Arg-193) were coloured yellow while two additional amino acid residues in SucC-C66S (B) specifically interacting with sucrose (Glu-296, His-310) were coloured yellow and were not found in other models. The mutated residue for each mutant was coloured cyan.

4.3.3. Saturated mutagenesis of Cys-66

Cys-66 was targeted and its simulated saturated mutagenesis analysis was performed. As summarized in Table 15, the predicted enzymes with substitutions of Cys into the other 19 amino acid residues showed that 15 of the 19 substitutions had higher affinity to sucrose compared to the wild type SucC (-3.65 kcal/mol). The C66S mutant exhibited the most improved affinity to sucrose (-4.14 kcal/mol). The residues Asp-64, Asp-122, Arg-193, Asp-194 and Glu-271 were predicted to be directly interacting with sucrose among all mutants while C66S surprisingly had two more residues (Glu-296, His-310) interacting with sucrose. These results suggested that C66S led to the modification of the microenvironment of the catalytic regions positively where the substrate was more accessible to the active site than wild type SucC as well as all the other predicted mutants. The only other mutation that had a binding energy above -4 kcal/mol was the C66Y mutation. Since Cys and Ser have very similar conformational structures that only differs in the side chains (-SH in Cys while -OH in Ser), it was predicted that the substitution of Cys to Ser may not lead to apparent changes on the active site conformation but may increase the hydrophilicity of the active site, which should favour the interactions between sucrose and the active sites through hydrogen bonds due to the presence of multiple hydroxyl groups. Therefore, the mutant C66S was chosen to be constructed for further studies.

Table 15: Summary of simulated saturated mutagenesis of residue Cys-66 in SucC, identifying the interacting residues and the partial binding models

Protein model	Binding energy (kcal/mol)	Binding residues	Surface model
SucC (wild type)	**-3.65**	**Asp^{64} Asp^{122} Arg^{193} Asp^{194} Glu^{271}**	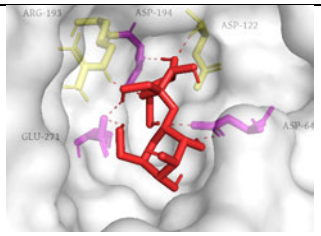
C66A	**-3.81**	**Asp^{64} Asp^{122} Arg^{193} Asp^{194} Glu^{271}**	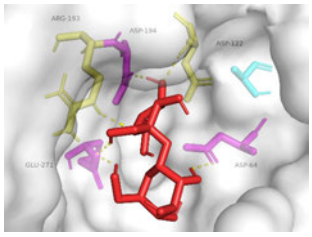
C66D	**-3.88**	**Asp^{64} Asp^{122} Arg^{193} Asp^{194} Glu^{271}**	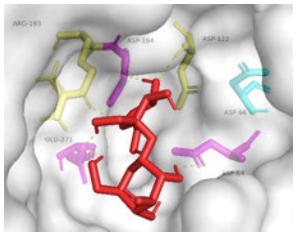

C66E	**-3.76**	**Asp^{64}** **Asp^{122}** **Arg^{193}** **Asp^{194}** **Glu^{271}**	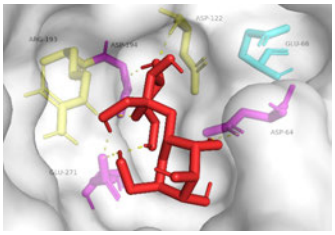
C66F	**-3.66**	**Asp^{64}** **Asp^{122}** **Arg^{193}** **Asp^{194}** **Glu^{271}**	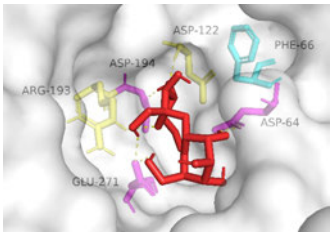
C66G	**-3.86**	**Asp^{64}** **Asp^{122}** **Arg^{193}** **Asp^{194}** **Glu^{271}**	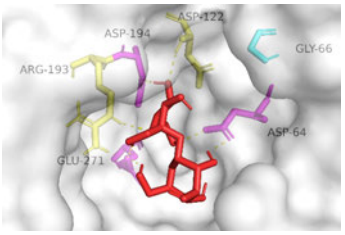
C66H	**-3.54**	**Asp^{64}** **Asp^{122}** **Arg^{193}** **Asp^{194}** **Glu^{271}**	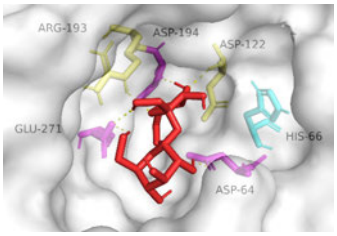
C66I	**-3.70**	**Asp^{64}** **Asp^{122}** **Arg^{193}** **Asp^{194}** **Glu^{271}**	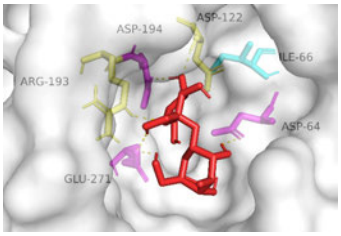
C66K	**-3.07**	**Asp^{64}** **Asp^{122}** **Arg^{193}** **Asp^{194}** **Glu^{271}**	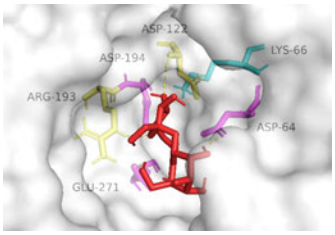
C66L	**-3.72**	**Asp^{64}** **Asp^{122}** **Arg^{193}** **Asp^{194}** **Glu^{271}**	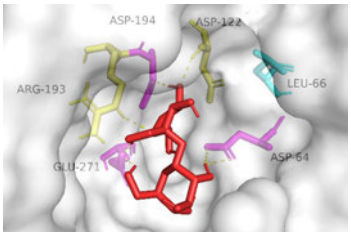

C66M	**-3.32**	**Asp^{64}** **Asp^{122}** **Arg^{193}** **Asp^{194}** **Glu^{271}**	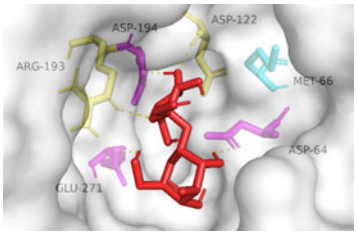
C66N	**-3.85**	**Asp^{64}** **Asp^{122}** **Arg^{193}** **Asp^{194}** **Glu^{271}**	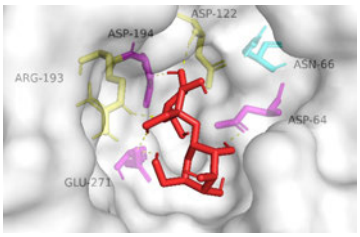
C66P	**-3.86**	**Asp^{64}** **Asp^{122}** **Arg^{193}** **Asp^{194}** **Glu^{271}**	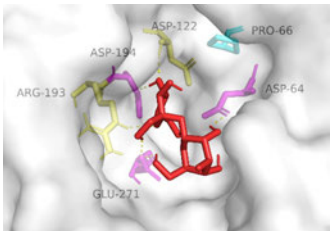
C66Q	**-3.84**	**Asp^{64}** **Asp^{122}** **Arg^{193}** **Asp^{194}** **Glu^{271}**	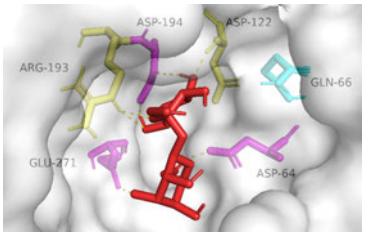
C66R	**-3.58**	**Asp^{64}** **Asp^{122}** **Arg^{193}** **Asp^{194}** **Glu^{271}**	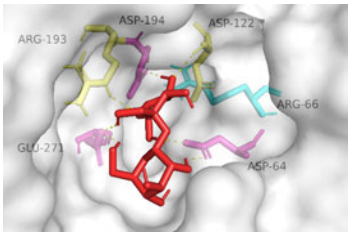
C66S	**-4.14**	**Asp^{64}** **Asp^{122}** **Arg^{193}** **Asp^{194}** **Glu^{271}** **Glu^{296}** **His^{310}**	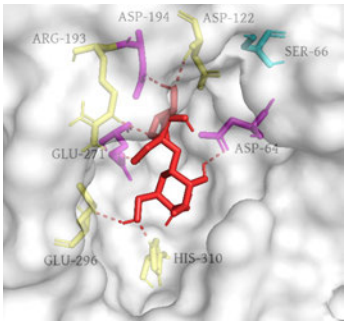
C66T	**-3.81**	**Asp^{64}** **Asp^{122}** **Arg^{193}** **Asp^{194}** **Glu^{271}**	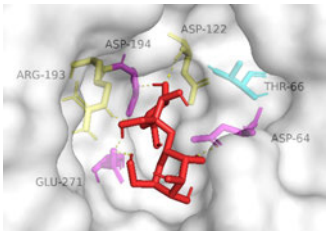

C66V	**-3.86**	**Asp^{64} Asp^{122} Arg^{193} Asp^{194} Glu^{271}**	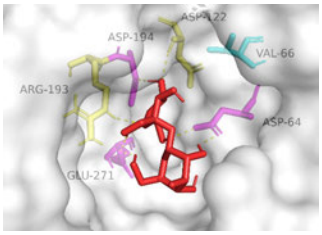
C66W	**-3.84**	**Asp^{64} Asp^{122} Arg^{193} Asp^{194} Glu^{271}**	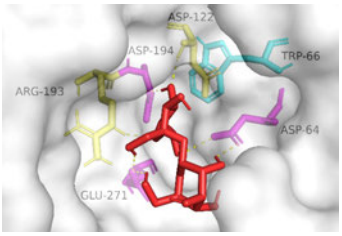
C66Y	**-4.12**	**Asp^{64} Asp^{122} Arg^{193} Asp^{194} Glu^{271}**	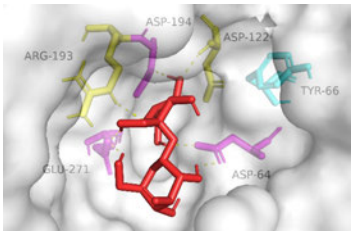

4.3.4. Sucrose access tunnel analysis

The sucrose access tunnel for mutant C66S and wild type SucC was further predicted and depicted in Figure 22. Two tunnels were modelled where tunnel one (T1) was responsible for transport of substrate to the active site (in green, Figure 22) and tunnel two (T2) for exit of products (in blue, Figure 22). It was found that the bottleneck region of the access tunnel of T1 for C66S was slightly reduced to 1.12 Å comparing to the wild type SucC (1.13 Å) but remained the same for T2 (0.71 Å). The length of the T1 tunnel for C66S was 18.90 Å which was longer but very close to that of wild type SucC (18.66 Å). The length of T2 tunnel decreased to 16.74 Å but only slightly compared with that of wild type SucC (16.81 Å). Lastly, the curvature of the T1 (1.23 Å) and T2 (1.15 Å) tunnels in C66S remained the same as that of SucC. This data proved that the substitution of Cys to Ser may not lead to a distinct change in the conformational structure of the substrate access and product exit tunnels. The tertiary structure of mutant C66S was further aligned with that of SucC. No apparent conformational changes occurred surrounding the active sites and the tertiary structures were highly overlapped (Figure 23).

In summary, the substitution of Cys-66 to Ser-66 (-SH to -OH group) was predicted to enhance the affinity between the substrate sucrose and the active sites by increasing the hydrophilicity surrounding the active site without significant alteration of the active site conformation.

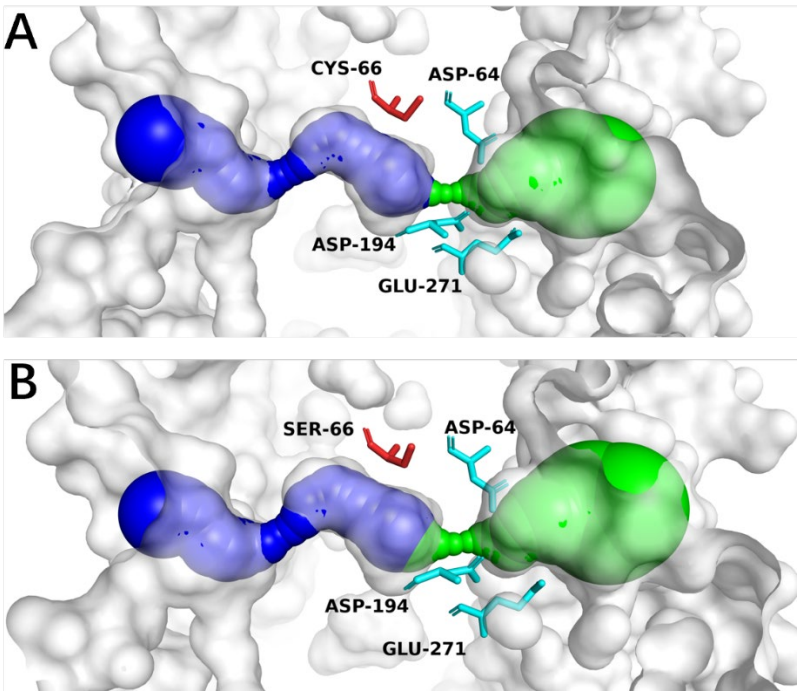

Figure 22: Structure analysis of WT-SucC (A) and SucC-C66S (B) depicting the modelled tunnels T1 (green) and T2 (blue). The catalytic triad (D64, D194 and E271) were coloured in cyan while Cys-66 (A) and Ser-66 (B) were coloured in red.

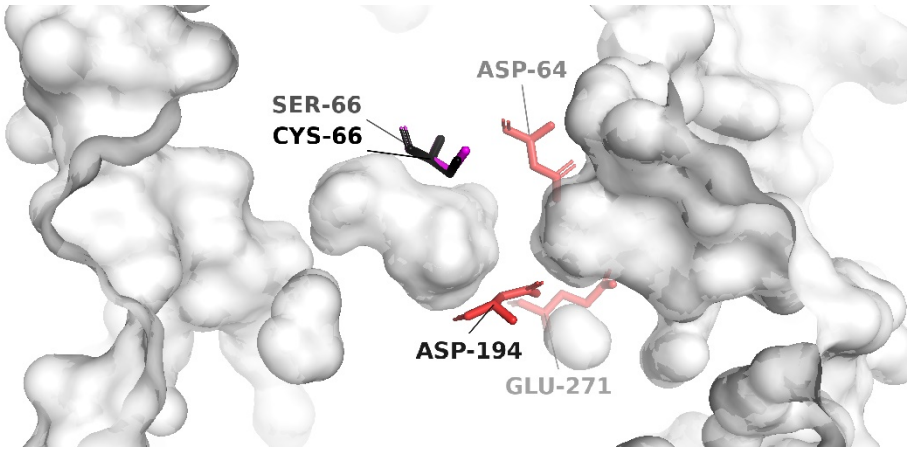

Figure 23: Superimposed tertiary structure alignments of C66S and SucC. The catalytic triad (D64, D194 and E271) were marked in red and labelled. The Cys-66 and Ser-66 residues showed no differences in their conformational structures.

4.3.5. Amplification of up-stream and down-stream fragments of mutations

Genomic DNA of *Pichia pastoris* GS115 was obtained as described previously in section 3.3.4. The up-stream and down-stream fragments of C66S, G273V and L313H were then amplified through the overlapping PCR technique with different sets of primers (Figure 24). The obtained PCR products were of expected sizes (Table 14), where C66S-up, C66S-down, G273V-up, G273V-down, L313H-up and L313H-down were 200 bp, 1700 bp, 800 bp, 1100 bp, 940 bp, 960 bp in size, respectively. The obtained bands were distinct and pure but not very bright, indicating a low yield of up-stream and down-stream fragments in the PCR.

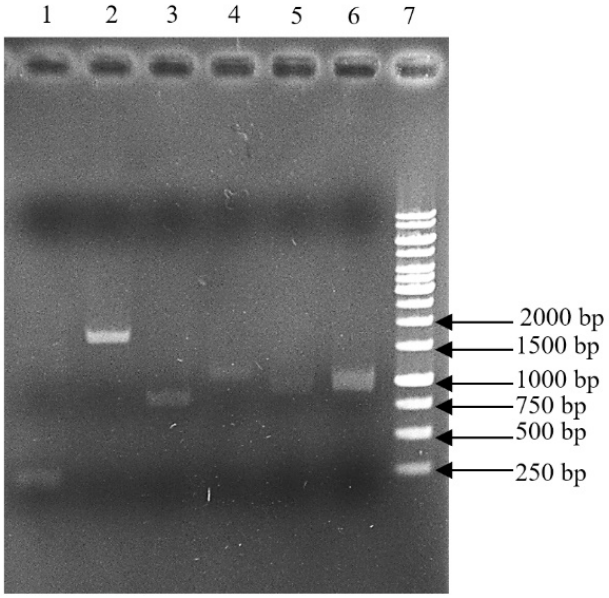

Figure 24: Visualization of up-stream and down-stream fragments after agarose gel (1.0%) electrophoresis at a constant 110 V for 30 minutes. From left to right, the bands were C66S-up (lane 1), C66S-down (lane 2), G273V-up (lane 3), G273V-down (lane 4), L313H-up (lane 5) and L313H-down (lane 6) which were 200 bp, 1700 bp, 800 bp, 1100 bp, 940 bp, 960 bp, respectively. Lane 7 was the molecular weight marker (GeneRuler 1 kb Plus DNA Ladder).

4.3.6. Cross-over PCR of C66S, G273V, L313H

The cross-over PCR products were obtained through cross-over PCR technique to produce full-length C66S, G273V and L313H DNA mutated genes (Figure 25). The obtained products were visualized by gel electrophoresis and were 1.9 kb. The bands for the recombined genes were very bright, indicating a high yield of crossover PCR products. Although the yield of desired products was high enough, strong non-specific amplifications were observed, suggesting the necessity for primer specificity adjustments. Primers may bind to unintended regions, leading to non-specific amplification. This may also be caused by an excessive use of DNA polymerase and inappropriate PCR program conditions that needs further improvements. These non-specific amplifications may affect the following applications of cloning processes, so that the screening processes were particularly crucial to eliminate the clones with incorrect inserts. Alternatively, the mutated genes could have been gel-purified, but this was not done.

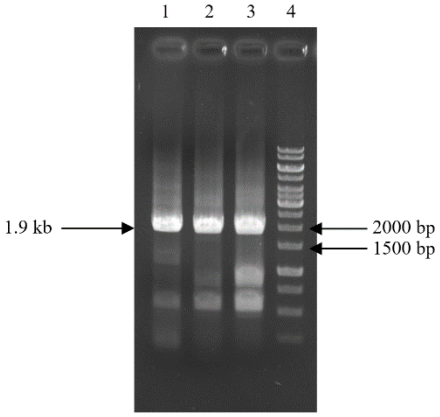

Figure 25: Cross-over PCR synthesis of C66S, G273V and L313H mutated genes after agarose gel (1.0%) electrophoresis at a constant 110 V for 30 minutes. From left to right, the bands were C66S (lane 1), G273V (lane 2) and L313H (lane 3), and all genes were 1.9 kb. Lane 4 was the molecular weight marker (GeneRuler 1 kb Plus DNA Ladder).

4.3.7. Ligation and heat-shock transformation into *E. coli* JM109

As described previously, the ligation was performed after insertion of foreign genes in between the *Avr*II and *Sna*BI sites (Figure 6). The pPIC9K was digested with *Avr*II and *Sna*BI (Table 5) and the inserts were digested by *Xba*I (Table 6) prior to ligation. Spread plates (Figure 26) of JM109 transformants (C66S, G273V and L313H) were inoculated after heat-shock transformation. The obtained transformants after 11 h incubation on LB-Amp plates at 37°C were round, creamy white and were of small sizes, which were the typical morphology of *E. coli* JM109 strains. They were closely packed, indicating

a high density of cells. They were evenly spread with good uniformity. Abundant transformants were obtained indicated an efficient ligation and heat-shock transformation. Twenty colonies from each plate were randomly selected and subjected to plasmid isolation for screening transformants with correct inserts.

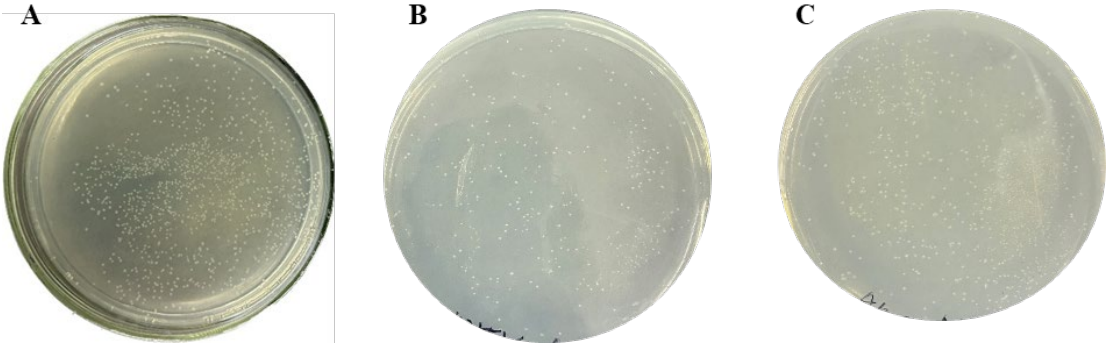

Figure 26: Spread plates of transformed *E. coli* JM109 cells for each mutation, C66S (A), G273V (B), L313H (C) on LB plates containing ampicillin (100 µg/mL) for 11 hours.

4.3.8. Screening for cloned SucC mutated genes

Twenty *E. coli* JM109 transformants were subcultured and plasmid extraction was performed followed by restriction enzyme digestion using *Hin*dIII to screen for correct transformants that contain the correct inserts. The principle for screening using *Hin*dIII digestion was explained in section 3.2.5.7. As shown in Figure 27, a clear and specific 2300 bp band was obtained for all mutants, indicating the correct C66S, G273V and L313H that were obtained. The *E. coli* JM109 transformants containing the desired recombinant vectors (pPIC9K-C66S, pPIC9K-G273V, pIC9K-L313H) were then subcultured and preserved for later use. The recombinant plasmids of pPIC9K-C66S, pPIC9K-G273V and pPIC9K-L313H were then isolated from their hosts and were transformed into *Pichia pastoris* GS115.

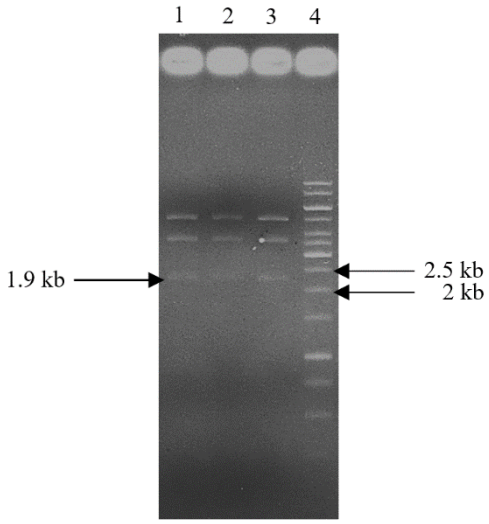

Figure 27: Recombinant pPIC9K plasmids digested by *Hin*dIII. pPIC9K-D64S (lane 1), pPIC9K-D194Q (lane 2) and pPIC9K-E271R (lane 3) contained bands of correct sizes (5000 bp, 3600 bp, 2300 bp, the 350 bp was too faint to be visualized). The 2300 bp band indicated the successful insertion of desired genes into pPIC9K.

4.3.9. Electrotransformation of mutated *sucC* genes into *P. pastoris* GS115

The recombinant plasmids pPIC9K-C66S, pPIC9K-G273V and pPIC9K-L313H were linearized by *Sal*I prior to transformation into *Pichia pastoris* GS115. The recombinant plasmids were electrotransformed into GS115 and cultivated on MD agar plates (Figure 28) to screen for histidine auxotrophs. The principle behind screening for *his*$^+$ auxotrophs was explained in section 3.3.10. Abundant transformants for C66S, G273V and L313H were obtained on MD plates. The transformants were then subcultured onto YPD plates containing 0.5 mg/mL geneticin (G418) to screen for high expression strains (Figure 29). Thirty-nine colonies for C66S, seventeen colonies for G273V and thirty-one colonies for L313H colonies were obtained. The reason some *his*$^+$ auxotrophs growing on MD plates and not growing on 0.5 mg/mL geneticin (G418) plates could be that the recombinant strains possessed low copy numbers of the geneticin resistance gene. It may also be due to incorrect homologous recombination between the recombinant pPIC9K plasmids and the GS115 genome which resulted in the disruption of the geneticin resistance gene in GS115. Therefore, it was vital to perform the antibiotic selection processes to isolate the correct recombinants after screening for *his*$^+$ auxotrophs on MD plates. A second screening process using a higher concentration of geneticin (G418) (2.0 mg/mL) was performed to screen for high expression strains with higher tolerance to geneticin. The best growing recombinants

for each mutant were subcultured and preserved for expression, suggesting a higher expression of the geneticin resistant gene as well as the adjacent *sucC* genes.

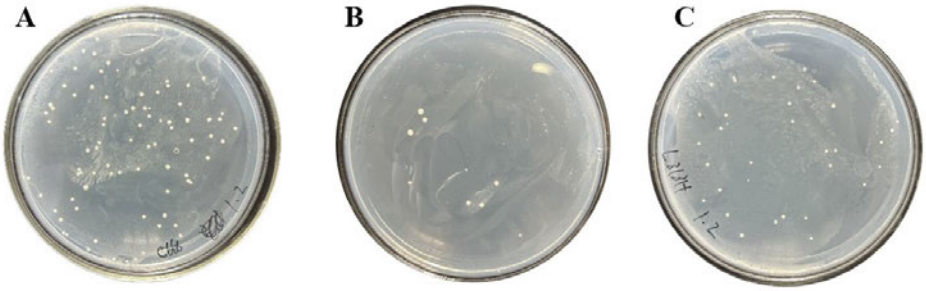

Figure 28: Transformants of *Pichia pastoris* GS115 after electroporation on MD plates to screen for *his*$^+$ auxotrophs. Plates were incubated at 30℃ for 48 hours. Abundant colonies for C66S (A), G273V (B) and L313H (C) were obtained.

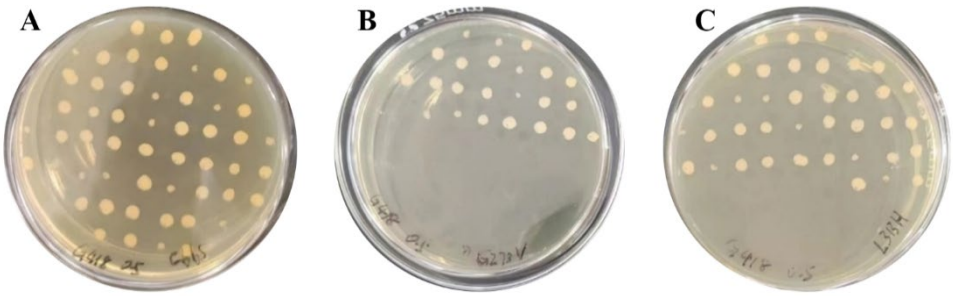

Figure 29： Screening for geneticin-resistant strains where the *his*$^+$ auxotrophs from MD plates were subcultured onto YPD agar plates containing 0.5 mg/mL geneticin (G418) and incubated at 30℃ for 72 hours. A was C66S, B was G273V and C was L313H.

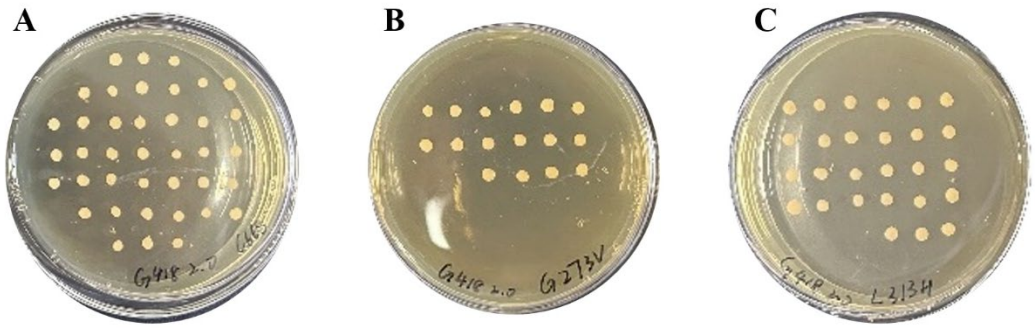

Figure 30: Screening for GS115 mutants having higher expression of SucC mutants using YPD plates having a higher concentration of geneticin (2.0 mg/mL). A was C66S, B was G273V and C was L313H.

4.3.10. Verification of GS115 transformants by colony PCR

The best growing GS115 transformants on YPD plates containing 2.0 mg/mL geneticin (G418) were subcultured and colony PCR was performed to verify if the SucC mutant genes were inserted into the GS115 chromosome. As shown in Figure 31, C66S, G273V and L313H were 1.9 kb and proved to be the same size as SucC. The GS115 mutants were then subcultured and preserved. After successful construction of three site-directed SucC mutants and insertion of these genes into *P. pastoris*, the next steps involved analysing expression of the mutated genes.

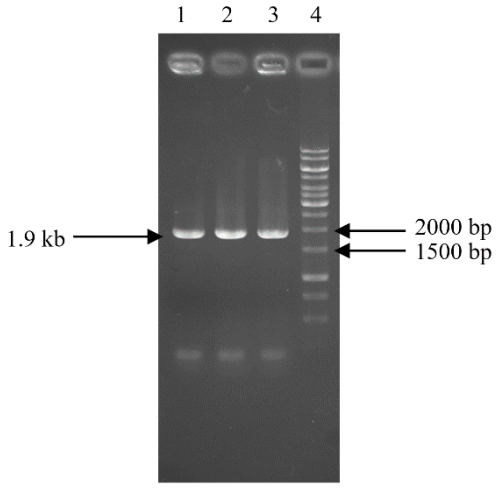

Figure 31: Amplification of C66S, G273V and L313H mutant genes after colony PCR. All three mutants were 1.9 kb.

4.3.11. Enzymatic activity determination

SucC, C66S, G273V and L313H enzymes were expressed during *P. pastoris* fermentation and their enzyme activities were determined using the method described previously in section 3.2.6 and section 3.2.7.2. The enzyme activity for SucC was much higher at 232±18.5 U/mL. The enzyme activity of the C66S mutant was determined to be 400 ±18.5 U/mL. However, no enzyme activity was detected for G273V and L313H (Table 16). It was therefore concluded that C66S had a higher expression level than wild type SucC and the G273V and L313H mutations led to complete loss of activity. However, it was necessary to prove the non-detection of enzyme activity was caused by the mutation of G273V and L313H, instead of the protein not being expressed in *P. pastoris*.

Table 16: Enzyme activity for SucC, C66S, G273V and L313H in *P. pastoris*

Enzyme	Enzyme activity (U/mL)
SucC	232 ±18.5
C66S	400 ±18.5
G273V	N.D*
L313H	N.D*

*N.D: not detected

4.3.12. Protein gel electrophoresis

The SDS-PAGE technique was used to verify if the enzymes were expressed or not. SucC, C66S, G273V and L313H were visualized by protein gel electrophoresis (Figure 32). These 4 enzymes were 70 kDa. SucC, C66S, G273V and L313H were all expressed. Since C66S, G273V and L313H were expressed, loss of enzyme activity for G273V and L313H were proved to be caused by the mutation. However, the target bands for all enzymes were very faint. The expression level of all these four proteins were similar as the brightness of these bands were similar. The identity of the brightest bands above the target bands is unknown. This band could be due to an unknown excreted protein or a residual medium component secreted after protein bands were also observed.

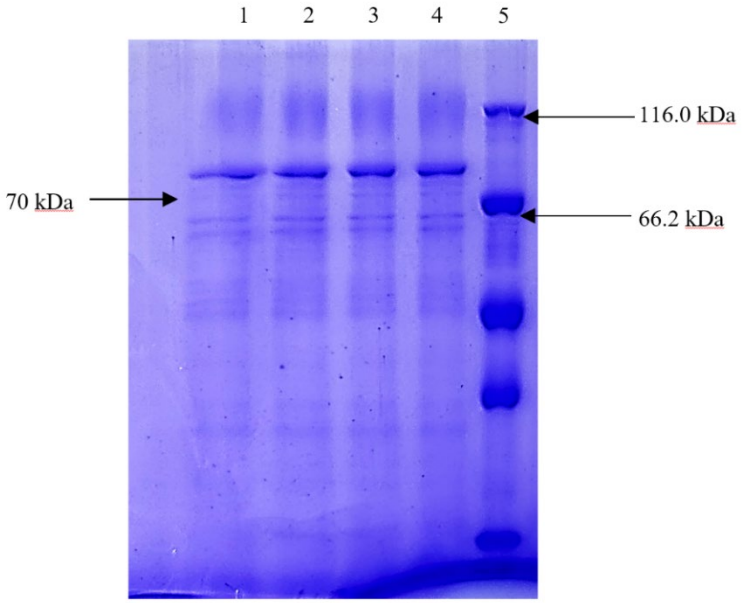

Figure 32: SDS-PAGE of SucC (lane 1), C66S (lane 2), G273V (lane 3) and L313H (lane 4) from *P. pastoris* supernatants.

4.3.13. SDS-PAGE of AKTA-purified enzymes

The purified enzymes SucC and C66S were electrophoresed by SDS-PAGE (Figure 33), in which desired bands (70 kDa) were obtained. The overall brightness of all bands were low due to the insufficient amount loaded on the gel. SucC and C66S bands were brighter than the marker bands, indicating a higher concentration. The obtained bands were distinct and pure, indicating a good purification of the enzymes after AKTA purification.

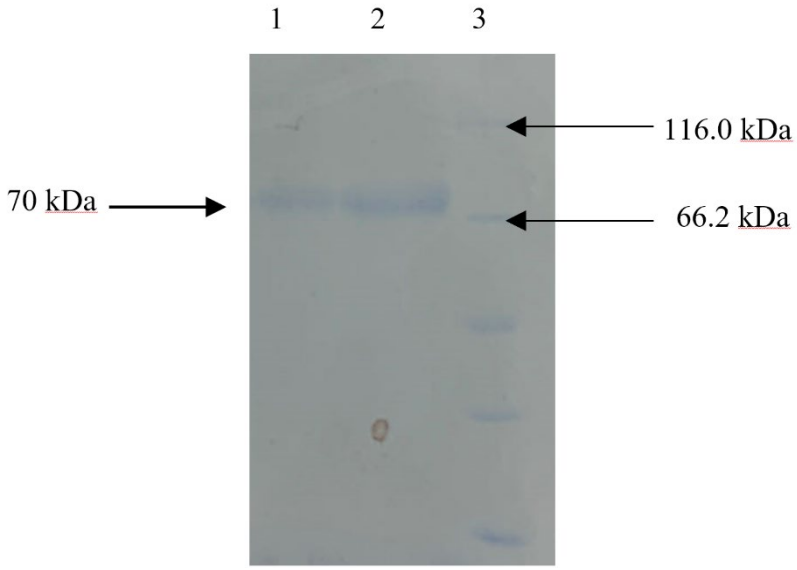

Figure 33: SDS-PAGE of purified SucC and C66S. SucC (lane 2) and C66S (lane 1) were 70 kDa, and no other bands were observed, indicating a high purity of enzymes obtained from AKTA purification.

4.3.14. Specific activity determination of SucC and C66S

The expressed SucC and C66S were purified by AKTA purification system and their concentration were determined using the Bradford assay described in 4.2.5. with a calibration curve (Appendix 1). The concentration of SucC and C66S were calculated as 0.038 mg/mL and 0.011 mg/mL, respectively. The enzyme activity of purified SucC and C66S were determined as 372 U/mL and 120 U/mL, respectively. Thus, the specific activity of SucC and C66S were then calculated as 10159.8 U/mg and 16386.8 U/mg, respectively. Remarkably, mutant C66S had an increase of 61.3% in its specific activity comparing to the wild type SucC. The enzyme's specific activity is a crucial parameter that reflects the efficiency of enzyme catalysis regarding per unit of protein mass (Xia et al., 2022). The increased specific activity indicates the mutation of C66S has led to a significant improvement in its catalytic rate per unit time per enzyme molecule. Meanwhile, it also implies that a lower amount of C66S enzyme molecules are required

to achieve the same level of reaction. This may contribute to cost savings in FOS production processes.

Table 17: Activity, concentration and specific activity of SucC and C66S after AKTA purification

	Activity (U/mL)	Concentration (mg/mL)	Specific activity (U/mg)
SucC	372	0.0366148	10159.8
C66S	120	0.0073229	16386.8

4.3.15. Enzymatic kinetics of SucC and C66S

The enzyme kinetics of SucC and C66S were determined through the reactions described in 4.2.8. and the data was plotted using Origin 9 software. The kinetic parameters of SucC and mutant C66S on catalysis of sucrose were summarized in Table 18. Mutant C66S presented a very similar V_{max} value (1.10 mM/min) to that of SucC but a very different K_m value. The K_m value of C66S decreased by 13.5% (71.14/82.21 mM) compared to that of SucC, indicating an increased affinity to sucrose in the catalysis. The k_{cat} value of C66S was increased by 21.6% (112.23/136.48 min^{-1}) compared to that of SucC. As a result, the catalytic efficiency (k_{cat}/K_m) of C66S (1.92 $min^{-1} \cdot mM^{-1}$) increased by 1.4-fold to that of WT-SucC (1.37 $min^{-1} \cdot mM^{-1}$). The catalytic efficiency signifies the enzyme's effectiveness in converting substrates into products where a higher k_{cat}/K_m value represents a greater catalytic efficiency of the enzyme (Nelson, 2019). In this case, the increase of catalytic efficiency of C66S to that of wild type SucC (1.4-fold) indicated a more rapid conversion of sucrose into FOS under optimal conditions, contributing to an enhanced reaction speed. The improvements of the catalytic efficiency of such fructosyltransferases were representatives of the industrial biocatalysts which influenced the overall productivity and cost-effectiveness of processes (Guio et al., 2012; Kashyap et al., 2015). A comprehensive study on enhancing the catalytic efficiency of an α-amylase signified its improved kinetic properties for specific applications of interest (Hernández-Heredia et al., 2022). Moreover, the continuous effort to improve the catalytic efficiency not only optimized existing enzymes but also provided valuable insights for enzyme engineering in which novel strategies and modifications were explored to enhance enzyme performance (Alvarado-Obando et al., 2022; Rakotoharisoa et al., 2023). The reactions on sucrose over different substrate concentrations was plotted in Figure 34.

Table 18. The kinetic parameters of SucC and mutant C66S on catalysis of sucrose

Enzyme	K_m (mM)	V_{max}	k_{cat} (min^{-1})	k_{cat}/K_m ($min^{-1} \cdot mM^{-1}$)
SucC	82.20	1.10	112.23	1.37
C66S	71.14	1.11	136.48	1.92

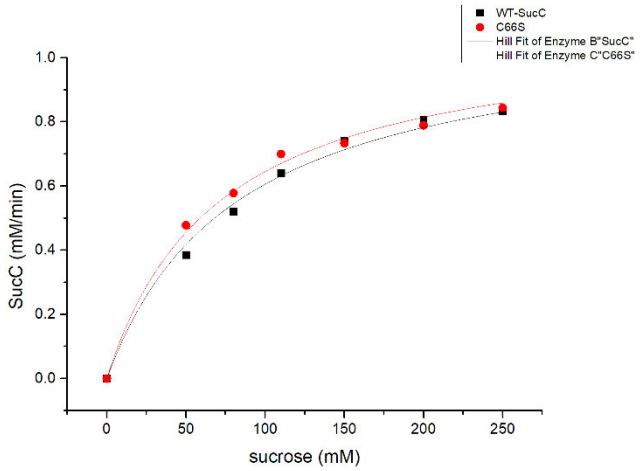

Figure 34: Predicted consumption of sucrose over different substrate concentrations from 50 to 250 mM that fits the Michaelis-Menten function. The value of V_{max} and K_m were given by the calculation from the Origin 9 software where V_{max} for both enzymes were determined as 1.10 mM/min and K_m for SucC and C66S was determined as 82.20 mM and 71.14 mM, respectively. The decrease of K_m value of C66S comparing to WT-SucC indicated a better affinity of enzyme to substrate.

4.3.16. Temperature and pH optima, thermostability and pH tolerance

The optimal reaction temperature and pH of mutant C66S were determined and are summarized in Figure 35 A&B. The mutant C66S had the maximum activity at 50˚C and pH 5.5, which are the same as that of SucC. The results indicated that the C66S mutation did not lead to a change of the temperature and pH optima.

The thermostability of C66S dropped significantly at 50˚C comparing to SucC (Figure 35C). This indicated that the mutant C66S led to the change of the active site rigidity so that the thermostability has decreased. The thermostability of an enzyme is affected by its tertiary structure conformation, salt bridge formed by charged residues, hydrogen bonds formed in the secondary and tertiary structure, the rigidity of amino acids and the hydrophobicity of protein (Nezhad et al., 2022). Typically, the disulfide (S-S) bridge formed by covalent linkages between Cys residues will greatly contribute to the stabilization of tertiary structure by improving the structural rigidity and

hydrophobicity (Jiao et al., 2022). As a result, the substitution of Cys-66 to Ser-66 that created a more hydrophilic environment surrounding the catalytic nucleophile (Asp-64) that led to an increase in catalytic efficiency but a slight drop of thermostability due to the reduced rigidity of active sites where the -SH group is changed to -OH group. The pH stability was similar at the optimum pH (5.5) but SucC was more stable in the acidic environment and C66S was more stable in the alkaline environment Figure 35D. The reason for this is unclear.

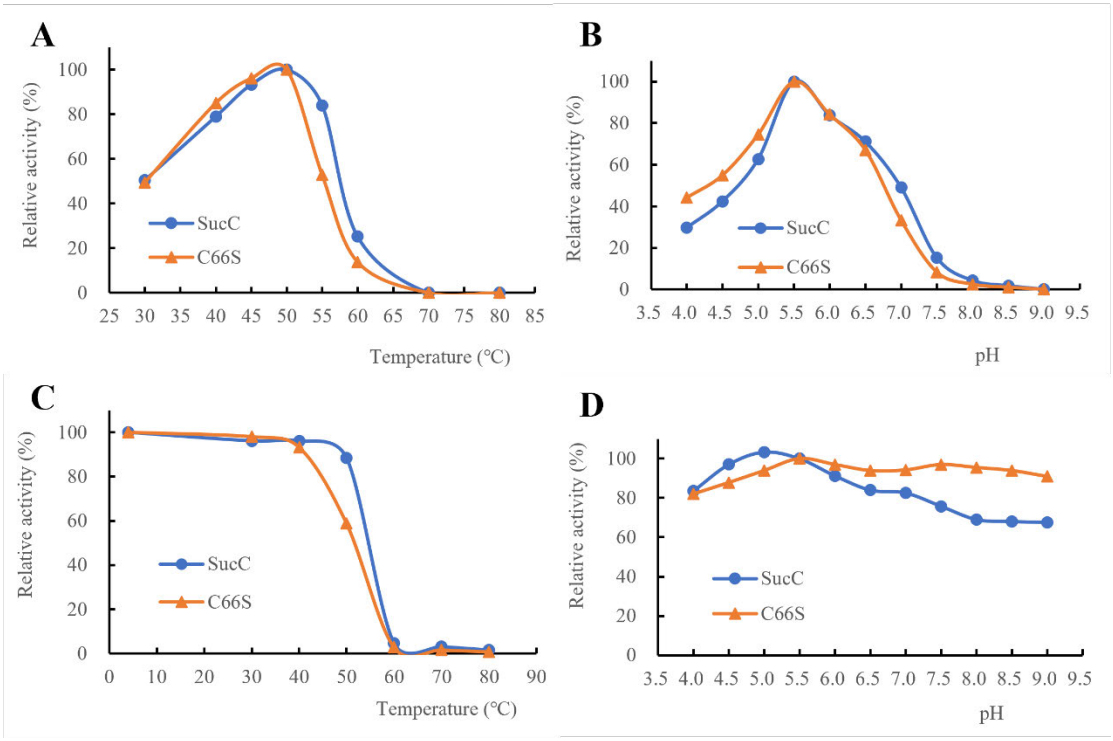

Figure 35: The effects of temperature and pH on the activities of SucC and mutant C66S. A: Temperature optimum; B: pH optimum; C: Thermostability at the temperatures from 4˚C to 80˚C for 1 h incubation; D: pH stability at pHs from 4.0 to 9.0 for 1 h incubation.

4.3.17. Sugar profiles of FOS production by C66S

Mutant C66S-mediated FOS formation from sucrose was conducted to further explore its catalytic performance and its potential for industrial application. The sugar profiles were analyzed by HPLC and the results are summarized in Figure 36. Initially, 400 g/L sucrose was supplied for FOS production over 6 hours. Although the same amounts of enzymes (9 U/g sucrose) were supplied for the FOS production, an obvious increase in the reaction rate catalyzed by C66S was observed where the amount of sucrose consumption as well as the FOS (DP_3, DP_4, DP_5) formation was more rapid than the reaction catalyzed by wild type SucC. Particularly, C66S consumed 21.23% (remaining sucrose 242.82/209.45 g/L) more sucrose and produced 20.39% (117.48/141.44 g/L)

more FOS than that catalyzed by wild SucC in the first hour, indicating a higher productivity in early stages of FOS productions. However, both reactions reached their endpoints by 4 h and the amount for sucrose consumptions (355 g/L) and FOS productions (250 g/L) were similar. These results validated the increased catalytic efficiency of C66S mediated a more efficient catalysis since k_{cat}/K_m was higher compared with wild SucC but did not change its substrate specificity. The detailed compositions of FOS preparations were also analyzed (Figure 36B). It was found that kestose (DP_3), nystose (DP_4) and fructofuranosylnystose (DP_5) were the main components of FOS after 6 hours of reaction. DP_3 (150 g/L) and DP_4 (90 g/L) were the main components of FOS while DP_5 formation was only detected after 3 hours for both reactions and at very low amounts (5 g/L). Glucose (100 g/L) was the main by-product. A very little amount of fructose (<5 g/L) was generated in both transfructosylating reactions and this result was not presented. The overall FOS production catalyzed by C66S was more efficient than that catalyzed by wild type SucC, where the formation of DP_3 was the most notable distinction between mutant C66S and wild type SucC where DP_3 reached its maximum yield after 2 h when catalyzed by C66S and was faster than that catalyzed by wild type SucC (3 h). DP_3 maximum yield for both enzymes were about 180 g/L and started to drop thereafter as DP_3 served as the substrate to form DP_4. However, the final spectrum of the generated FOS (DP_3, DP_4, DP_5), glucose and fructose could not be distinguished between these two catalytic reactions, indicating no detectable changes in the FOS sugar profile using the C66S enzyme. The C66S enzyme had increased catalytic efficiency in transfructosylation without altering the enzyme's substrate specificity. This observation further substantiated that the substitution of Cys-66 to Ser-66 in SucC led to an increased hydrophilic microenvironment surrounding the catalytic region, increasing its affinity to sucrose, and eventually improved its performance in catalytic efficiency during FOS production. The results of sugar profiles also demonstrated that the C66S variant was a competitively advantageous candidate for industrial production of FOS compared with wild type SucC.

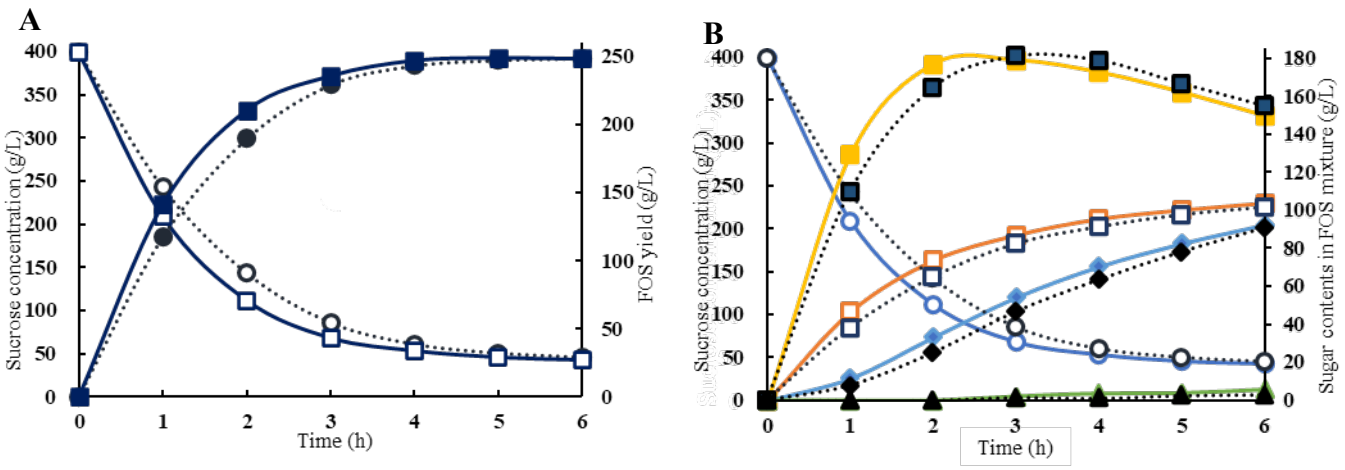

Figure 36: The time-course of FOS formation from sucrose. The FOS preparation was carried out in 100 mL reaction volume with 400 g/L sucrose solution and 9 U/g enzyme at 50˚C and pH 5.5 for 6 h. The contents of sugars in the reaction mixture were determined by HPLC. A: The residual sucrose (open rectangle or circle) and total FOS (solid rectangle or circle) catalysed by mutant C66S (solid line) or SucC (dot line). B: The sugar profiles (Circle: sucrose; Rectangle: glucose; Solid square: DP_3; Solid diamond: DP_4; Solid triangle: DP_5) in the reaction mixture catalysed by C66S (solid lines) or SucC (dot lines).

CHAPTER 5: GENERAL DISCUSSION AND CONCLUSION

The fructosyltansferase, SucC, used in this study was functionally expressed in *P. pastoris* GS115 and has been applied in food industry to make fructooligosaccharides for over 10 years in China. Although it is widely applied, there is a lack of fundamental studies on this specific enzyme regarding tertiary structural analysis, bioinformatics simulations and structure-function relationships. To further improve the catalytic efficiency of this enzyme to meet the higher demand of FOS production catalysed by fructosyltransferase in industry, it is vital to reveal the structure of SucC where the amino acid residues involved in catalysis will be determined so that an accurate enzymatic mechanism can be proposed. Once the structure of SucC is determined, strategies can then be designed to modify the enzyme's structure that results in a desired modified function. The SucC was modelled through SWISS-MODELLING using a template of the crystal structure of another fructofuranosidase (PDB ID: 5XH8) that is most closely related to each other in the protein databases. It is well known that conserved amino acid sequences have similar structure and function meaning that their conservation will maintain the similar structure and function of protein domains. The catalytic residues in SucC were initially determined as D64, D194 and E271. These residues form a catalytic triad as evidenced by homologous alignment between the other six fructosyltransferases or fructofuranosidases with identified catalytic residues. There is a large difference in overall amino acid sequence similarity between these seven enzymes, but the active sites are highly identical. Due to the high homogeneity of SucC to the fructofuranosidase (5XH8) which was originally cloned from *A. kawachii*, the overall 3-D structure of SucC was then predicted (Nagaya et al., 2017) (Figure 8B).

Although the active sites and the overall structure of SucC were determined through bioinformatics analysis, it was vital to empirically prove the validity of the proposed active sites in SucC. Considering that amino acid sequences are highly conserved, it is therefore assumed that the evolution of specific amino acid residues with important functions has selected against their substitution by other residues, to prevent the loss of function in the enzyme (Chikunova and Ubbink, 2022). The proposed catalytic triad (D64, D194, E271) in SucC would be validated if these three sites are proven to be non-substitutable by the other 19 amino acids. The 19 mutations on these three amino acids were initially done by tertiary structure modelling, followed by predicting the interactions between the resultant mutated enzymes and sucrose through molecular docking processes. 57 predicted interactions between sucrose and the mutated SucC variants which were generated, 29 docking models showed non-specific binding when compared to the docking of wild type SucC to sucrose (Table 11). This suggested a

collapse of enzyme structure with loss of enzyme activity. Among the remaining 28 interaction models, D64S, D194Q and E271R showed the best affinity to sucrose in each catalytic site. If these three mutants were constructed and enzyme activity was found to have been lost experimentally, it can be safely assumed that the other mutations in the 28 models would also lose their enzyme activities. No enzyme activity was detected for D64S, D194Q and E271R after physical construction of the mutants, followed by fermentation and enzyme assays (Table 12). These results proved that these three bioinformatically identified catalytic residues play a significant role in the catalytic mechanism and can not be substituted by other amino acid residues. Therefore, D64, D194 and E271 are validated to form the catalytic triad of the SucC where D64 acts as a catalytic nucleophile, D194 acts as a transition-state stabilizer and E271 acts as a general acid/base catalyst (Chuankhayan et al., 2010; Nagaya et al., 2017; Olarte-Avellaneda et al., 2018). The utilization of bioinformatics analysis to determine the enzyme active sites and as a support technique to predict the interactions between substrates and enzymes as well as their mutants helps researchers better understand the structure and function of enzymes and greatly reduces the amount of experimental work required for designing and screening of mutants. The above statement was shown to be true in this study.

To further improve the catalytic efficiency of SucC to meet the higher demand for fructosyltransferases used in industry to produce FOS, rational mutagenesis of SucC was carried out. The substitution of certain amino acids in an enzyme may lead to changes in its structure and function which may result in changes in enzyme activity or kinetics, an altered substrate specificity, better or weaker enzyme stability, and even a loss or gain of novel functions (Al-Raawi and Kanhere, 2023). Three mutants (C66S, G273V, L313H) proposed in Chapter 3 to increase the enzyme's catalytic efficiency were constructed and their genes were cloned and expressed in the genome of *P. pastoris*. C66S expression (400 ±18.5 U/mL) was better than wild type SucC (232 ±18.5 U/mL) while no enzyme activity was detected for the other two mutants, G273V and L313H. This meant that their mutations led to a complete loss of enzyme activity. Expressed enzymes were purified and characterized in specific activity and it was found that C66S had an increased specific activity of 1.63-fold compared to SucC (Table 17). The mutant C66S showed a better affinity to sucrose (-4.14 kcal/mol) compared to the wild type SucC interacting with sucrose (-3.65 kcal/mol) in the catalytic sites predicted by AutoDock. There are an additional two amino acid residues interacting with sucrose (Glu-296, His-310) for C66S. This can be explained as the substitution of Cys-66 to Ser-66 in SucC resulted in the modification of the structure in the catalytic region, making the catalytic domain interacting with sucrose more easily. In Chapter 4, the

C66S enzyme had the highest affinity to sucrose, while the other two variants had a lower affinity than SucC (Figure 21). This suggests that any binding energy lower than that of the wild type enzyme for its substrate may completely abolish enzyme activity. C66S was predicted to have better affinity to sucrose than the wild type SucC and this was supported by the kinetic study which showed the better affinity of C66S to sucrose with a lower K_m value and a better k_{cat} value. The structure of Cys and Ser differs in their side chain where a Cys contains a thiol (-SH) group and a Ser contains a hydroxyl group (-OH). Both structures are simple and similar which theoretically did not lead to major changes of protein conformations. However, the -OH group is more hydrophilic than the -SH group, providing a more hydrophilic environment in the catalytic domain when Cys-66 is mutated to Ser-66. The substrate sucrose contains multiple -OH groups which means a more hydrophilic environment favours the interactions between sucrose and the active sites. Thus, the increase of catalytic activity of C66S may be due to a more hydrophilic environment which promotes the transfructosylation enzymatic reaction when the substrate is sucrose. The construction of G273V was an attempt to create a more hydrophobic environment around the catalytic triad that was hypothesized to favour transfructosylation as the released fructosyl unit during the catalysis must react with another sucrose molecule to form kestose, otherwise free fructose will be formed as the final product instead of joining into another sucrose molecule (Chu et al., 2022). However, the constructed G273V and L313H lost their activities, which may be explained as the Gly-273 takes part in the stabilization and maintenance of the structure in the catalytic regions where the substitution of Gly to Val may lead to the collapse of the catalytic regions that resulted in the loss of activity. Leu is often involved in forming ionic interactions and salt bridges within proteins and its loss indicated the importance of this residue in playing vital roles involved in the enzymatic mechanisms. The docking results of G273V and L313H showed reduced affinity to sucrose compared to wild type SucC. As mentioned before, the negatively charged active site pocket in a fructosyltransferase (PDB ID:3LF7) from *A. japonicus* was determined and the residues Lys-82, Phe-121, Asp-122, Ile-146, His-147, Arg-193, Glu-296, His-310, Tyr-342, Ala-343, Phe-376 and Glu-380 were homologous to the identified negatively charged active site pocket in 3LF7 (Chuankhayan et al., 2010). On the other hand, the complete loss of activity caused by G273V and L313H proved the importance of Gly-273 and Lys-313 that are non-substitutable and are vital for the enzymatic mechanism. This also suggests that binding energy scores lower than that for the wild type enzyme and sucrose may result in complete loss of activity, not just reduced activity. The combination of in silico simulations and in vitro mutagenesis served as a powerful tool in enzyme engineering, which can significantly impact the artificial evolution of enzymes.

Although the catalytic efficiency of C66S was increased comparing to wild type SucC, the thermostability of C66S decreased about 20% compared to wild type SucC when incubating the enzymes at its optimal temperature for 1 hour (Figure 35C). The thermostability of an enzyme is affected by its tertiary structure conformation, salt bridges formed by charged residues, hydrogen bonds formed in the secondary and tertiary structure, the rigidity of amino acids and the hydrophobicity of the protein (Nezhad et al., 2022). Typically, the disulfide (S-S) bridge formed by covalent linkages between Cys residues will greatly contribute to the stabilization of tertiary structure by improving the structural rigidity and hydrophobicity (Jiao et al., 2022). As a result, the substitution of Cys-66 to Ser-66 that created a less hydrophobic environment around the catalytic nucleophile (Asp-64) led to an increase in catalytic efficiency but a slight drop of thermostability due to the reduced rigidity of active sites when the -SH group was changed to an -OH group. Besides specific activity and thermostability, the other characteristics of C66S were similar to wild type SucC.

Lastly, the application of SucC-C66S to produce FOS compared to SucC was assessed through sugar profiles. The consumption of sucrose and the formation of FOS catalysed by C66S was about 10% faster than wild type SucC in the first two hours and both reactions reached the endpoint around 5 hours later (Figure 36). The summary of the FOS production distinctly showed detailed compositions of substrate and products in the reaction mixture from 1 to 6 hours. According to the National Food Safety Standard in China of the regulation on FOS products (GB/T 23528.2-2021), the commercialization of FOS composed of DP_3, DP_4, DP_5 and DP_6 produced from sucrose must exceed 50% (g/100 g) of the reaction mixture (residual sucrose + glucose + fructose + FOS). Therefore, the FOS produced by SucC-C66S met the requirement in the second hour (52.7%) while SucC only generated 47.4% FOS at the same time. The produced FOS that met the standard from 400 g/L sucrose catalysed by SucC-C66S was made in less than 2 hours while it took more than 2 hours catalysed by SucC. Therefore, C66S increased the catalytic efficiency for commercial FOS production compared to wild type SucC. The process now saves time and this improved enzyme will be a suitable candidate for industrial application for manufacturing FOS.

To conclude, the fructosyltransferase, SucC, which was originally cloned from *A. niger* was used in this study for bioinformatics characterization and site-directed mutagenesis. The tertiary structure of SucC was determined where specifically the catalytic residues (D64, D194 and E271) were identified and validated by homologous alignment and saturation mutagenesis. The constructed mutants were biochemically characterized

through comprehensive analysis of enzyme structures, simulations of saturated mutagenesis, molecular docking for screening candidate mutants and eventually by enzyme assays. The enzyme variant, C66S, exhibited a more hydrophilic microenvironment surrounding the active site without significant conformational changes and was more favourable for fructooligosaccharide production compared with the wild type SucC. Moreover, it is notable that these findings have provided valuable insights for guiding further enzyme evolution studies.

REFERENCES

Aachary, A.A., Prapulla, S.G., 2011. Xylooligosaccharides (XOS) as an emerging prebiotic: microbial synthesis, utilization, structural characterization, bioactive properties, and applications. Comprehensive Reviews in Food Science and Food Safety 10, 2–16

Alméciga-Díaz, C.J., Gutierrez, Á.M., Bahamon, I., Rodríguez, A., Rodríguez, M.A., Sánchez, O.F., 2011. Computational analysis of the fructosyltransferase enzymes in plants, fungi and bacteria. Gene 484, 26–34

Al-Raawi, D., Kanhere, A., 2023. Site-directed mutagenesis protocol to determine the role of amino acid residues in polycomb group (pcg) protein function, in: Lanzuolo, C., Marasca, F. (Eds.), Polycomb Group Proteins, Methods in Molecular Biology. Springer US, New York, NY, pp. 79–89

Alvarado-Obando, M., Contreras, N., León, D., Botero, L., Beltran, L., Díaz, D., Rodríguez-López, A., Reyes, L.H., Alméciga-Díaz, C.J., Sánchez, O.F., 2022. Engineering a heterologously expressed fructosyltransferase from *Aspergillus oryzae* N74 in *Komagataella phaffii* (*Pichia pastoris*) for kestose production. New Biotechnology 69, 18–27

Álvaro-Benito, M., De Abreu, M., Portillo, F., Sanz-Aparicio, J., Fernández-Lobato, M., 2010. New insights into the fructosyltransferase activity of *Schwanniomyces occidentalis* β-Fructofuranosidase, emerging from nonconventional codon usage and directed mutation. Applied and Environmental Microbiology 76, 7491–7499

Antošová, M., Polakovič, M., 2001. Fructosyltransferases: the enzymes catalyzing production of fructooligosaccharides. Chemical Papers 55, 350–358

Bachman, J., 2013. Site-directed mutagenesis. Methods Enzymology 529, 241–248

Balamurugan, V., Reddy, G.R., Suryanarayana, V.V.S., 2007. *Pichia pastoris*: a notable heterologous expression system for the production of foreign proteins—vaccines

Ballinger, R.A., 1971. A History of Sugar Marketing. U.S. Department of Agriculture, Economic Research Service. Agricultural Economic Report No. 197, Washington, DC

Baurhoo, B., Phillip, L., Ruiz-Feria, C.A., 2007. Effects of purified lignin and mannan oligosaccharides on intestinal integrity and microbial populations in the ceca and litter of broiler chickens. Poultry Science 86, 1070–1078

Berezovskaya, Y., Varakina-Mitrail, K., Nechaeva, V., Kholodova, I., 2020. Biotic nutritional components in baby formula: possible solution for infantile colic management. Functional Foods in Health and Disease 10, 368

Bhandari, S., Poudel, D.K., Marahatha, R., Dawadi, S., Khadayat, K., Phuyal, S., Shrestha, S., Gaire, S., Basnet, K., Khadka, U., 2021. Microbial enzymes used in bioremediation. Journal of Chemistry 2021, 1–17

Birnboim, H., Doly, J., 1979. A rapid alkaline extraction procedure for screening recombinant plasmid DNA. Nucleic Acids Research 7, 1513–1523

Bradford, M.M., 1976. A rapid and sensitive method for the quantitation of microgram quantities of protein utilizing the principle of protein-dye binding. Analytical Biochemistry 72, 248–254

Buller, R., Lutz, S., Kazlauskas, R.J., Snajdrova, R., Moore, J.C., Bornscheuer, U.T., 2023. From nature to industry: Harnessing enzymes for biocatalysis. Science 382, eadh8615

Campbell, J.M., Bauer, L.L., Fahey, G.C., Hogarth, A., Wolf, B.W., Hunter, D.E., 1997. Selected fructooligosaccharide (1-kestose, nystose, and 1F-β-fructofuranosylnystose) composition of foods and feeds. Journal of Agricultural and Food Chemistry 45, 3076–3082

Carter, J.N., 1987. Sucrose production as affected by root yield and sucrose concentration of sugarbeets. J Am Soc Sugar Beet Technol 24, 14–31

Chakraborty, P., Di Cera, E., 2017. Induced fit is a special case of conformational selection. Biochemistry 56, 2853–2859

Chen, Y., Sotomayor, M., Capponi, S., Hariharan, B., Sahu, I.D., Haase, M., Lorigan, G.A., Kuhn, A., White, S.H., Dalbey, R.E., 2022. A hydrophilic microenvironment in the substrate-translocating groove of the YidC membrane insertase is essential for enzyme function. Journal of Biological Chemistry 298, 101690

Chen, Y., Xie, Y., Ajuwon, K.M., Zhong, R., Li, T., Chen, L., Zhang, H., Beckers, Y., Everaert, N., 2021. Xylo-oligosaccharides, preparation and application to human and animal health: A review. Frontiers in Nutrition 8:731930

Cheng, Y.-S., Chen, C.-C., Huang, J.-W., Ko, T.-P., Huang, Z., Guo, R.-T., 2015. Improving the catalytic performance of a GH11 xylanase by rational protein engineering. Applied Microbiology and Biotechnology 99, 9503–9510

Chikunova, A., Ubbink, M., 2022. The roles of highly conserved, non-catalytic residues in class A β-lactamases. Protein Science 31, e4328

Choukade, R., Kango, N., 2021. Production, properties, and applications of fructosyltransferase: a current appraisal. Critical Reviews in Biotechnology 41, 1178–1193

Chovancova, E., Pavelka, A., Benes, P., Strnad, O., Brezovsky, J., Kozlikova, B., Gora, A., Sustr, V., Klvana, M., Medek, P., 2012. CAVER 3.0: a tool for the analysis of transport pathways in dynamic protein structures. PLoS Computational Biology 8: e1002708, 8(10), 2012

Chu, J., Tian, Y., Li, Q., Liu, G., Yu, Q., Jiang, T., He, B., 2022. Engineering the β-fructofuranosidase Fru6 with promoted transfructosylating capacity for fructooligosaccharide production. Journal of Agricultural and Food Chemistry. 70, 9694–9702

Chuankhayan, P., Hsieh, C.-Y., Huang, Y.-C., Hsieh, Y.-Y., Guan, H.-H., Hsieh, Y.-C., Tien, Y.-C., Chen, C.-D., Chiang, C.-M., Chen, C.-J., 2010. Crystal

structures of *Aspergillus japonicus* fructosyltransferase complex with donor/acceptor substrates reveal complete subsites in the active site for catalysis. Journal of Biological Chemistry 285, 23251–23264

Copeland, R. A. (1997). Enzymes: a practical introduction to structure, mechanism, and data analysis. Biomedicine & Pharmacotherapy, 4(51), 187

Davani-Davari, D., Negahdaripour, M., Karimzadeh, I., Seifan, M., Mohkam, M., Masoumi, S.J., Berenjian, A., Ghasemi, Y., 2019. Prebiotics: definition, types, sources, mechanisms, and clinical applications. Foods 8, 92.

de Menezes, C.R., Silva, Í.S., Pavarina, É.C., Guímaro Dias, E.F., Guímaro Dias, F., Grossman, M.J., Durrant, L.R., 2009. Production of xylooligosaccharides from enzymatic hydrolysis of xylan by the white-rot fungi Pleurotus. International Biodeterioration & Biodegradation 63, 673–678

de Paulo Farias, D., de Araújo, F.F., Neri-Numa, I.A., Pastore, G.M., 2019. Prebiotics: Trends in food, health and technological applications. Trends in Food Science & Technology 93, 23–35

Dekker, P.J.T., Daamen, C.B.G., 2011. Enzymes exogenous to milk in dairy technology | β-D-Galactosidase, in: Fuquay, J.W. (Ed.), Encyclopedia of Dairy Sciences (Second Edition). Academic Press, San Diego, pp. 276–283

Denji, K.A., Mansour, M.R., Akrami, R., Ghobadi, S., Jafarpour, S.A., Mirbeygi, S.K., 2015. Effect of dietary prebiotic mannan oligosaccharide (MOS) on growth performance, intestinal microflora, body composition, haematological and blood serum biochemical parameters of rainbow trout (*Oncorhynchus mykiss*) juveniles. Journal of Fisheries and Aquatic Science 10, 255

Dhanjal, J.K., Malik, V., Radhakrishnan, N., Sigar, M., Kumari, A., Sundar, D., 2019. Computational Protein Engineering Approaches for Effective Design of New Molecules, in: Ranganathan, S., Gribskov, M., Nakai, K., Schönbach, C. (Eds.), Encyclopedia of Bioinformatics and Computational Biology. Academic Press, Oxford, pp. 631–643

Dimitroglou, A., Merrifield, D.L., Spring, P., Sweetman, J., Moate, R., Davies, S.J., 2010. Effects of mannan oligosaccharide (MOS) supplementation on growth performance, feed utilisation, intestinal histology and gut microbiota of gilthead sea bream (*Sparus aurata*). Aquaculture 300, 182–188

Dumon, C., Varvak, A., Wall, M.A., Flint, J.E., Lewis, R.J., Lakey, J.H., Morland, C., Luginbuhl, P., Healey, S., Todaro, T., 2008. Engineering hyperthermostability into a GH11 xylanase is mediated by subtle changes to protein structure. Journal of Biological Chemistry 283, 22557–22564

Eggleston, G., 2019. History of sugar and sweeteners, in: Chemistry's Role in Food Production and Sustainability: Past and Present, ACS Symposium Series. American Chemical Society, pp. 63–74

Fischer, E., 1894. Einfluss der Configuration auf die Wirkung der Enzyme. Berichte der deutschen chemischen Gesellschaft 27, 2985–2993

Flamm, G., Glinsmann, W., Kritchevsky, D., Prosky, L., Roberfroid, M., 2001. Inulin and oligofructose as dietary fiber: A review of the evidence. Critical Reviews in Food Science and Nutrition 41, 353–362

Flores-Maltos, D.A., Mussatto, S.I., Contreras-Esquivel, J.C., Rodríguez-Herrera, R., Teixeira, J.A., Aguilar, C.N., 2016. Biotechnological production and application of fructooligosaccharides. Critical Reviews in Biotechnology 36, 259–267Fogarty, W.M., Kelly, C.T., 2012. Microbial enzymes and biotechnology. Springer Science & Business Media

Foligné, B., Daniel, C., Pot, B., 2013. Probiotics from research to market: the possibilities, risks and challenges. Current Opinion in Microbiology 16, 284–292

Fooks, L.J., Gibson, G.R., 2002. Probiotics as modulators of the gut flora. British Journal of Nutrition 88, s39–s49

Gänzle, M.G., 2011. Lactose and Oligosaccharides | Lactose: Galacto-Oligosaccharides, in: Fuquay, J.W. (Ed.), Encyclopedia of Dairy Sciences (Second Edition). Academic Press, San Diego, pp. 209–216

Ghazi, I., Fernandez-Arrojo, L., Garcia-Arellano, H., Ferrer, M., Ballesteros, A., Plou, F.J., 2007. Purification and kinetic characterization of a fructosyltransferase from Aspergillus aculeatus. Journal of Biotechnology 128, 204–211

González-Delgado, I., López-Muñoz, M.-J., Morales, G., Segura, Y., 2016. Optimisation of the synthesis of high galacto-oligosaccharides (GOS) from lactose with β-galactosidase from *Kluyveromyces lactis*. International Dairy Journal 61, 211–219

Guerrero, C., Vera, C., Conejeros, R., Illanes, A., 2015. Transgalactosylation and hydrolytic activities of commercial preparations of β-galactosidase for the synthesis of prebiotic carbohydrates. Enzyme and Microbial Technology 70, 9–17

Guio, F., Rugeles, L.D., Rojas, S.E., Palomino, M.P., Camargo, M.C., Sánchez, O.F., 2012. Kinetic modeling of fructooligosaccharide production using *Aspergillus oryzae* N74. Applied Biochemistry and Biotechnology 167, 142–163

Halas, V., Nochta, I., 2012. Mannan oligosaccharides in nursery pig nutrition and their potential mode of action. Animals 2, 261–274

Harish, K., Varghese, T., 2006. Probiotics in humans–evidence based review. Calicut Medical Journal J 4, e3

Hemsley, A., Arnheim, N., Toney, M.D., Cortopassi, G., Galas, D.J., 1989. A simple method for site-directed mutagenesis using the polymerase chain reaction. Nucleic Acids Research 17, 6545–6551

Henry, R.J., Darbyshire, B., 1980. Sucrose: sucrose fructosyltransferase and fructan: fructan fructosyltransferase from *Allium cepa*. Phytochemistry 19, 1017–1020

Hernández-Heredia, S., Peña-Castro, J.M., Aguilar-Uscanga, M.G., Olvera, C., Nolasco-Hipólito, C., Del Moral, S., 2022. AmyJ33, a truncated amylase with improved catalytic properties. Biotechnology Letters 44, 1447–1463

Higgins, A., Thorburn, P., Archer, A., Jakku, E., 2007. Opportunities for value chain research in sugar industries. Agricultural Systems 94, 611–621

Holzapfel, W.H., Schillinger, U., 2002. Introduction to pre-and probiotics. Food Research International 35, 109–116.

Hussain, H., Chong, N.F.-M., 2016. Combined overlap extension PCR method for improved site directed mutagenesis. BioMed Research International, 2016

Ibrahim O. 2018. Functional oligosaccharides: chemicals structure, manufacturing, health benefits, applications and regulations. Journal of Food Chemistry & Nanotechnology 4(4): 65-76

Ibrahim, O. 2021. Technological aspects of fructo-oligosaccharides (FOS), production processes, physiological properties, applications and health benefits. Journal of Food Chemistry and Nanotechnology 7(2): 41-46

Iqbal, S., Nguyen, T.-H., Nguyen, T.T., Maischberger, T., Haltrich, D., 2010. β-Galactosidase from Lactobacillus plantarum WCFS1: biochemical characterization and formation of prebiotic galacto-oligosaccharides. Carbohydrate Research 345, 1408–1416

Jiao, L., Chi, H., Xia, B., Lu, Z., Bie, X., Zhao, H., Lu, F., Chen, M., 2022. Thermostability improvement of L-asparaginase from *Acinetobacter soli* via consensus-designed cysteine residue substitution. Molecules 27, 6670

Kabel, M.A., Kortenoeven, L., Schols, H.A., Voragen, A.G., 2002. In vitro fermentability of differently substituted xylo-oligosaccharides. Journal of Agricultural and Food Chemistry 50, 6205–6210

Kang, Z., Zhang, J., Jin, P., Yang, S., 2015. Directed evolution combined with synthetic biology strategies expedite semi-rational engineering of genes and genomes. Bioengineered 6, 136–140

Kashyap, R., Palai, T., Bhattacharya, P.K., 2015. Kinetics and model development for enzymatic synthesis of fructo-oligosaccharides using fructosyltransferase. Bioprocess and Biosystems Engineering 38, 2417–2426

Kaushik, S., Marques, S.M., Khirsariya, P., Paruch, K., Libichova, L., Brezovsky, J., Prokop, Z., Chaloupkova, R., Damborsky, J., 2018. Impact of the access tunnel engineering on catalysis is strictly ligand-specific. The FEBS Journal 285, 1456–1476

Kawakami, A., Yoshida, M., 2002. Molecular Characterization of Sucrose:Sucrose 1-Fructosyltransferase and Sucrose:Fructan 6-Fructosyltransferase Associated with Fructan Accumulation in Winter Wheat during Cold Hardening. Bioscience, Biotechnology, and Biochemistry 66, 2297–2305

Kechagia, M., Basoulis, D., Konstantopoulou, S., Dimitriadi, D., Gyftopoulou, K., Skarmoutsou, N., Fakiri, E.M., 2013. Health benefits of probiotics: a review. International Scholarly Research Notices, 2013

Kherade, M., Solanke, S., Tawar, M., Wankhede, S., 2021. Fructooligosaccharides: A comprehensive review. Journal of Ayurvedic and Herbal Medicine 7, 193–200

Kingsley, L.J., Lill, M.A., 2015. Substrate tunnels in enzymes: Structure–function relationships and computational methodology. Proteins 83, 599–611

Kokkonen, P., Bednar, D., Pinto, G., Prokop, Z., Damborsky, J., 2019. Engineering enzyme access tunnels. Biotechnology Advances 37, 107386

Koshland Jr, D.E., 1958. Application of a theory of enzyme specificity to protein synthesis. Proceedings of the National Academy of Sciences 44, 98–104

Koudelakova, T., Chaloupkova, R., Brezovsky, J., Prokop, Z., Sebestova, E., Hesseler, M., Khabiri, M., Plevaka, M., Kulik, D., Kuta Smatanova, I., 2013. Engineering enzyme stability and resistance to an organic cosolvent by modification of residues in the access tunnel. Angewandte Chemie 125, 2013–2017

Laemmli, U.K., 1970. Cleavage of structural proteins during the assembly of the head of bacteriophage T4. nature 227, 680–685

Lafraya, Á., Sanz-Aparicio, J., Polaina, J., Marín-Navarro, J., 2011. Fructo-oligosaccharide synthesis by mutant versions of *Saccharomyces cerevisiae* invertase. Applied and Environmental Microbiology 77, 6148–6157

Lammens, W., Le Roy, K., Schroeven, L., Van Laere, A., Rabijns, A., Van den Ende, W., 2009. Structural insights into glycoside hydrolase family 32 and 68 enzymes: functional implications. Journal of Experimental Botany 60, 727–740

Latif, A., Shehzad, A., Niazi, S., Zahid, A., Ashraf, W., Iqbal, M.W., Rehman, A., Riaz, T., Aadil, R.M., Khan, I.M., 2023. Probiotics: mechanism of action, health benefits and their application in food industries. Frontiers in Microbiology 14

Lescheid, D.W., 2014. Probiotics as regulators of inflammation: A review. Functional foods in health and disease 4, 299–311

Li, Q., Sun, B., Jia, H., Hou, J., Yang, R., Xiong, K., Xu, Y., Li, X., 2017. Engineering a xylanase from *Streptomyce rochei* L10904 by mutation to improve its catalytic characteristics. International Journal of Biological Macromolecules 101, 366–372

Lu, Y., Zen, K.-C., Muthukrishnan, S., Kramer, K.J., 2002. Site-directed mutagenesis and functional analysis of active site acidic amino acid residues D142, D144 and E146 in *Manduca sexta* (tobacco hornworm) chitinase. Insect Biochemistry and Molecular Biology 32, 1369–1382

Lu, Z., Li, X., Zhang, R., Yi, L., Ma, Y., Zhang, G., 2019. Tunnel engineering to accelerate product release for better biomass-degrading abilities in lignocellulolytic enzymes. Biotechnology for Biofuels 12, 1–9

Ma, D., Cheng, Z., Han, L., Guo, J., Peplowski, L., Zhou, Z., 2024. Structure-oriented engineering of nitrile hydratase: Reshaping of substrate access tunnel and binding pocket for efficient synthesis of cinnamamide. International Journal of Biological Macromolecules 254, 127800

Macfarlane, G.T., Steed, H., Macfarlane, S., 2008. Bacterial metabolism and health-related effects of galacto-oligosaccharides and other prebiotics. Journal of Applied Microbiology 104, 305–344

Macfarlane, H.S.S., 2009. Mechanisms of prebiotic impact on health. Prebiotics and Probiotics Science and Technology 1, 135–161

Madhu, A., Chakraborty, J.N., 2017. Developments in application of enzymes for textile processing. Journal of Cleaner Production 145, 114–133

Maischberger, T., Leitner, E., Nitisinprasert, S., Juajun, O., Yamabhai, M., Nguyen, T.-H., Haltrich, D., 2010. β-Galactosidase from *Lactobacillus pentosus*: Purification, characterization and formation of galacto-oligosaccharides. Biotechnology Journal 5, 838–847

Manoochehri, H., Hosseini, N.F., Saidijam, M., Taheri, M., Rezaee, H., Nouri, F., 2020. A review on invertase: Its potentials and applications. Biocatalysis and Agricultural Biotechnology 25, 101599

Marques, S., Brezovsky, J., Damborsky, J., 2016. Role of tunnels and gates in enzymatic catalysis. Understanding Enzymes: Function, Design, Engineering, and Analysis 421–463

Mathlouthi, M., Reiser, P., 1995. Sucrose: properties and applications. Springer Science & Business Media

Meiering, E.M., Serrano, L., Fersht, A.R., 1992. Effect of active site residues in barnase on activity and stability. Journal of Molecular Biology 225, 585–589

Mhetras, N., Mapre, V., Gokhale, D., 2019. Xylooligosaccharides (XOS) as emerging prebiotics: Its production from lignocellulosic material. Advances in Microbiology 9, 14–20

Mnisi, M.S., Dlamini, C.S., 2012. The concept of sustainable sugarcane production: Global, African and South African perceptions. African Journal of Agricultural Research 7, 4337–4343

Morris, G.M., Huey, R., Lindstrom, W., Sanner, M.F., Belew, R.K., Goodsell, D.S., Olson, A.J., 2009. AutoDock4 and AutoDockTools4: Automated docking with selective receptor flexibility. Journal of Computational Chemistry 30, 2785–2791

Mudannayake, D.C., Jayasena, D.D., Wimalasiri, K.M., Ranadheera, C.S., Ajlouni, S., 2022. Inulin fructans–food applications and alternative plant sources: a review. International Journal of Food Science & Technology 57, 5764–5780

Nagaya, M., Kimura, M., Gozu, Y., Sato, S., Hirano, K., Tochio, T., Nishikawa, A., Tonozuka, T., 2017. Crystal structure of a β-fructofuranosidase with high transfructosylation activity from *Aspergillus kawachii*. Bioscience, Biotechnology, and Biochemistry 81, 1786–1795

Nelson, A., 2019. Catalytic machinery of enzymes expanded. Nature 570, 172–173

Nezhad, N.G., Rahman, R.N.Z.R.A., Normi, Y.M., Oslan, S.N., Shariff, F.M., Leow, T.C., 2022. Thermostability engineering of industrial enzymes through structure modification. Applied Microbiology and Biotechnology 106, 4845–4866

Ni, D., Chen, Z., Tian, Y., Xu, W., Zhang, W., Kim, B.-G., Mu, W., 2022. Comprehensive utilization of sucrose resources via chemical and biotechnological processes: A review. Biotechnology Advances 60, 107990

Nobre, C., Teixeira, J.A., Rodrigues, L.R., 2015. New trends and technological challenges in the industrial production and purification of fructo-oligosaccharides. Critical Reviews in Food Science and Nutrition 55, 1444–1455

Olarte-Avellaneda, S., Rodríguez-López, A., Patiño, J.D., Alméciga-Díaz, C.J., Sánchez, O.F., 2018. *In silico* analysis of the structure of fungal fructooligosaccharides-synthesizing enzymes. Interdisciplinary Sciences: Computational Life Sciences 10, 53–67

O'sullivan, M.G., Thornton, G., O'sullivan, G.C., Collins, J.K., 1992. Probiotic bacteria: myth or reality? Trends in Food Science & Technology 3, 309–314

Pang, C., Yin, X., Zhang, G., Liu, S., Zhou, J., Li, J., Du, G., 2021. Current progress and prospects of enzyme technologies in future foods. Systems Microbiology and Biomanufacturing 1, 24–32

Park, H.-Y., Kim, H.-J., Lee, J.-K., Kim, D., Oh, D.-K., 2008. Galactooligosaccharide production by a thermostable β-galactosidase from *Sulfolobus solfataricus*. World Journal of Microbiology and Biotechnology 24, 1553–1558

Parvez, S., Malik, K.A., Ah Kang, S., Kim, H.-Y., 2006. Probiotics and their fermented food products are beneficial for health. Journal of Applied Microbiology 100, 1171–1185

Picazo, B., Flores-Gallegos, A.C., Muñiz-Márquez, D.B., Flores-Maltos, A., Michel-Michel, M.R., de la Rosa, O., Rodríguez-Jasso, R.M., Rodríguez-Herrera, R., Aguilar-González, C.N., 2019. Enzymes for fructooligosaccharides production: achievements and opportunities, in: Enzymes in Food Biotechnology. Elsevier, pp. 303–320

Pico, J., Vidal, N.P., Widjaja, L., Falardeau, L., Albino, L., Martinez, M.M., 2021. Development and assessment of GC/MS and HPAEC/PAD methodologies for the quantification of α-galacto-oligosaccharides (GOS) in dry beans (*Phaseolus vulgaris*). Food Chemistry 349, 129151

Pinto, M.C.C., Dutra, L., Fé, L.X.S.G.M., Freire, D.M.G., Manoel, E.A., Cipolatti, E.P., 2023. Chapter 15 - Immobilized biocatalysts for hydrolysis of polysaccharides, in: Goldbeck, R., Poletto, P. (Eds.), Polysaccharide-Degrading Biocatalysts, Foundations and Frontiers in Enzymology. Academic Press, pp. 385–407

Plaza-Diaz, J., Ruiz-Ojeda, F.J., Gil-Campos, M., Gil, A., 2019. Mechanisms of action of probiotics. Advances in Nutrition 10, S49–S66

Pons, T., Naumoff, D.G., Martínez-Fleites, C., Hernández, L., 2004. Three acidic residues are at the active site of a β-propeller architecture in glycoside hydrolase families 32, 43, 62, and 68. Proteins: Structure, Function, and Bioinformatics 54, 424–432

Prada, M., Saraiva, M., Garrido, M.V., Sério, A., Teixeira, A., Lopes, D., Silva, D.A., Rodrigues, D.L., 2022. Perceived associations between excessive sugar intake and health conditions. Nutrients 14, 640

Precedence Research, 2022. Prebiotic ingredients market size, share, report 2023-2032. Available at: https://www.precedenceresearch.com/prebiotic-ingredients-market. Accessed: 20 December 2023

Prokop, Z., Gora, A., Brezovsky, J., Chaloupkova, R., Stepankova, V., Damborsky, J., 2012. Engineering of protein tunnels: Keyhole-lock-key model for catalysis by the enzymes with buried active sites. Protein Engineering Handbook 3, 421–464

Queneau, Y., Jarosz, S., Lewandowski, B., Fitremann, J., 2007. Sucrose chemistry and applications of sucrochemicals. Advances in Carbohydrate Chemistry and Biochemistry 61, 217–292

Rakotoharisoa, R.V., Seifinoferest, B., Zarifi, N., Miller, J.D.M., Rodriguez, J.M., Thompson, M.C., Chica, R.A., 2023. Design of efficient artificial enzymes using crystallographically-enhanced conformational sampling. bioRxiv 2023-11. 564846

Raman, M., Saiprasad, G.V.S., Madhavakrishna, K., 2019. From seed to feed: assessment and alleviation of Raffinose Family Oligosaccharides (RFOs) of seed-and sprout-flours of soybean [Glycine max (L.) Merr.]-a commercial aspect. International Food Research Journal 26

Raveendran, S., Parameswaran, B., Ummalyma, S.B., Abraham, A., Mathew, A.K., Madhavan, A., Rebello, S., Pandey, A., 2018. Applications of microbial enzymes in food industry. Food Technology and Biotechnology 56, 16

Roberfroid, M., Gibson, G.R., Hoyles, L., McCartney, A.L., Rastall, R., Rowland, I., Wolvers, D., Watzl, B., Szajewska, H., Stahl, B., 2010. Prebiotic effects: metabolic and health benefits. British Journal of Nutrition 104, S1–S63

Robinson, P.K., 2015. Enzymes: principles and biotechnological applications. Essays in Biochemistry 59, 1–41

Roduner, E., 2014. Understanding catalysis. Chemical Society Reviews. 43, 8226–8239

Rosenfeld, L., Heyne, M., Shifman, J.M., Papo, N., 2016. Protein engineering by combined computational and *in vitro* evolution approaches. Trends in Biochemical Sciences 41, 421–433

Rowley, J., Decker, S.R., Michener, W., Black, S., 2013. Efficient extraction of xylan from delignified corn stover using dimethyl sulfoxide. 3 Biotech 3, 433–438

Sabater-Molina, M., Larqué, E., Torrella, F., Zamora, S., 2009. Dietary fructooligosaccharides and potential benefits on health. Journal of Physiology and Biochemistry 65, 315–328

Sahu, O., 2018. Assessment of sugarcane industry: Suitability for production, consumption, and utilization. Annals of Agrarian Science 16, 389–395

Sainz-Polo, M.A., Ramírez-Escudero, M., Lafraya, A., González, B., Marín-Navarro, J., Polaina, J., Sanz-Aparicio, J., 2013. Three-dimensional structure of Saccharomyces invertase: Role of a non-catalytic domain in oligomerization and substrate specificity. Journal of Biological Chemistry 288, 9755–9766

Sako, T., Tanaka, R., 2011. Prebiotics | Types, in: Fuquay, J.W. (Ed.), Encyclopedia of Dairy Sciences (Second Edition). Academic Press, San Diego, pp. 354–364

Sánchez-Martínez, M.J., Soto-Jover, S., Antolinos, V., Martínez-Hernández, G.B., López-Gómez, A., 2020. Manufacturing of short-chain fructooligosaccharides: From laboratory to industrial scale. Food Engineering Reviews 12, 149–172

Sangeetha, P.T., Ramesh, M.N., Prapulla, S.G., 2005. Recent trends in the microbial production, analysis and application of Fructooligosaccharides. Trends in Food Science & Technology 16, 442–457

Sarao, L.K., Arora, M., 2017. Probiotics, prebiotics, and microencapsulation: A review. Critical Reviews in Food Science and Nutrition 57, 344–371

Schrodinger, 2015. The PyMOL Molecular Graphics System, Version 1.8

Sen, A., Isaacs, N., Geldenhuys, M., Govender, S., Vallabh, V.T., Fleishman, Z., Ndlawana, Y., 2019. The history of sugar. Available at http://hdl.handle.net/11427/30588. Accessed: 20 December 2023

Seo, E.-J., Kim, M.-J., Park, S.-Y., Park, S., Oh, D.-K., Bornscheuer, U., Park, J.-B., 2022. Enzyme access tunnel engineering in baeyer-villiger monooxygenases to improve oxidative stability and biocatalyst performance. Advanced Synthesis & Catalysis 364, 555–564

Singh, R.S., Singh, R.P., 2010. Production of fructooligosaccharides from inulin by endoinulinases and their prebiotic potential. Food Technology and Biotechnology 48, 435

Singh, R.S., Singh, T., Singh, A.K., 2019. Enzymes as diagnostic tools, in: Advances in Enzyme Technology. Elsevier, pp. 225–271

Singh, S., Anand, R., 2021. Tunnel Architectures in Enzyme Systems that Transport Gaseous Substrates. ACS Omega 6, 33274–33283

Sirisansaneeyakul, S., Lertsiri, S., Tonsagunrathanachai, P., Luangpituksa, P., 2000. Enzymatic production of fructo-oligosaccharides from sucrose. Agriculture and Natural Resources 34, 262–269

Slavin, J., 2013. Fiber and prebiotics: Mechanisms and health benefits. Nutrients 5, 1417–1435

Song, L., Siguier, B., Dumon, C., Bozonnet, S., O'Donohue, M.J., 2012. Engineering better biomass-degrading ability into a GH11 xylanase using a directed evolution strategy. Biotechnology for biofuels 5, 1–16

Souza, A.F.C. e, Gabardo, S., Coelho, R. de J.S., 2022. Galactooligosaccharides: Physiological benefits, production strategies, and industrial application. Journal of Biotechnology 359, 116–129

Studer, G., Rempfer, C., Waterhouse, A.M., Gumienny, R., Haas, J., Schwede, T., 2020. QMEANDisCo—distance constraints applied on model quality estimation. Bioinformatics 36, 1765–1771

Tamura, K., Stecher, G., Kumar, S., 2021. MEGA11: molecular evolutionary genetics analysis version 11. Molecular Biology and Evolution 38, 3022–3027

Thompson, J.D., Higgins, D.G., Gibson, T.J., 1994. CLUSTAL W: Improving the sensitivity of progressive multiple sequence alignment through sequence weighting, position-specific gap penalties and weight matrix choice. Nucleic Acids Research 22, 4673–4680

Torrecillas, S., Montero, D., Izquierdo, M., 2014. Improved health and growth of fish fed mannan oligosaccharides: potential mode of action. Fish & Shellfish Immunology 36, 525–544

Torres, D.P., Gonçalves, M. do P.F., Teixeira, J.A., Rodrigues, L.R., 2010. Galacto-oligosaccharides: production, properties, applications, and significance as prebiotics. Comprehensive Reviews in Food Science and Food Safety 9, 438–454

Tungland, B., 2018. Chapter 7 - Overview of prebiotics: Membership, physiological effects and their health attributes, in: tungland, b. (ed.), human microbiota in health and disease. Academic Press, pp. 289–348

Urrutia, P., Rodriguez-Colinas, B., Fernandez-Arrojo, L., Ballesteros, A.O., Wilson, L., Illanes, A., Plou, F.J., 2013. Detailed analysis of galactooligosaccharides synthesis with β-galactosidase from *Aspergillus oryzae*. Journal of Agricultural and Food Chemistry 61, 1081–1087

Vega, R., Zuniga-Hansen, M.E., 2014. A new mechanism and kinetic model for the enzymatic synthesis of short-chain fructooligosaccharides from sucrose. Biochemical Engineering Journal 82, 158–165

Vera, C., Illanes, A., Guerrero, C., 2021. Enzymatic production of prebiotic oligosaccharides. Current Opinion in Food Science 37, 160–170

Vulevic, J., Tzortzis, G., Juric, A., Gibson, G.R., 2018. Effect of a prebiotic galactooligosaccharide mixture (B-GOS®) on gastrointestinal symptoms in adults selected from a general population who suffer with bloating, abdominal pain, or flatulence. Neurogastroenterology & Motility 30, e13440

Wang, L., Diao, S., Sun, Y., Jiang, S., Liu, Y., Wang, H., Wei, D., 2021. Rational engineering of *Acinetobacter tandoii* glutamate dehydrogenase for asymmetric synthesis of L -homoalanine through biocatalytic cascades. Catal. Sci. Technol. 11, 4208–4215

Wang, X., Ma, R., Xie, X., Liu, W., Tu, T., Zheng, F., You, S., Ge, J., Xie, H., Yao, B., 2017. Thermostability improvement of a Talaromyces leycettanus xylanase by rational protein engineering. Scientific Reports 7, 15287

Waterhouse, A., Bertoni, M., Bienert, S., Studer, G., Tauriello, G., Gumienny, R., Heer, F.T., de Beer, T.A.P., Rempfer, C., Bordoli, L., Lepore, R., Schwede, T., 2018. SWISS-MODEL: homology modelling of protein structures and complexes. Nucleic Acids Research 46, W296–W303

White, J.S., 2014. Sucrose, HFCS, and fructose: history, manufacture, composition, applications, and production, in: Rippe, J.M. (Ed.), Fructose, High Fructose Corn Syrup, Sucrose and Health. Springer New York, New York, NY, pp. 13–33

White, L.A., Newman, M.C., Cromwell, G.L., Lindemann, M.D., 2002. Brewers dried yeast as a source of mannan oligosaccharides for weanling pigs. Journal of Animal Science 80, 2619–2628

Williams, N.T., 2010. Probiotics. American Journal of Health-System Pharmacy 67, 449–458.

Woodley, J.M., 2022. Integrating protein engineering into biocatalytic process scale-up. Trends in Chemistry 4:371–373

Xia, Y., Guo, W., Han, L., Shen, W., Chen, X., Yang, H., 2022. Significant improvement of both catalytic efficiency and stability of fructosyltransferase from *Aspergillus niger* by structure-guided engineering of key residues in the conserved sequence of the catalytic domain. Journal of Agricultural and Food Chemistry 70, 7202–7210

Yang, K., Huang, B., Amanze, C., Yan, Z., Qiu, G., Liu, X., Zhou, H., Zeng, W., 2022. Hydrophilicity-based engineering of the active pocket of D-amino acid oxidase leading to highly improved specificity toward D-glufosinate. Angewandte Chemie International Edition 61, e202212720

Yoo, E.-H., Lee, S.-Y., 2010. Glucose biosensors: an overview of use in clinical practice. Sensors 10, 4558–4576

Yoshikawa, J., Amachi, S., Shinoyama, H., Fujii, T., 2006. Multiple β-fructofuranosidases by *Aureobasidium pullulans* DSM2404 and their roles in fructooligosaccharide production. FEMS Microbiology Letters 265, 159–163

Yuan, X.-L., Goosen, C., Kools, H., Van Der Maarel, M.J.E.C., Van Den Hondel, C.A.M.J.J., Dijkhuizen, L., Ram, A.F.J., 2006. Database mining and transcriptional analysis of genes encoding inulin-modifying enzymes of Aspergillus niger. Microbiology 152, 3061–3073

Zhang, J., Liu, C., Xie, Y., Li, N., Ning, Z., Du, N., Huang, X., Zhong, Y., 2017. Enhancing fructooligosaccharides production by genetic improvement of the industrial fungus *Aspergillus niger* ATCC 20611. Journal of Biotechnology 249, 25–33

Zhang, S., Lv, S., Li, Y., Wei, D., Zhou, X., Niu, X., Yang, Z., Song, W., Zhang, Z., Peng, D., 2023. Prebiotics modulate the microbiota–gut–brain axis and ameliorate cognitive impairment in APP/PS1 mice. European Journal of Nutrition 62, 2991–3007

Zhu, J.Y., Pan, X., 2022. Efficient sugar production from plant biomass: Current status, challenges, and future directions. Renewable and Sustainable Energy Reviews 164, 112583